

			MAXSS ATBD ESA Contract 4000132954/20/I-NB Delivery D21, Version 1.0.0 Date 28/01/2022 Page 1
---	--	--	---

MAXSS:

**Storm Atlas Algorithm Theoretical Baseline
Document**

(ATBD, preliminary version)

(ATBD)

Doc. No.: ATBD_stormAtlas-v0.1

Issue: 0

No.:

Version: 1.0.0

Date: 28 Janvier 2022

Document prepared under ESA Contract Number: 4000132954/20/I-NB

1 TABLE OF CONTENTS

1 Table of contents.....	2
2 Introduction.....	5
2.1 Storm Atlas objective.....	5
2.2 Document objective and organisation.....	6
2.3 Reference documents.....	6
3 MARINE EXTREME ATLAS INPUT DATA.....	11
3.1 Storm tracks.....	11
3.1.1 Tropical Cyclones tracks.....	11
3.1.2 Extra-Tropical Cyclones tracks.....	12
3.1.3 Polar Lows tracks.....	13
3.2 Gridded EO data.....	13
3.2.1 Sea Surface Salinity data.....	13
3.2.1.1 Satellite SSS data.....	13
3.2.1.2 In Situ analysed SSS data.....	14
3.2.2 Sea Surface Temperature.....	14
3.2.2.1 Satellite SST data.....	14
3.2.2.1.1 GHRSSST Level 4 MW_IR_OI Global Foundation Sea Surface Temperature analysis version 5.0 from REMSS.....	14
3.2.2.1.2 ESA Climate Change Initiative (CCI) v2.1 SST Level 4 Analysis.....	15
3.2.2.2 In Situ analyzed SST data.....	15
3.2.3 Sea Level Anomalies.....	15
3.2.4 Ocean Color products.....	16
3.2.5 Atmospheric data.....	17
3.2.5.1 Multi-satellite Precipitation Analysis (TMPA).....	17
3.2.5.2 ERA5 Total Precipitation, Evaporation, and wind component data.....	18
3.2.5.3 Surface Wind Vector.....	20
3.2.6 In Situ Analyzed Ocean Salinity and Temperature profiles.....	20
3.3 Along-track / Swath Observations.....	20

- 3.3.1 sea surface heights anomalies..... 20
- 3.3.2 Sea State..... 21
- 3.3.3 Surface Wind Speed from Individual Sensors..... 21
- 4 STORM ATLAS GENERATION: STEP1: STORM TRACK PRE-SELECTION..... 24
 - 4.1 Tropical Cyclones tracks..... 24
 - 4.1.1.1 Source selection for East Pacific basin..... 26
 - 4.1.1.2 Source selection for North Atlantic basin..... 28
 - 4.1.1.3 Source selection for North Indian basin..... 29
 - 4.1.1.4 Source selection for South Indian basin..... 30
 - 4.1.1.5 Source selection for West Pacific basin..... 32
 - 4.1.1.6 Source selection for South Pacific basin..... 34
 - 4.1.1.7 TC tracks selection summary..... 35
 - 4.1.2 Extra-Tropical Cyclones tracks..... 36
 - 4.1.3 Polar Low tracks..... 40
- 5 Storm Atlas Generation: step 2 Coarse Collocation..... 41
 - 5.1 Tropical Cyclones scales..... 42
 - 5.2 ETC characteristic scales..... 42
 - 5.3 Polar Lows characteristic scales..... 43
 - 5.4 Recovery time for SST and SSS response..... 43
 - 5.5 SSH and SLA long term response..... 44
 - 5.6 Upper ocean Biological response time scale..... 45
- 6 Storm Atlas Generation: step 3 Refined Collocation..... 53
- 7 Storm Atlas Generation: step 4 Data Extraction and Pre-processing..... 54
 - 7.1 Gridded data..... 54
 - 7.1.1 Extraction method..... 54
 - 7.1.2 Gridded product currently included into the MAXSS Storm Atlas..... 56
 - 7.1.3 Output Content and Nomenclature..... 56
 - 7.1.3.1 Content..... 56
 - 7.1.3.2 Nomenclature..... 57
 - 7.2 Along-Track and Swath Data..... 59

			<p style="text-align: right;"> MAXSS ATBD ESA Contract 4000132954/20/I-NB Delivery D21, Version 1.0.0 Date 06/10/2021 Page 4 </p>
---	--	--	---

7.2.1 Extraction method..... 59

7.2.2 Swath Data currently included into the Storm Atlas..... 63

7.2.3 Output Content and Nomenclature..... 63

7.3 Argo floats..... 64

7.4 Data Organization and Access..... 65

8 Annex 1 Example of format for gridded data..... 68

9 Annex 2: Example of format for along-track data..... 85

10 Annex 3: Example of format for ARGO float data..... 108

2 INTRODUCTION

This document is the Algorithm Theoretical Basis Document for the MAXSS Storm Atlas.

2.1 Storm Atlas objective

The Storm Atlas is a collection of observations from multiple satellite, insitu or model sources matching up storm tracks of **Tropical Cyclones (TC)**, **Extra-Tropical Storms (ETC)** and **Polar Lows (PL)**. These observations, in the Storm Atlas, are grouped per storm and per source of data.

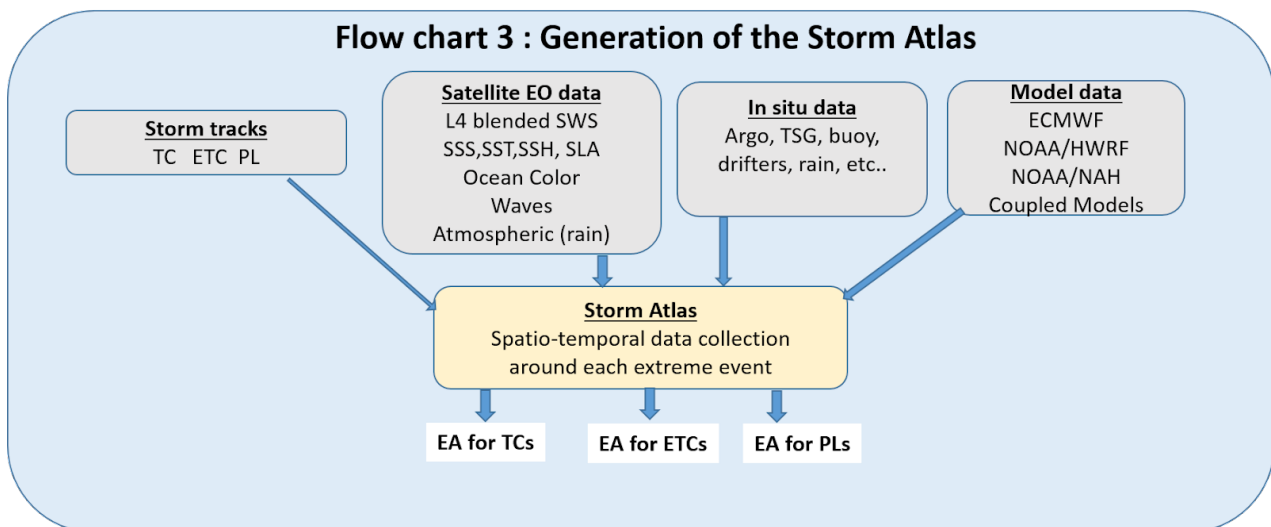


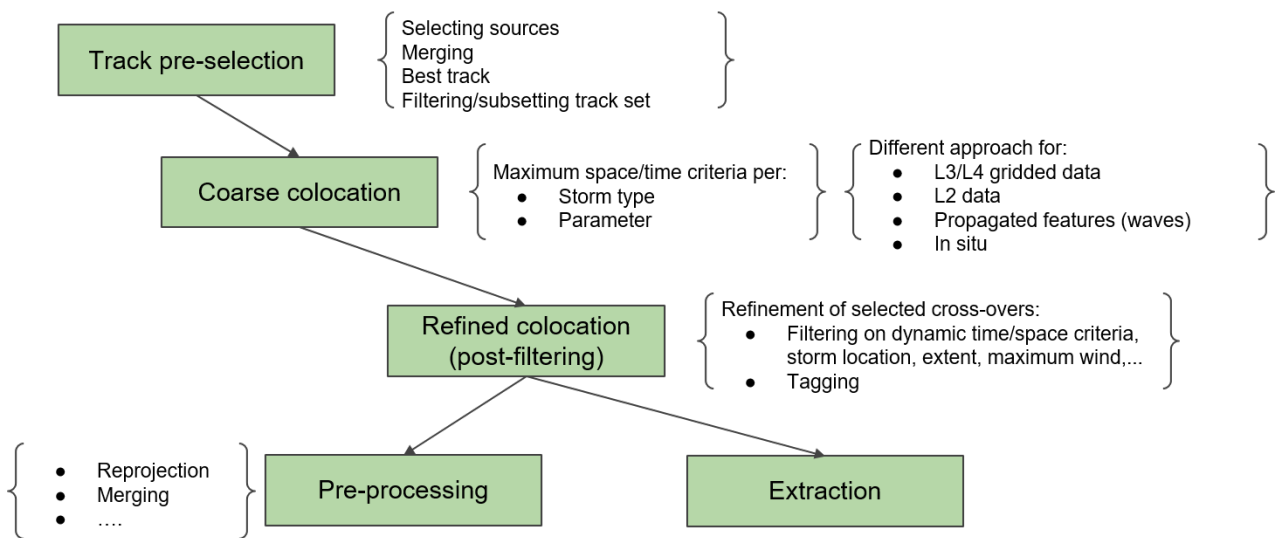
Figure 1: Steps for building the storm-Atlas.

The general scheme for building the Storm Atlas consists of the following steps, as illustrated also in figure 1:

- the **selection** of the reference storms for which observations will be collected. The best known tracks for each storm are evaluated, merged together per type of storm (TC, ETC or PL), and interpolated to the hour if necessary. These storm tracks are made available in different formats as a separate product.
- **coarse collocation** between the selected tracks and the sources of data to be matched with is then performed. **Coarse collocation** means in this context that fixed time and search radius collocation criteria are used for all storms of a given type and for a given source dataset. They are not dependent on the storm development stage or spatial extent for instance. Such refinement in the storm/data sources matching or characterization of each individual matchup can be done at a

later stage, referred to as **refined collocation**, which is not performed in the first version of the Storm Atlas.

- the **extraction** of the source data is then performed and the extracted data are collated into a single output file for each storm/data source association.



2.2 Document objective and organisation

This document describes how the Storm Atlas was generated. It details the following aspects:

- the selection of **input datasets** that are used to form the atlas
- the selection of the **best and most relevant tracks** for each source of storm tracks
- the **collocation** procedure for each type of observation input
- the **refined collocation** and **characterization** of each storm collocation (not covered in version 1.0 of the Storm Atlas)

2.3 Reference documents

Babin SM, Carton JA, Dickey TD, Wiggert JD (2004) Satellite evidence of hurricane-induced phytoplankton blooms in an oceanic desert. *J Geophys Res Oceans* 109:C03043

Boutin J., Reul Nicolas, Koehler J., Martin A, Catany R., Guimbarde Sebastien, Rouffi F., Vergely J.L., Arias M., Chakroun M., Corato G., Estella Perez V., Hasson A., Josey S., Khvorostyanov D., Kolodziejczyk Nicolas, Mignot J., Olivier L., Reverdin G., Stammer D., Supply Alexandre, Thouvenin masson C., Turiel A., Vialard J., Cipollini P., Donlon

			<p style="text-align: right;">MAXSS ATBD ESA Contract 4000132954/20/I-NB Delivery D21, Version 1.0.0 Date 06/10/2021 Page 7</p>
---	--	--	---

C., Sabia R., Mecklenburg S. (2021). Satellite based Sea Surface Salinity designed for Ocean and Climate Studies . Journal Of Geophysical Research-oceans , 126(11), e2021JC017676 (28p.) .

Chen, F. and Y. Fu, (2015) Contribution of tropical cyclone rainfall at categories to total precipitation over the Western North Pacific from 1998 to 2007, Sci. China Earth Sci. 58: 2015. doi:10.1007/s11430-015-5103-9.

Chen Y, Tang D (2012) Eddy-feature phytoplankton bloom induced by a tropical cyclone in the South China sea. Int J Remote Sens 33:7444–7457

Chiang TL, Wu CR, Oey LY (2011) Typhoon kai-tak: an ocean’s perfect storm. J Phys Oceanogr 41:221–233

Combot, C., Mouche, A., Knaff, J., Zhao, Y., Zhao, Y., Vinour, L., Quilfen, Y., & Chapron, B. (2020). Extensive High-Resolution Synthetic Aperture Radar (SAR) Data Analysis of Tropical Cyclones: Comparisons with SFMR Flights and Best Track, Monthly Weather Review, 148(11), 4545-4563. Retrieved Feb 22, 2022, from <https://journals.ametsoc.org/view/journals/mwre/148/11/MWR-D-20-0005.1.xml>

Dacre, H. F., Hawcroft, M. K., Stringer, M. A., & Hodges, K. I. (2012). An Extratropical Cyclone Atlas: A Tool for Illustrating Cyclone Structure and Evolution Characteristics, Bulletin of the American Meteorological Society, 93(10), 1497-1502. Retrieved Feb 22, 2022, from <https://journals.ametsoc.org/view/journals/bams/93/10/bams-d-11-00164.1.xml>

Dare, R. A., & McBride, J. L. (2011). Sea Surface Temperature Response to Tropical Cyclones, Monthly Weather Review, 139(12), 3798-3808. Retrieved Feb 22, 2022, from <https://journals.ametsoc.org/view/journals/mwre/139/12/mwr-d-10-05019.1.xml>

Foltz GR, Balaguru K, Leung LR (2015) A reassessment of the integrated impact of tropical cyclones on surface chlorophyll in the western subtropical North Atlantic. Geophys Res Lett 42:1158–1164

Gaillard F., Reynaud T., Thierry V., Kolodziejczyk N., Von Schuckmann K. (2016). In-situ based reanalysis of the global ocean temperature and salinity with ISAS: variability of the heat content and steric height. Journal of Climate, 29(4), 1305-1323. <https://doi.org/10.1175/JCLI-D-15-0028.1>

Good, S.A.; Embury, O.; Bulgin, C.E.; Mittaz, J. (2019): ESA Sea Surface Temperature Climate Change Initiative (SST_cci): Level 4 Analysis Climate Data Record, version 2.1. Centre for Environmental Data Analysis, 22 August 2019. doi:10.5285/62c0f97b1eac4e0197a674870afe1ee6.

Gramscianinov, C. B., Campos, R. M., de Camargo, R., Hodges, K., Guedes Soares, C. and da Silva Dias, P. L. (2020) Analysis of Atlantic extratropical storm tracks characteristics in 41 years of ERA5 and CFSR/CFSv2 databases. Ocean Engineering, 216. 108111. ISSN 0029-8018

- Hanshaw MN, Lozier MS, Palter JB (2008) Integrated impact of tropical cyclones on sea surface chlorophyll in the North Atlantic. *Geophys Res Lett* 35:L01601
- Hoskins, B. J. and Hodges, K. I. (2002) New perspectives on the Northern Hemisphere winter storm tracks. *Journal of the Atmospheric Sciences*, 59 (6). pp. 1041-1061. ISSN 1520-0469 doi: [https://doi.org/10.1175/1520-0469\(2002\)059<1041:NPOTNH>2.0.CO;2](https://doi.org/10.1175/1520-0469(2002)059<1041:NPOTNH>2.0.CO;2)
- Hoskins, B. J. and Hodges, K. I. (2005) A new perspective on Southern hemisphere storm-tracks. *Journal of Climate*, 18 (20). pp. 4108-4129. ISSN 1520-0442 doi: <https://doi.org/10.1175/JCLI3570.1>
- Huang PS, Sanford TB, Imberger J (2009) Heat and turbulent kinetic energy budgets for surface layer cooling induced by the passage of Hurricane Frances (2004). *J Geophys Res Oceans* 114:C12023
- Huang SM, Oey LY (2015) Right-side cooling and phytoplankton bloom in the wake of a tropical cyclone. *J Geophys Res Oceans* 120:5735–5748
- Hung CC, Chung CC, Gong GC, Jan S, Tsai Y, Chen KS, Chou WC, Lee MA, Chang Y, Chen MH, Yang WR, Tseng CJ, Gawarkiewicz G (2013) Nutrient supply in the Southern East China sea after Typhoon Morakot. *J Mar Res* 71:133–149
- Jiang, H. and E.J. Zipser, (2010) Contribution of Tropical Cyclones to the Global Precipitation from Eight Seasons of TRMM Data: Regional, Seasonal, and Interannual Variations. *Journal of Climate* 23:6, 1526-1543.
- Jiang, H., C. Liu, and E. D. Zipser (2011), A TRMM-based tropical cyclones cloud and precipitation feature database, *J. Appl. Meteorol. Climatol.*, 50, 1255–1274.
- Jin W, Liang C, Hu J, Meng Q, Lü H, Wang Y, Lin F, Chen X, Liu X (2020) Modulation effect of mesoscale eddies on sequential typhoon-induced oceanic responses in the South China Sea. *Remote Sens* 12:3059
- Kimball, S. K., & Mulekar, M. S. (2004). A 15-Year Climatology of North Atlantic Tropical Cyclones. Part I: Size Parameters, *Journal of Climate*, 17(18), 3555-3575. Retrieved Feb 22, 2022, from https://journals.ametsoc.org/view/journals/clim/17/18/1520-0442_2004_017_3555_aycona_2.0.co_2.xml
- Knaff, J. A., S. P. Longmore, and D. A. Molnar, 2014: An objective satellite-based tropical cyclone size climatology. *J. Climate*, 27, 455–476, <https://doi.org/10.1175/JCLI-D-13-00096.1>.
- Knapp, K. R., M. C. Kruk, D. H. Levinson, H. J. Diamond, and C. J. Neumann, 2010: The International Best Track Archive for Climate Stewardship (IBTrACS): Unifying Tropical Cyclone Data. *Bull. Amer. Meteor. Soc.*, 91, 363–376, <https://doi.org/10.1175/2009BAMS2755.1>.
- Kolodziejczyk Nicolas, Prigent-Mazella Annaig, Gaillard Fabienne (2017). ISAS-15 temperature and salinity gridded fields. SEANOE. <https://doi.org/10.17882/52367>

			<p style="text-align: right;">MAXSS ATBD ESA Contract 4000132954/20/I-NB Delivery D21, Version 1.0.0 Date 06/10/2021 Page 9</p>
---	--	--	---

Lin I-I, Liu WT, Wu C-C, Wong GTF, Hu C, Chen Z, Liang W-D, Yang Y, Liu K-K (2003b) New evidence for enhanced ocean primary production triggered by tropical cyclone. *Geophys Res Lett* 30:1718

Lin YC, Oey LY (2016) Rainfall-enhanced blooming in typhoon wakes. *Sci Rep* 6:31310

Lonfat, M., F. D. Marks, and S. S. Chen, (2004) Precipitation distribution in tropical cyclones using the Tropical Rainfall Measuring Mission (TRMM) microwave imager: A global perspective. *Mon. Wea. Rev.*, 132, 1645–1660, doi:10.1175/1520-0493(2004)132,1645:PDITCU.2.0.CO;2.

Mei, W., & Pasquero, C. (2013). Spatial and Temporal Characterization of Sea Surface Temperature Response to Tropical Cyclones, *Journal of Climate*, 26(11), 3745-3765. Retrieved Feb 22, 2022, from <https://journals.ametsoc.org/view/journals/clim/26/11/jcli-d-12-00125.1.xml>

Merchant, C.J., Embury, O., Bulgin, C.E. et al. Satellite-based time-series of sea-surface temperature since 1981 for climate applications. *Sci Data* 6, 223 (2019). <https://doi.org/10.1038/s41597-019-0236-x>

Mooers CNK (1975) Several effects of a baroclinic current on the cross-stream propagation of inertial-internal waves. *Geophys Fluid Dyn* 6:245–275

Morimoto A, Kojima S, Jan S, Takahashi D (2009) Movement of the Kuroshio axis to the Northeast shelf of Taiwan during typhoon events. *Estuar Coast Shelf Sci* 82:547–552

Pan G, Chai F, Tang D, Wang D (2017) Marine phytoplankton biomass responses to typhoon events in the South China Sea based on physical–biogeochemical model. *Ecol Modell* 356:38–47

Prat, O. P., and B. R. Nelson (2013), Mapping the world's tropical cyclone rainfall contribution over land using the TRMM Multi-satellite Precipitation Analysis, *Water Resour. Res.*, 49, 7236–7254, doi:10.1002/wrcr.20527.

Remote Sensing Systems. 2017. MWIR optimum interpolated SST data set. Ver. 5.0. PO.DAAC, CA, USA. Dataset accessed [YYYY-MM-DD] at <https://doi.org/10.5067/GHMWI-4FR05>

Roberts, J. F., Champion, A. J., Dawkins, L. C., Hodges, K. I., Shaffrey, L. C., Stephenson, D. B., Stringer, M. A., Thornton, H. E. and Youngman, B. D. (2014) The XWS open access catalogue of extreme European windstorms from 1979 to 2012. *Natural Hazards and Earth System Sciences*, 14. pp. 2487-2501. ISSN 1561-8633 doi: <https://doi.org/10.5194/nhess-14-2487-2014>

Sathyendranath, S, Brewin, RJW, Brockmann, C, Brotas, V, Calton, B, Chuprin, A, Cipollini, P, Couto, AB, Dingle, J, Doerffer, R, Donlon, C, Dowell, M, Farman, A, Grant, M, Groom, S, Horseman, A, Jackson, T, Krasemann, H, Lavender, S, Martinez-Vicente, V, Mazeran, C, Mélin, F, Moore, TS, Müller, D, Regner, P, Roy, S, Steele, CJ, Steinmetz, F,

Swinton, J, Taberner, M, Thompson, A, Valente, A, Zühlke, M, Brando, VE, Feng, H, Feldman, G, Franz, BA, Frouin, R, Gould, Jr., RW, Hooker, SB, Kahru, M, Kratzer, S, Mitchell, BG, Muller-Karger, F, Sosik, HM, Voss, KJ, Werdell, J, and Platt, T (2019) An ocean-colour time series for use in climate studies: the experience of the Ocean-Colour Climate Change Initiative (OC-CCI). *Sensors*: 19, 4285. doi:10.3390/s19194285

Sathyendranath, S.; Jackson, T.; Brockmann, C.; Brotas, V.; Calton, B.; Chuprin, A.; Clements, O.; Cipollini, P.; Danne, O.; Dingle, J.; Donlon, C.; Grant, M.; Groom, S.; Krasemann, H.; Lavender, S.; Mazeran, C.; Mélin, F.; Müller, D.; Steinmetz, F.; Valente, A.; Zühlke, M.; Feldman, G.; Franz, B.; Frouin, R.; Werdell, J.; Platt, T. (2021): ESA Ocean Colour Climate Change Initiative (Ocean_Colour_cci): Version 5.0 Data. NERC EDS Centre for Environmental Data Analysis, 19 May 2021. doi:10.5285/1dbe7a109c0244aaad713e078fd3059a.

<http://dx.doi.org/10.5285/1dbe7a109c0244aaad713e078fd3059a>

Shang S, Li L, Sun F, Wu J, Hu C, Chen D, Ning X, Qiu Y, Zhang C, Shang S (2008) Changes of temperature and bio-optical properties in the South China sea in response to typhoon lingling, 2001. *Geophys Res Lett* 35:L10602

Shibano R, Yamanaka Y, Okada N, Chuda T, Suzuki SI, Niino H, Toratani M (2011) Responses of marine ecosystem to typhoon passages in the western subtropical North Pacific. *Geophys Res Lett* 38:L18608

Sinclair, M.R., 1994. An objective cyclone climatology for the Southern Hemisphere. *Mon. Wea. Rev.* 122, 2239–2256.

Siswanto E, Morimoto A, Kojima S (2009) Enhancement of phytoplankton primary productivity in the Southern East China sea following episodic typhoon passage. *Geophys Res Lett* 36:L11603

Sun, J.; Vecchi, G.; Soden, B. Sea Surface Salinity Response to Tropical Cyclones Based on Satellite Observations. *Remote Sens.* 2021, 13, 420. <https://doi.org/10.3390/rs13030420>

Xu F, Yao Y, Oey L, Lin Y (2017a) Impacts of pre-existing ocean cyclonic circulation on sea surface chlorophyll-a concentrations off northeastern Taiwan following episodic typhoon passages. *J Geophys Res Oceans* 122:6482–6497

Yin X, Wang Z, Liu Y, Xu Y (2007) Ocean response to typhoon ketsana traveling over the Northwest Pacific and a numerical model approach. *Geophys Res Lett* 34:L21606

Zhao H, Pan J, Han G, Devlin AT, Zhang S, Hou Y (2017) Effect of a fast-moving tropical storm washi on phytoplankton in the northwestern South China sea. *J Geophys Res Oceans* 122:3404–3416

Zhao B, Qiao F, Wang G (2008) The effects of the non-breaking surface wave-induced vertical mixing on the forecast of tropical cyclone tracks. *Chin Sci Bull* 59:3075–3084

			<p style="text-align: right;">MAXSS ATBD ESA Contract 4000132954/20/I-NB Delivery D21, Version 1.0.0 Date 06/10/2021 Page 11</p>
---	--	--	--

3 MARINE EXTREME ATLAS INPUT DATA

The following input data are used to build up the storm Atlas.

3.1 Storm tracks

Storm tracks and associated storm parameters are collected to build up the Atlas covering the period 2010-2020 for Tropical cyclones, Extra-Tropical Cyclones, and Polar Lows. In fact, this categorization forms the basic skeleton on which the storm Atlas is built. The data sources and analyses are different for Tropical Cyclones, Extra-Tropical cyclones, and Polar lows. The project relies on the data sources for storm tracks described in further details in the following subsections.

3.1.1 Tropical Cyclones tracks

For building the present Atlas of Tropical Cyclones (TCs), we use the TC tracks from the International Best Track Archive for Climate Stewardship, IBTrACS (Knapp et al., 2010). We use the last version available: v04. It is accessible at <https://www.ncdc.noaa.gov/ibtracs/index.php?name=ib-v4-access>). IBTrACS provides global tropical cyclone best track data in a centralized location to aid our understanding of the distribution, frequency, and intensity of tropical cyclones worldwide. The World Meteorological Organization Tropical Cyclone Program has endorsed IBTrACS as an official archiving and distribution resource for tropical cyclone best track data. The data are available in many formats. We collected only the files in netcdf format. The WMO uses data from the WMO-sanctioned Regional Specialized Meteorological Centre (RSMC) / Tropical Cyclones Warning Centre (TCWC) in each basin. This data consolidates global tropical cyclone data at a central location, are available in a single file or subsets and is the most complete global set of historical tropical cyclones available. It includes data from 12 different agencies or historical databases.

Key limitations are the changing operational procedures and observing systems which have led to significant heterogeneity in the best track record but these weakly affect the last ten years of data which concern the present Atlas. In addition, storms may have conflicting data from multiple sources. We selected the data as described in 4. From the database, for each year, each basin and each named storm, we collected the 3 to 6-hourly time series of:

- storm center tracks,
- maximum sustained wind speed V_{max} ,
- radius of maximum wind (R_{max}),
- wind radii at 34, 50, and 64 kts in each geophysical storm quadrant (R_{34}, R_{50} ,

			<p style="text-align: right;">MAXSS ATBD ESA Contract 4000132954/20/I-NB Delivery D21, Version 1.0.0 Date 06/10/2021 Page 12</p>
---	--	--	--

and R64), as well as the storm translation speed (V_t) and track propagation direction.

As these tracks are available at varying sampling time (6 hourly, 3 hourly or others), all track locations and associated parameters (listed above) were interpolated to an hourly time step using a PCHIP (Piecewise Cubic Hermite Interpolating Polynomial) 1-D monotonic cubic interpolation.

3.1.2 Extra-Tropical Cyclones tracks

For Extra Tropical Cyclones (ETC), the Atlas relies on a suite of input products derived by the university of reading (Hoskins and Hodges, 2002 & 2005; Dacre et al. 2012; Roberts et al., 2014; Gramcianinov et al., 2020) from the fifth ECMWF model reanalysis (ERA5; Hersbach and Dee, 2016). The atmospheric variables used in this work are on a 210 km (1.88° at the equator, T63) horizontal grid with 1-hourly outputs. The cyclones are identified and tracked in the reanalysis using the TRACK program (Hodges, 1994; 1995; 1999) following the preprocessing steps described in Hoskins and Hodges (2002; 2005). The cyclonic features were identified using the relative vorticity, which is computed using the zonal and meridional wind components at 850 hPa in spherical coordinates to avoid latitudinal bias (Sinclair, 1997). Sinclair (1994) highlighted the benefit of using vorticity instead of mean sea level pressure (MSLP) for the detection of cyclones in mid-latitudes, where the surface pressure gradient can be strong so that cyclones appear without a closed isobar. For this reason, the use of vorticity allows the early identification of cyclones that would only be detected by MSLP when intensification occurs or they move to higher latitudes. The vorticity field contains many small scale structures, particularly at the high resolution, which can cause problems during the identification process and tracking on the synoptic scale. To prevent this issue and focus on synoptic scales, the vorticity was spectrally filtered by converting to the spectral representation and truncating to T42, tapering the spectral coefficients to smooth the data. Large-scale atmospheric features were also removed by setting zonal wavenumbers ≤ 5 to zero. Hoskins and Hodges (2002) and Gramcianinov et al., (2020) present more details about the filtering and tracking method. The cyclone track database is derived for winter and summer periods, covers 2010-2020 and both hemispheres and provides storm center at hourly time steps. It also includes vorticity tracks, MSLP, and maximum winds. For each season and hemisphere, there is 1 file including non-exhaustively:

- TRACK_ID (identifier number of the storm)
- FIRST_PT (start of track)
- NUM_PTS (number of samples in the track)
- index (identifier index of the storm) and for each storm track ID, the files include hourly time series of time
- longitude (longitude values are the actual tracked locations in the vorticity

			MAXSS ATBD ESA Contract 4000132954/20/I-NB Delivery D21, Version 1.0.0 Date 06/10/2021 Page 13
---	--	--	--

- max)
- latitude
- relative_vorticity
- air_pressure_at_sea_level (minimum pressure location are given as longitude_1 & latitude_1)
- wind_speed_925 (max wind speed at geopotential height 925mb) (maximum sws at 925mb height location are given as longitude_2 & latitude_2)
- wind_speed_10m (maximum sws at 10 m height location are given as longitude_3 & latitude_3)

3.1.3 Polar Lows tracks

For Polar Lows, the Atlas is based on the storm track database determined over the Nordic and Barents seas from the associated cloud signatures on satellite Thermal Infra-Red Imagery by Rojo et al. (2019), which is covering 2010-2019. Other PL track databases will be investigated in the next version of the ATBD to extend the PL database from other sources (e.g., STARS dataset <http://polarlow.met.no/stars-dat>, Noer et al., 2011; for Antarctica, www.sail.msk.ru/antarctica, Verezhenskaya et al, 2017).

3.2 Gridded EO data

3.2.1 Sea Surface Salinity data

3.2.1.1 Satellite SSS data

The Atlas uses as input the ESA Sea Surface Salinity Climate Change Initiative (CCI) products (Boutin et al., 2021). These are global, level 4, multi-sensor (SMOS, Aquarius and SMAP) Sea Surface Salinity maps covering the jan 2010- Sep 2020 period. We use the v03.21 dataset which is obtained at a spatial resolution of 50 km and a time resolution of 1 week. It has been spatially sampled on a 25 km EASE (Equal Area Scalable Earth) grid and 1 day of time sampling. In addition to salinity, information on errors are provided. For more information see the user guide and other product documentation available from the Sea Surface Salinity CCI web page:

<https://catalogue.ceda.ac.uk/uuid/fad2e982a59d44788eda09e3c67ed7d5>

Compared to the previous version of the data, version 3 SSS and associated uncertainties are more precise and cover a longer period (Jan 2010-sept 2020); version 3 SSS are provided closer to land than version 2 SSS, with a possible degraded quality. We can remove these additional near land data by using the lsc_qc flag.

			<p style="text-align: right;">MAXSS ATBD ESA Contract 4000132954/20/I-NB Delivery D21, Version 1.0.0 Date 06/10/2021 Page 14</p>
---	--	--	--

3.2.1.2 In Situ analysed SSS data

In situ 1/2° resolution monthly analyses of sea surface salinity generated from Argo profilers at 5 m depth by the In Situ Analysis System (Kolodziejczyk et al., 2017) are used to estimate pre-storm SSS properties. The In Situ Analysis System (ISAS) was developed to produce gridded fields of temperature and salinity that preserve as much as possible the time and space sampling capabilities of the Argo network of profiling floats. ISAS is based on Optimal Interpolation method. Since the first global re-analysis performed in 2009, the system has been extended to accommodate all types of vertical profile as well as time series. ISAS gridded fields are entirely based on in-situ measurements. The system aims at monitoring the time evolution of ocean properties for climatic studies and allowing easy computation of climate indices. Delayed Mode (D) profiles are used as much as possible and extra visual check is carried out. The ISAS procedure and products are described in Gaillard et al. (2016). We use the ISAS20_ARGO release which is interpolated on 187 standard depth levels between 0-5500 m depth and 0.5°x0.5° global horizontal grid. ISAS20 use the version 8 of ISAS and updated statistics to produce the monthly analysis (Monthly Climatology and annual STD computed from WOA18A5B7). ISAS20 gridded fields analyze the Argo and Deep-Argo temperature and salinity data alone between 2002-2020. We used the most recent dataset update ISAS-20.

3.2.2 Sea Surface Temperature

3.2.2.1 Satellite SST data

The Atlas is currently using the two following satellite SST analyses:

3.2.2.1.1 *GHRSSST Level 4 MW_IR_OI Global Foundation Sea Surface Temperature analysis version 5.0 from REMSS*

A Group for High Resolution Sea Surface Temperature (GHRSSST) global Level 4 sea surface temperature analysis produced daily on a 0.09-degree grid at Remote Sensing Systems is used as input to the storm Atlas. This product uses optimal interpolation (OI) from both microwave (MW) sensors including the Global Precipitation Measurement (GPM) Microwave Imager (GMI), the Tropical Rainfall Measuring Mission (TRMM) Microwave Imager (TMI), the NASA Advanced Microwave Scanning Radiometer-EOS (AMSRE), the Advanced Microwave Scanning Radiometer 2 (AMSR2) onboard the GCOM-W1 satellite, and WindSat operates on the Coriolis satellite, and infrared (IR) sensors such as the Moderate Resolution Imaging Spectroradiometer (MODIS) on the NASA Aqua and Terra platform and the Visible Infrared Imaging Radiometer Suite (VIIRS) on board the Suomi-NPP satellite. The through-cloud capabilities of microwave radiometers provide a valuable picture of global sea surface temperature (SST) while infrared radiometers (i.e., MODIS) have a higher spatial resolution. This analysis does not use any in situ SST data such as drifting buoy SST. Comparing with previous version 4.0

			MAXSS ATBD ESA Contract 4000132954/20/I-NB Delivery D21, Version 1.0.0 Date 06/10/2021 Page 15
---	--	--	--

dataset, the version 5.0 has made the updates in several areas, including the diurnal warming model, the sensor-specific error statistics (SSES) for each microwave sensor, the sensor correlation model, and the quality mask.

3.2.2.1.2 *ESA Climate Change Initiative (CCI) v2.1 SST Level 4 Analysis*

The Atlas uses as input the ESA Climate Change Initiative (CCI) v2.1 SST Level 4 Analysis Climate Data Record (CDR), which provides a globally-complete daily analysis of **sea surface temperature (SST)** on a 0.05 degree regular latitude - longitude grid (Good et al., 2020). It combines data from both the Advanced Very High Resolution Radiometer (AVHRR) and Along Track Scanning Radiometer (ATSR) SST Climate Data Records, using a data assimilation method to provide SSTs where there were no measurements. These data cover the 2010-2016 period of the Atlas. The data provide independently quantified SSTs to a quality suitable for climate research. The 0.05°x0.05° pixel SSTs median uncertainty is 0.18 K (Merchant et al., 2019). SSTs derived from IR radiances are sensitive to the variation in temperature of the skin layer of the ocean (depth of few microns). Note that the L4 CCI SST product is derived from the IR SSTs that are adjusted to 20 cm depth and to a local time representative of the daily average SST. For the period 2016-2020, we use the same product from C3S (<https://cds.climate.copernicus.eu/cdsapp#!/dataset/satellite-sea-surface-temperature?tab=overview>).

3.2.2.2 **In Situ analyzed SST data**

In situ 1/2° resolution monthly analyses of sea surface temperature generated from Argo profilers at 5 m depth by the In Situ Analysis System (Kolodziejczyk et al., 2017) are used to estimate pre-storm SST properties.

3.2.3 **Sea Level Anomalies**

The SEALEVEL_GLO_PHY_L4_MY_008_047 data are used as input to the storm Atlas: it is a satellite global sea level product downloaded from the Copernicus Marine Environment Monitoring Service ([CMEMS](#)). Altimeter satellite gridded Sea Level Anomalies (SLA) computed with respect to a twenty-year **2012** mean. The SLA is estimated by Optimal Interpolation, merging the measurement from the different altimeter missions available. The product gives additional variables (i.e. Absolute Dynamic Topography and geostrophic currents (absolute and anomalies)). This product is processed by the DUACS multi-mission altimeter data processing system. It serves in near-real time the main operational oceanography and climate forecasting centers in Europe and worldwide. It processes data from all altimeter missions: Jason-3, Sentinel-3A, HY-2A,

			<p style="text-align: right;">MAXSS ATBD ESA Contract 4000132954/20/I-NB Delivery D21, Version 1.0.0 Date 06/10/2021 Page 16</p>
---	--	--	--

Saral/AltiKa, Cryosat-2, Jason-2, Jason-1, T/P, ENVISAT, GFO, ERS1/2. It provides a consistent and homogeneous catalogue of products for varied applications, both for near real time applications and offline studies. To produce maps of Sea Level Anomalies (SLA) and Absolute Dynamic Topography (ADT) in delayed-time (REPROCESSED), the system uses the along-track altimeter missions from products called SEALEVEL_*PHY_L3_MY_008*. Finally an Optimal Interpolation is made merging all the flying satellites in order to compute gridded SLA and ADT. The geostrophic currents are derived from sla (geostrophic velocities anomalies, ugos and vgos variables) and from adt (absolute geostrophic velocities, ugos and vgos variables).

3.2.4 Ocean Color products

The ocean color data of the storm Atlas are estimated based on the input Ocean-Colour ESA Climate Change Initiative (OC_CCI) version 5 L3S products which are global, level 3, binned multi-sensor time-series of satellite ocean-colour data with a particular focus for use in climate studies (Sathyendranath et al., 2021). The approach that was adopted for generating the ocean-colour time series for climate studies (Sathyendranath et al., 2019) is using data from the MERIS (MEdium spectral Resolution Imaging Spectrometer) sensor of the European Space Agency; the SeaWiFS (Sea-viewing Wide-Field-of-view Sensor) and MODIS-Aqua (Moderate-resolution Imaging Spectroradiometer-Aqua) sensors from the National Aeronautics and Space Administration (USA); and VIIRS (Visible and Infrared Imaging Radiometer Suite) from the National Oceanic and Atmospheric Administration (USA). The time series covers the period from late 1997 to end of 2018. Taking the user requirements into account, a series of objective criteria were established, against which available algorithms for processing ocean-colour data were evaluated and ranked. The algorithms that performed best with respect to the climate user requirements were selected to process data from the satellite sensors. The dataset (v5.0) is created by band-shifting and bias-correcting SeaWiFS, MODIS, VIIRS and OLCI data to match MERIS data, merging the datasets and computing per-pixel uncertainty estimates. Overlapping data were used to correct for mean biases between sensors at every pixel. The remote-sensing reflectance data derived from the sensors were merged, and the selected in-water algorithm was applied to the merged data to generate maps of chlorophyll concentration, inherent optical properties at SeaWiFS wavelengths, and the diffuse attenuation coefficient at 490 nm. The merged products were validated against in situ observations. The uncertainties established on the basis of comparisons with in situ data were combined with an optical classification of the remote-sensing reflectance data using a fuzzy-logic approach, and were used to generate uncertainties (root mean square difference and bias) for each product at each pixel. We used the following variables in the L3S products:

- phytoplankton chlorophyll-a concentration;
- absorption coefficients for dissolved and detrital material, and,

			<p style="text-align: right;">MAXSS ATBD ESA Contract 4000132954/20/I-NB Delivery D21, Version 1.0.0 Date 06/10/2021 Page 17</p>
---	--	--	--

- the diffuse attenuation coefficient for downwelling irradiance for light of wavelength 490 nm.

This dataset contains all their Version 5.0 generated ocean colour products on a geographic projection at 4 km spatial resolution and for the storm Atlas, we used the daily composites covering the period 2010 - 2020.

3.2.5 Atmospheric data

3.2.5.1 Multi-satellite Precipitation Analysis (TMPA)

Rain rate data from the Tropical Rainfall Measuring Mission (TRMM) Multi-satellite Precipitation Analysis (TMPA) (TRMM multi-satellite precipitation analysis) over the period 2010-2020 is used here to estimate accumulated rainfall under storms. Specifically, we used the research quality dataset, labeled TRMM3B42 (V.7), which provides precipitation estimates at 3-hourly resolution on a $0.25^\circ \times 0.25^\circ$ grid. This product depends on input from two different types of sensors, namely microwave and IR [Huffman et al., 2007]. This product has already been used in numerous studies to estimate rainfall under TCs, e.g., see works presented in Lonfat et al., (2004); Jiang and Zisper (2010), Jiang et al., (2011); Hu and Meehl (2009), Prat and Nelson (2013 a&b), Jourdain et al. (2013) or Chen and Fu (2015). TRMM3B42 is a blended product whose error characteristics are difficult to quantify and have changed with time with the increasing availability of microwave observations (Venugopal and Wallace, 2016). Chen et al., (2013) have compared TC rainfall from TRMM3B42 product to an ensemble of gauge records in close to oceanic conditions (e.g., with gauges installed on small islands or atolls). They have estimated that 3B42 overestimates TC rainfall by 14% particularly in the presence of orographic effects. TMPA nevertheless shows reasonable skill in detecting tropical cyclone rainfall with superior performances to detect heavy rain events over the ocean than over coastal and island sites. There are very few rain gauge observations over the ocean: the TRMM3B42 data thus provide a good source of temporally and spatially varying information for analysis of TC rainfall variations.

Note that on October 07, 2014, routine production ended for the TRMM Precipitation Radar (PR) precipitation estimates. Since PR is no longer available, the TMI/PR combined instrument (TCI) estimates are also no longer available. As products 3B42 use the TCI estimates as the satellite calibrator, September 2014 is the last month these products were produced in this way. In an effort to continue 3B42/3B43 available and usable, TMPA climatological calibrations/adjustments have been adapted for use in the 3B42 [Bolvin and Huffman, 2015]. October 2014 is the first month of the climatologically calibrated/adjusted 3B42/3B43: there is therefore a possible discontinuity in the record as a result. TRMM has recently been succeeded by the Global Precipitation Measurement mission (GPM) for which there exists a 30mn $0.1^\circ \times 0.1^\circ$ resolution blended product [IMERG; Huffman et al., 2015]. Note that the TMPA products are limited to a latitudinal

band [50°S-50°N]

3.2.5.2 ERA5 Total Precipitation, Evaporation, and wind component data

ERA5 provides hourly estimates of a large number of atmospheric, land and oceanic climate variables. The data cover the Earth on a 30km grid and resolve the atmosphere using 137 levels from the surface up to a height of 80km. ERA5 includes information about uncertainties for all variables at reduced spatial and temporal resolutions.

We extracted the following atmospheric variables from ERA5 hourly data on single levels from 1979 to present (<https://cds.climate.copernicus.eu/cdsapp#!/dataset/reanalysis-era5-single-levels?tab=overview>) :

Evaporation	m of water equivalent	This parameter is the accumulated amount of water that has evaporated from the Earth's surface, including a simplified representation of transpiration (from vegetation), into vapour in the air above. This parameter is accumulated over a particular time period which depends on the data extracted. For the reanalysis, the accumulation period is over the 1 hour ending at the validity date and time. For the ensemble members, ensemble mean and ensemble spread, the accumulation period is over the 3 hours ending at the validity date and time. The ECMWF Integrated Forecasting System (IFS) convention is that downward fluxes are positive. Therefore, negative values indicate evaporation and positive values indicate condensation.
Total precipitation	m	This parameter is the accumulated liquid and frozen water, comprising rain and snow, that falls to the Earth's surface. It is the sum of large-scale precipitation and convective precipitation. Large-scale precipitation is generated by the cloud scheme in the ECMWF Integrated Forecasting System (IFS). The cloud scheme represents the formation and dissipation of clouds and large-scale precipitation due to changes in atmospheric quantities (such as pressure, temperature and moisture) predicted directly by the IFS at spatial scales of the grid box or larger. Convective precipitation is generated by the convection scheme in the IFS, which represents convection at spatial scales smaller than the grid box. This parameter does not include fog, dew or the precipitation that evaporates in the atmosphere before

		<p>it lands at the surface of the Earth. This parameter is accumulated over a particular time period which depends on the data extracted. For the reanalysis, the accumulation period is over the 1 hour ending at the validity date and time. For the ensemble members, ensemble mean and ensemble spread, the accumulation period is over the 3 hours ending at the validity date and time. The units of this parameter are depth in metres of water equivalent. It is the depth the water would have if it were spread evenly over the grid box. Care should be taken when comparing model parameters with observations, because observations are often local to a particular point in space and time, rather than representing averages over a model grid box.</p>
--	--	--

We also extracted the following atmospheric variables from “ERA5 hourly data on pressure levels from 1979 to present” at:

<https://cds.climate.copernicus.eu/cdsapp#!/dataset/reanalysis-era5-pressure-levels?tab=overview>

U-component of wind	m s ⁻¹	This parameter is the eastward component of the wind. It is the horizontal speed of air moving towards the east. A negative sign indicates air moving towards the west. This parameter can be combined with the V component of wind to give the speed and direction of the horizontal wind.
V-component of wind	m s ⁻¹	This parameter is the northward component of the wind. It is the horizontal speed of air moving towards the north. A negative sign indicates air moving towards the south. This parameter can be combined with the U component of wind to give the speed and direction of the horizontal wind.

The wind component data were only extracted at levels of 200 mb and 800 mb in order to evaluate the large-scale vertical wind-shear vector data.

All ERA5 data were downloaded from the Copernicus Climate Change Service (C3S) (2017): ERA5: Fifth generation of ECMWF atmospheric reanalyses of the global climate . Copernicus Climate Change Service Climate Data Store (CDS), date of access.

			<p style="text-align: right;">MAXSS ATBD ESA Contract 4000132954/20/I-NB Delivery D21, Version 1.0.0 Date 06/10/2021 Page 20</p>
---	--	--	--

<https://cds.climate.copernicus.eu/cdsapp#!/home>

3.2.5.3 Surface Wind Vector

We use as input to the storm Atlas the MAXSS blended Level 4 preliminary product version which gives hourly surface wind speed and direction on a 0.25°x0.25° rectangular lat/lon grid.

3.2.6 In Situ Analyzed Ocean Salinity and Temperature profiles

In situ 1/2° resolution monthly analyses are used to estimate pre-storm sub-surface properties. Vertical salinity S , temperature T , and density ρ are interpolated bi-linearly in time and space from the monthly ISAS fields. We use the ISAS20_ARGO release which is interpolated on 187 standard depth levels between 0-5500 m depth and 0.5°x0.5° global horizontal grid. ISAS20 use the version 8 of ISAS and updated statistics to produce the monthly analysis (Monthly Climatology and annual STD computed from WOA18A5B7). ISAS20 gridded fields analyze the Argo and Deep-Argo temperature and salinity data alone between 2002-2020. We used the most recent dataset update ISAS-20.

3.3 Along-track / Swath Observations

3.3.1 sea surface heights anomalies

To characterize the sea surface heights anomalies (SLA) changes within the storms, we used the reprocessed Altimeter satellite along-track sea surface heights anomalies (SLA) computed with respect to a twenty-year 2012 mean and made available by CMEMS¹. All the missions are homogenized with respect to a reference mission. The product gives additional variables (e.g. Absolute Dynamic Topography, ADT) that can be used to change the physical content for specific needs. This product is processed by the DUACS multi-mission altimeter data processing system. It serves in near-real time the main operational oceanography and climate forecasting centers in Europe and worldwide. It processes data from all altimeter missions: Jason-3, Sentinel-3A/B, HY-2A, Saral/AltiKa, Cryosat-2, Jason-2, Jason-1, T/P, ENVISAT, GFO, ERS1/2. It provides a consistent and homogeneous catalogue of products for varied applications, both for near real time applications and offline studies. To produce SLA in delayed-time (REPROCESSED), the system uses the Geophysical Data Records which are computed from a Precise Orbit Ephemeris (POE) and are delivered within 3 months depending on the mission. Reanalysis

¹https://resources.marine.copernicus.eu/product-detail/SEALEVEL_GLO_PHY_L3_MY_008_062/INFORMATION

			<p style="text-align: right;">MAXSS ATBD ESA Contract 4000132954/20/I-NB Delivery D21, Version 1.0.0 Date 06/10/2021 Page 21</p>
---	--	--	--

products are more precise than NRT products. The system acquires and then synchronizes altimeter data and auxiliary data; each mission is homogenized using the same models and corrections. The Input Data Quality Control checks that the system uses the best altimeter data. The multi-mission cross-calibration process removes any residual orbit error, or long wavelength error (LWE), as well as large scale biases and discrepancies between various data flows; all altimeter fields are interpolated at crossover locations and dates. After a repeat-track analysis, a mean profile, which is peculiar to each mission, or a Mean Sea Surface (MSS) (when the orbit is non repetitive) is subtracted to compute sea level anomaly. The MSS is available via the Aviso+ dissemination². Data are then cross validated, filtered from residual noise and small scale signals (sla_filtered variable). The ADT (Absolute Dynamic Topography, adt_filtered variable) is then computed as follows:

$$\text{adt_filtered} = \text{sla_filtered} + \text{MDT}$$

where MDT is the Mean Dynamic Topography distributed by Aviso+³.

3.3.2 Sea State

The ESA Sea State Climate Change Initiative (CCI) project has produced global multi-sensor time-series of along-track satellite altimeter significant wave height data (referred to as Level 2P (L2P) data) with a particular focus for use in climate studies. This dataset contains the Version 3 Remote Sensing Significant Wave Height product, along-track at approximately 6 km spatial resolution, separated per satellite and pass, including all measurements with flags, corrections and extra parameters from other sources. These are expert products with rich content and no data loss. The altimeter data used in the Sea State CCI dataset come from multiple satellite missions spanning from 1991 to 2018 (ERS-1, ERS-2, Topex, Envisat, GFO, CryoSat-2, Jason-1, Jason-2, Jason-3, SARAL, Sentinel-3 A), from which we used over the 2010-2020 time frame only the followings: Envisat, CryoSat-2, Jason-1, Jason-2, Jason-3, SARAL, Sentinel-3 A. Many altimeters are bi-frequency (Ku-C or Ku-S) and only measurements in the Ku band were used, for consistency reasons, being available on each altimeter but SARAL (Ka band).

In addition we used SAR Wave Mode SWH observations from the CCI Sea State version 3 dataset for Envisat, Sentinel-1 A and Sentinel-1 B.

These products⁴ are used as input to the storm Atlas.

²<http://www.aviso.altimetry.fr/en/data/products/auxiliary-products/mss.html>

³<http://www.aviso.altimetry.fr/en/data/products/auxiliary-products/mdt.html>

⁴<https://catalogue.ceda.ac.uk/uuid/f91cd3ee7b6243d5b7d41b9beaf397e1>

3.3.3 Surface Wind Speed from Individual Sensors

Individual measurements from Scatterometers and Radiometers (see list in the tables below) were re-calibrated by the project using SFMR data and are used as inputs to the Storm Atlas.

Scatterometers	Format	Period	Source	Frequency
ASCAT-A	NetCDF-4	Full period	ICM	C-band
ASCAT-B	NetCDF-4	11/2012 – 12/2020	ICM	C-band
ASCAT-C	NetCDF-4	01/2019 – 12/2020	ICM	C-band
OceanSat-2	NetCDF-4	01/2010 - 02/2014	ICM	Ku-band
RapidScat	NetCDF-4	11/2014 - 08/2016	ICM	Ku-band
Scatsat-1	NetCDF-4	01/2017 – 12/2020	ICM	Ku-band
HY-2A	NetCDF-4	02/2012 - 04/2015	ICM	Ku-band
HY-2B	NetCDF-4	01/2019 – 12/2020	ICM	Ku-band
HY-2C		11/2020 – 12/2020		Ku-band
CFOSAT		01/2019 – 12/2020		Ku-band

Radiometers	Format	Period	Source	Frequency
SMOS	NetCDF-4	01/2010 – 12/2020	ICM	L-band
SMAP	NetCDF-4	04/2015 – 12/2020	ICM	L-band

WindSat	NetCDF-4	01/2003 12/2020	–	ICM	Channels (GHz): 6.8; 10.7; 18.7; 23.8; 37.0
AMSR2	NetCDF-4	07/2012 12/2020	–	ICM	Channels (GHz): 6.93; 7.3; 10.65; 18.7; 23.8; 36.5; 89.0
SSMI / SSMIS	Bytemap	Full period		REMSS	Channels (GHz): 19.35; 23.235; 37.0; 85.5
GMI	Bytemap	03/2014 12/2020	–	REMSS	Channels (GHz): 10.65; 18.7; 23.8; 36.5; 89.0; 165.5; 183.31
TMI	Bytemap	01/2010 12/2014	–	REMSS	Channels (GHz): 10.65; 19.35; 21.3; 37.0; 85.5
AMSRE	Bytemap	01/2010 10/2011	–	REMSS	Channels (GHz): 6.93; 10.65; 18.7; 23.8; 36.5; 89.0

4 STORM ATLAS GENERATION: STEP1: STORM TRACK PRE-SELECTION

Methodology: Step 1 Track pre-selection

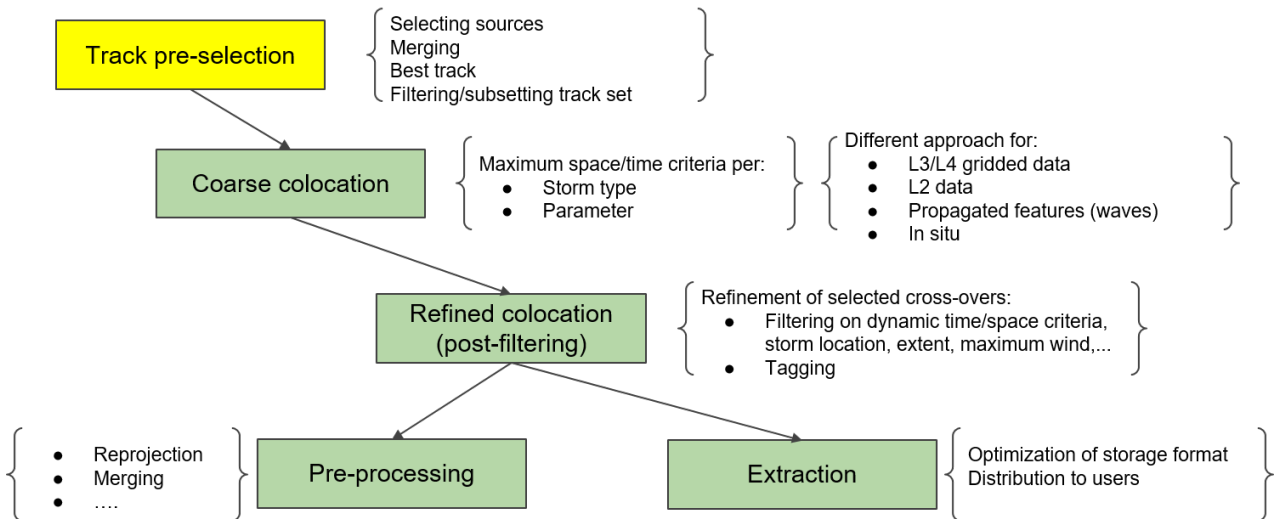


Figure 2: Atlas building algorithm Step 1: The storm Track pre-selection

As illustrated in Figure 2, the first step to build the Storm Atlas consists in selecting the sources for the storm tracks, merging them into consistent and complete storm track databases over 2010-2020 for each storm basin, seasons and type of storms, interpolated to the hour when necessary. The consolidated storm tracks are made available as a separate product, but also included within each extracted observation product.

The approaches used to pre-select tropical Cyclones, Extra-tropical Cyclones, and polar lows are described successively in the following subsections.

4.1 Tropical Cyclones tracks

Best track data in IBTrACS has many source agencies and datasets. IBTrACS makes every effort to provide data exactly as it was provided by the agency (or source data). To select the source for each storm track in each basin, we performed analyses of the number of tracks per sources and basin and the duration of the tracks. As found for all basins (see Figure 3), USA is the most comprehensive source (global) although there are significant missing number of tracks in the Indian Ocean compared to other sources (40% missing compared to New Delhi and 20% missing compared to the one from the Australian Bureau

of Meteorology). However, there are few missing tracks in USA compared to others.

	usa	tokyo	hko	newdelhi	reunion	bom	nadi	wellington	ds824	td9636	td9635	neumann	mlc
usa	0	827	810	1018	990	993	1019	1037	1075	1075	1075	1075	1075
tokyo	4	0	0	250	252	252	252	252	252	252	252	252	252
hko	7	20	0	269	272	272	272	272	272	272	272	272	272
newdelhi	40	95	94	0	97	97	97	97	97	97	97	97	97
reunion	5	90	90	90	0	81	90	90	90	90	90	90	90
bom	20	102	102	102	93	0	92	92	102	102	102	102	102
nadi	0	56	56	56	56	46	0	19	56	56	56	56	56
wellington	6	44	44	44	44	34	7	0	44	44	44	44	44
ds824	0	0	0	0	0	0	0	0	0	0	0	0	0
td9636	0	0	0	0	0	0	0	0	0	0	0	0	0
td9635	0	0	0	0	0	0	0	0	0	0	0	0	0
neumann	0	0	0	0	0	0	0	0	0	0	0	0	0
mlc	0	0	0	0	0	0	0	0	0	0	0	0	0

usa_lat	1075
tokyo_lat	252
hko_lat	272
newdelhi_lat	97
reunion_lat	90
bom_lat	102
nadi_lat	56
wellington_lat	44
ds824_lat	0
td9636_lat	0
td9635_lat	0
neumann_lat	0
mlc_lat	0
lon	1154
time	1154
lat	1154

total number of tracks
per center

Figure 3: for each WMO RSMC centre (column), the left table is showing the number of missed tracks with respect to other centers (lines) over 2010-2020. The total number of tracks per center over the period is shown in the right table.

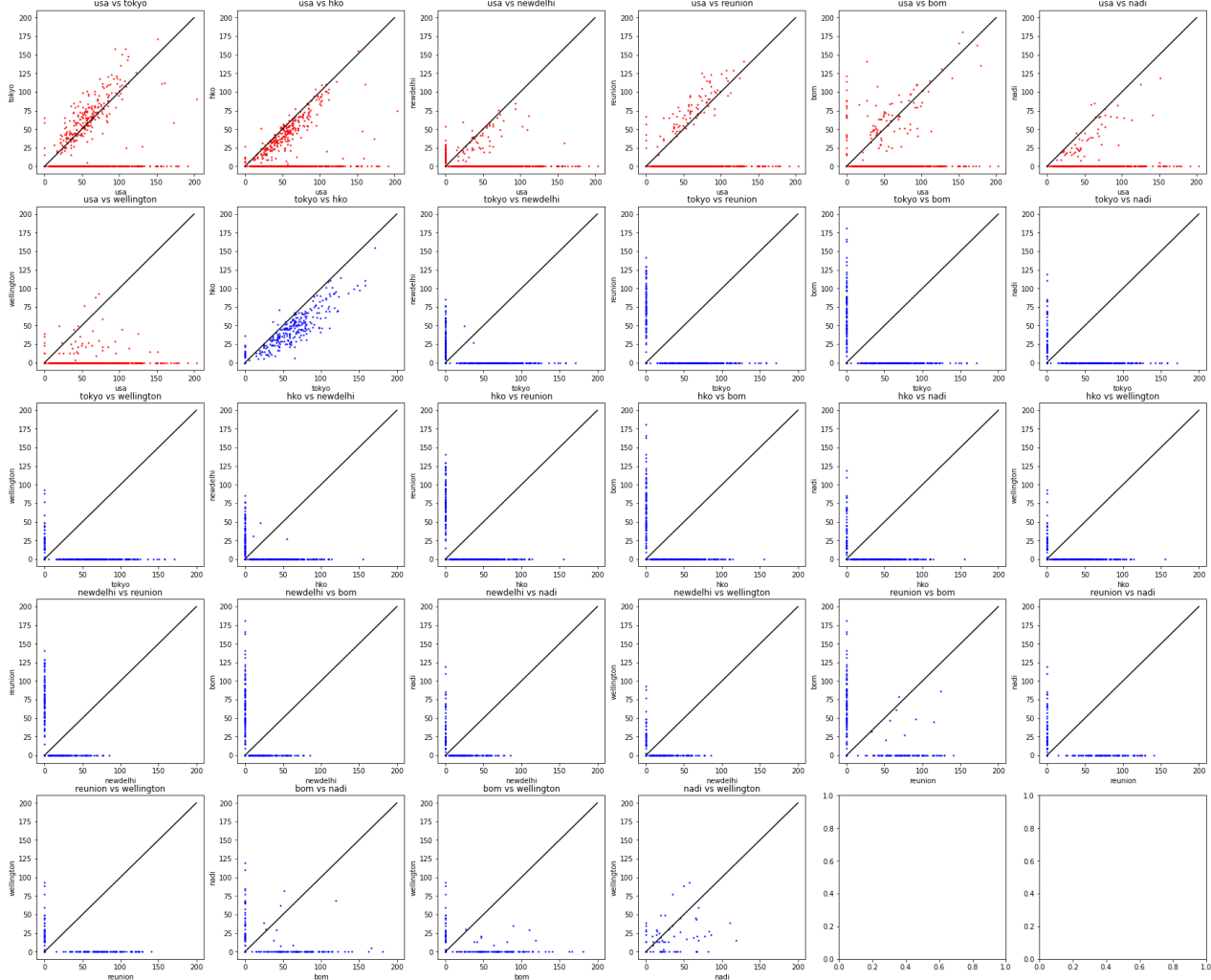


Figure 4: duration (in time steps) of the TC tracks of one center with respect the others (see title in each panel).

As shown in Figure 4, the main overlap for the number of tracks is between USA and others, then between JMA and HKO. USA (in red in the figure) is the source for which the tracks duration is generally the longer, except for JMA & Reunion. While this is indicative at global scale, the selection of the track source have been conducted specifically for each basin. We first selected the source with the higher number of tracks for each basin and completed with the missing tracks from other sources. If a track is found in several sources, the longer track duration is selected in priority.

4.1.1.1 Source selection for East Pacific basin

For the East Pacific basin, USA is only missing 31 tracks from JMA (“tokyo” in above

table) but JMA is missing 226 tracks from USA. The additional 31 JMA tracks are however less than 3 time steps: there is therefore no benefit in using JMA in addition to USA. The final source selected for the East Pacific TC tracks is therefore defined as : USA only and the 261 TC tracks are shown in Figure 5.

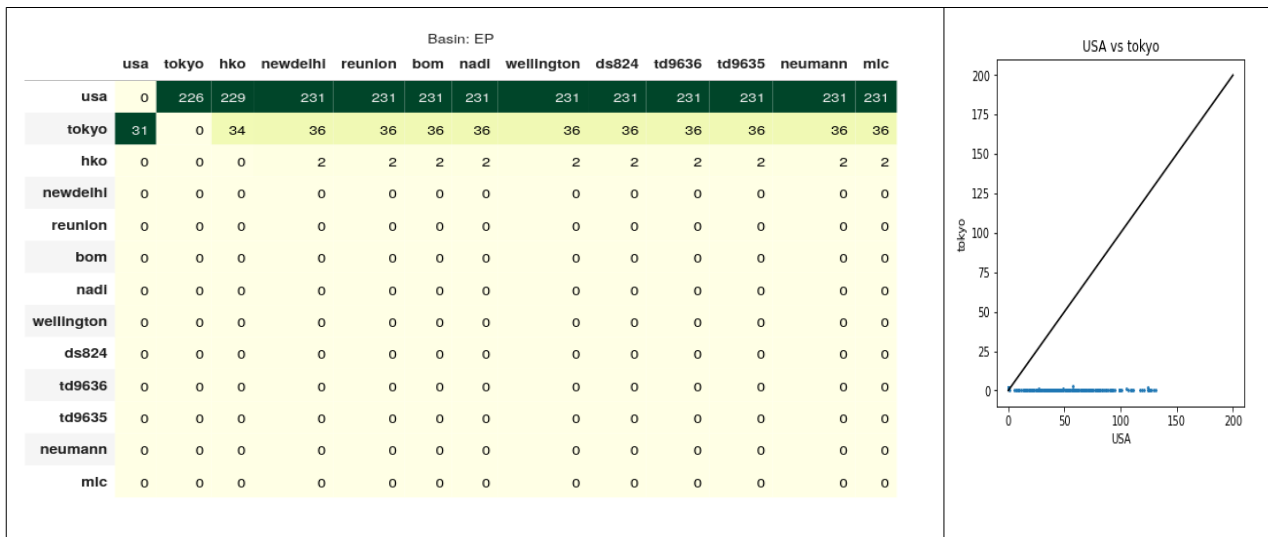


Figure 5: (Left) number of missed tracks with respect to other centers (lines) for each WMO RSMC center (column), over 2010-2020 and for the East Pacific. (Right) : duration (in time steps) of the TC tracks of JMA center with respect USA.

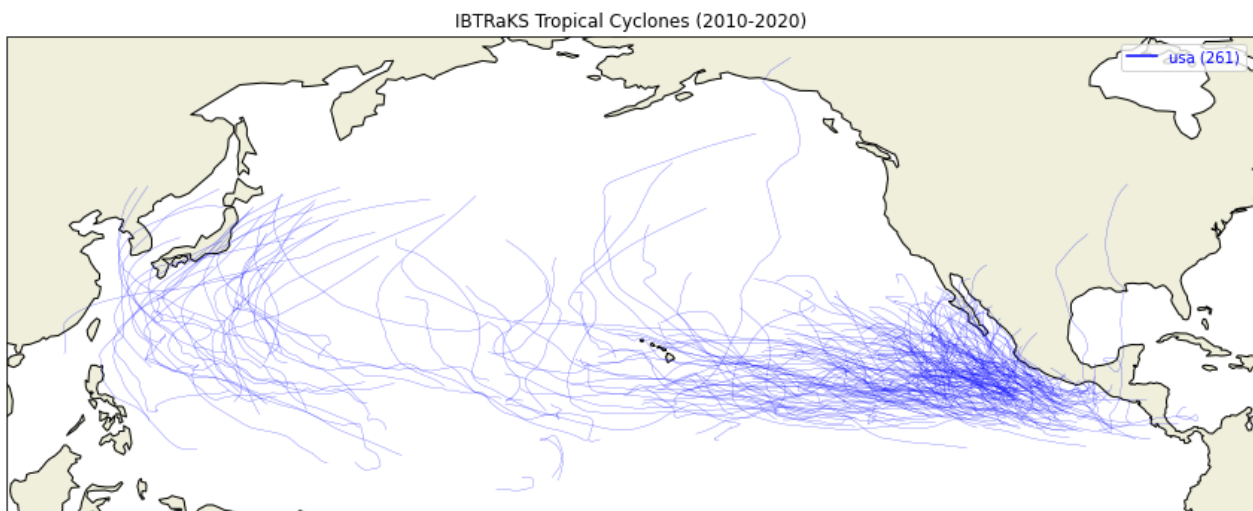


Figure 6: map of the TC tracks selected from the IBTRACS's USA source for the East Pacific over 2010-2020

4.1.1.2 Source selection for North Atlantic basin

As illustrated in Figure 7, North-Atlantic is only covered by USA source. The final source selected for the North Atlantic TC tracks is therefore defined as : USA only and the 200 TC tracks from that source over 2010-2020 are shown in Figure 8.

	usa	tokyo	hko	newdelhi	reunion	bom	nadi	wellington	ds824	td9636	td9635	neumann	mlc
usa	0	200	200	200	200	200	200	200	200	200	200	200	200
tokyo	0	0	0	0	0	0	0	0	0	0	0	0	0
hko	0	0	0	0	0	0	0	0	0	0	0	0	0
newdelhi	0	0	0	0	0	0	0	0	0	0	0	0	0
reunion	0	0	0	0	0	0	0	0	0	0	0	0	0
bom	0	0	0	0	0	0	0	0	0	0	0	0	0
nadi	0	0	0	0	0	0	0	0	0	0	0	0	0
wellington	0	0	0	0	0	0	0	0	0	0	0	0	0
ds824	0	0	0	0	0	0	0	0	0	0	0	0	0
td9636	0	0	0	0	0	0	0	0	0	0	0	0	0
td9635	0	0	0	0	0	0	0	0	0	0	0	0	0
neumann	0	0	0	0	0	0	0	0	0	0	0	0	0
mlc	0	0	0	0	0	0	0	0	0	0	0	0	0

Figure 7: number of missed tracks with respect to other centers (lines) for each WMO RSMC centre (column), over 2010-2020 and for the North Atlantic.

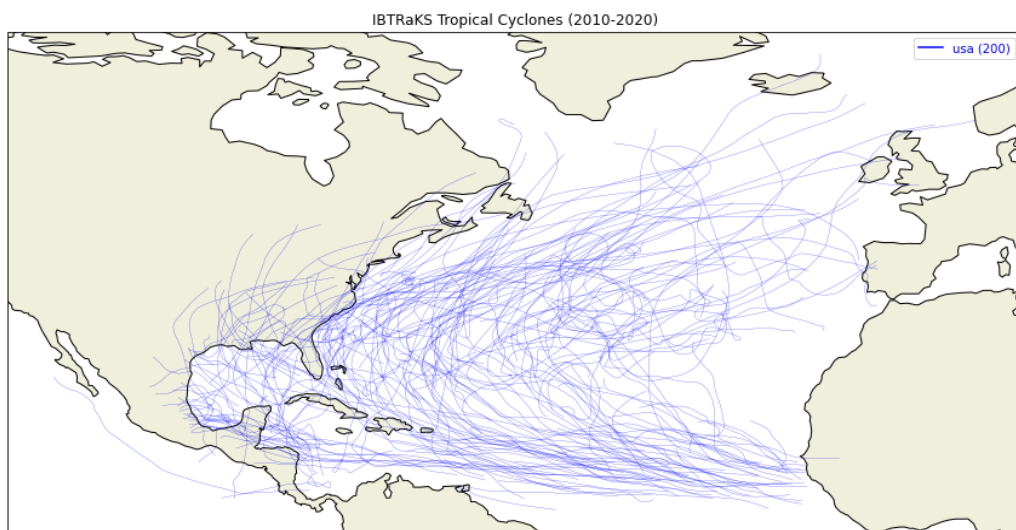


Figure 8: map of the TC tracks selected from the IBTRACS's USA source for the North Atlantic over 2010-2020

4.1.1.3 Source selection for North Indian basin

USA is missing 40 tracks from New Delhi and New Delhi is missing only 6 tracks from USA. However, when tracks are found in both sources, USA tracks are longer in time and the later is therefore selected as the preferred source. The final sources selected for the North Indian TC tracks is therefore defined as : USA \cup New Delhi (with priority: USA when available in both sources). The final TC tracks (64 from USA and 40 from New Delhi) over 2010-2020 are shown in Figure 11.

Basin: NI

	usa	tokyo	hko	newdelhi	reunion	bom	nadi	wellington	ds824	td9636	td9635	neumann	mlc
usa	0	62	62	6	63	63	63	63	63	63	63	63	63
tokyo	1	0	1	1	2	2	2	2	2	2	2	2	2
hko	0	0	0	0	1	1	1	1	1	1	1	1	1
newdelhi	40	96	96	0	97	97	97	97	97	97	97	97	97
reunion	0	0	0	0	0	0	0	0	0	0	0	0	0
bom	0	0	0	0	0	0	0	0	0	0	0	0	0
nadi	0	0	0	0	0	0	0	0	0	0	0	0	0
wellington	0	0	0	0	0	0	0	0	0	0	0	0	0
ds824	0	0	0	0	0	0	0	0	0	0	0	0	0
td9636	0	0	0	0	0	0	0	0	0	0	0	0	0
td9635	0	0	0	0	0	0	0	0	0	0	0	0	0
neumann	0	0	0	0	0	0	0	0	0	0	0	0	0
mlc	0	0	0	0	0	0	0	0	0	0	0	0	0

Figure 9: number of missed tracks from each WMO RSMC centre (column) with respect to other centers (lines), over 2010-2020 and for the North Indian basin.

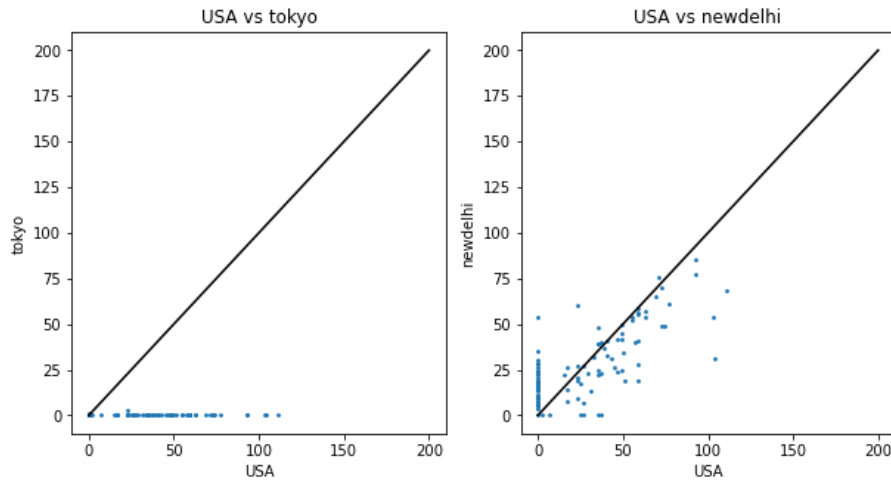


Figure 10: duration (in time steps) of the TC tracks of JMA center with respect USA (bottom left) and of New Delhi center with respect USA (bottom Right).

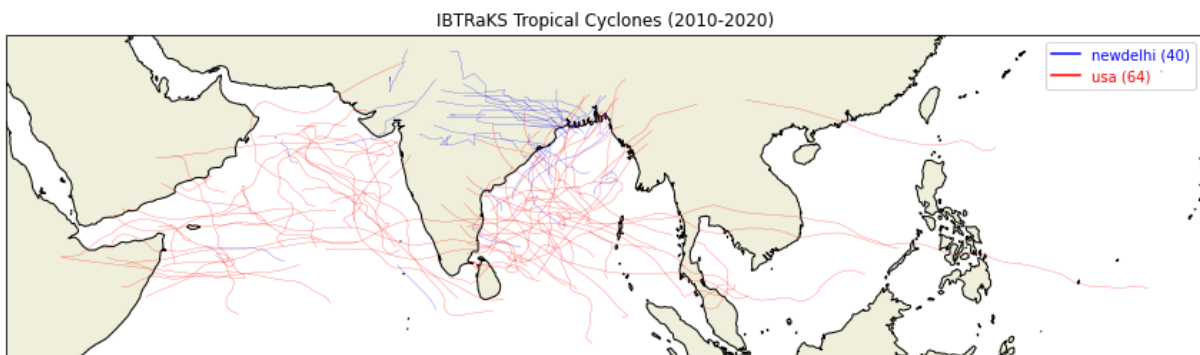


Figure 11: map of the TC tracks selected from the IBTrACS's USA \cup New Delhi sources for the North Indian basin over 2010-2020

4.1.1.4 Source selection for South Indian basin

USA is only missing 5 tracks from Reunion and 16 from BoM, each of them missing many more from USA. The selection is therefore USA \cup BoM \cup Reunion (for consistency with other basins - USA first - and to have radii wherever possible). The final TC tracks (165 from USA, 15 from BoM and 5 from La Réunion) over 2010-2020 are shown in Figure 14.

Basin: SI

	usa	tokyo	hko	newdelhi	reunion	bom	nadi	wellington	ds824	td9636	td9635	neumann	mlc
usa	0	176	176	176	91	123	176	176	176	176	176	176	176
tokyo	0	0	0	0	0	0	0	0	0	0	0	0	0
hko	0	0	0	0	0	0	0	0	0	0	0	0	0
newdelhi	0	0	0	0	0	0	0	0	0	0	0	0	0
reunion	5	90	90	90	0	81	90	90	90	90	90	90	90
bom	16	69	69	69	60	0	69	69	69	69	69	69	69
nadi	0	0	0	0	0	0	0	0	0	0	0	0	0
wellington	0	0	0	0	0	0	0	0	0	0	0	0	0
ds824	0	0	0	0	0	0	0	0	0	0	0	0	0
td9636	0	0	0	0	0	0	0	0	0	0	0	0	0
td9635	0	0	0	0	0	0	0	0	0	0	0	0	0
neumann	0	0	0	0	0	0	0	0	0	0	0	0	0
mlc	0	0	0	0	0	0	0	0	0	0	0	0	0

Figure 12: number of missed tracks from each WMO RSMC centre (column) with respect to other centers (lines), over 2010-2020 and for the South Indian basin.

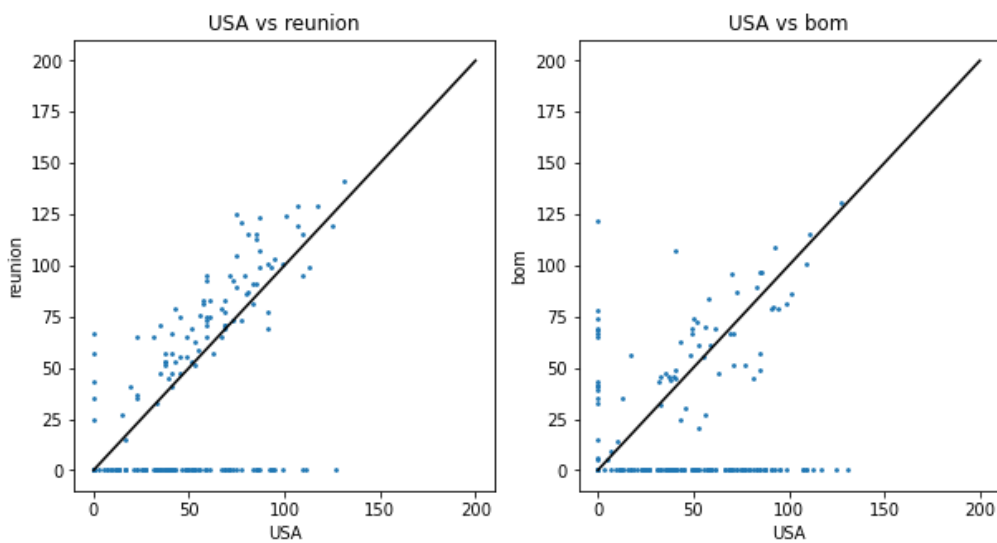


Figure 13: duration (in time steps) of the TC tracks of La Réunion center with respect USA (left) and of BoM center with respect USA (bottom Right) for the South Indian Basin.

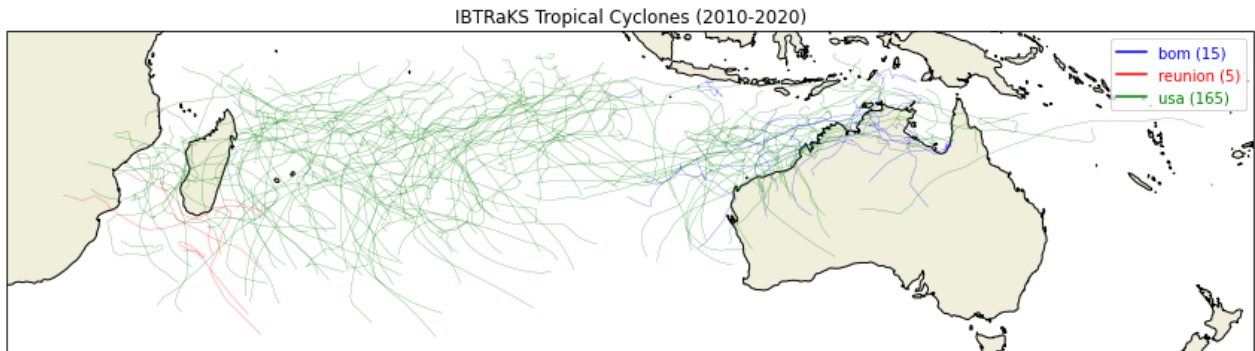


Figure 14: map of the TC tracks selected from the IBTRACS's USA \cup BoM \cup Reunion sources for the South Indian basin over 2010-2020.

4.1.1.5 Source selection for West Pacific basin

In the West Pacific, USA is only missing 5 tracks from JMA and 8 from HKO, each of them missing many more from USA (78 and 61). JMA (Tokyo) tracks are longer than USA and HKO are shorter than USA.

The final sources selected for West Pacific TC tracks is therefore defined as : USA \cup JMA \cup HKO (for consistency with other basins - USA first - and to have radii wherever possible). The final TC tracks (325 from USA, 3 from JMA and 4 from HKO) over 2010-2020 are shown in Figure 17.

Basin: WP

	usa	tokyo	hko	newdelhi	reunion	bom	nadi	wellington	ds824	td9636	td9635	neumann	mlc
usa	0	78	61	325	325	325	325	325	325	325	325	325	325
tokyo	5	0	0	252	252	252	252	252	252	252	252	252	252
hko	8	20	0	272	272	272	272	272	272	272	272	272	272
newdelhi	0	0	0	0	0	0	0	0	0	0	0	0	0
reunion	0	0	0	0	0	0	0	0	0	0	0	0	0
bom	0	0	0	0	0	0	0	0	0	0	0	0	0
nadi	0	0	0	0	0	0	0	0	0	0	0	0	0
wellington	0	0	0	0	0	0	0	0	0	0	0	0	0
ds824	0	0	0	0	0	0	0	0	0	0	0	0	0
td9636	0	0	0	0	0	0	0	0	0	0	0	0	0
td9635	0	0	0	0	0	0	0	0	0	0	0	0	0
neumann	0	0	0	0	0	0	0	0	0	0	0	0	0
mlc	0	0	0	0	0	0	0	0	0	0	0	0	0

Figure 15: number of missed tracks from each WMO RSMC centre (column) with respect to other centers (lines), over 2010-2020 and for the West Pacific basin.

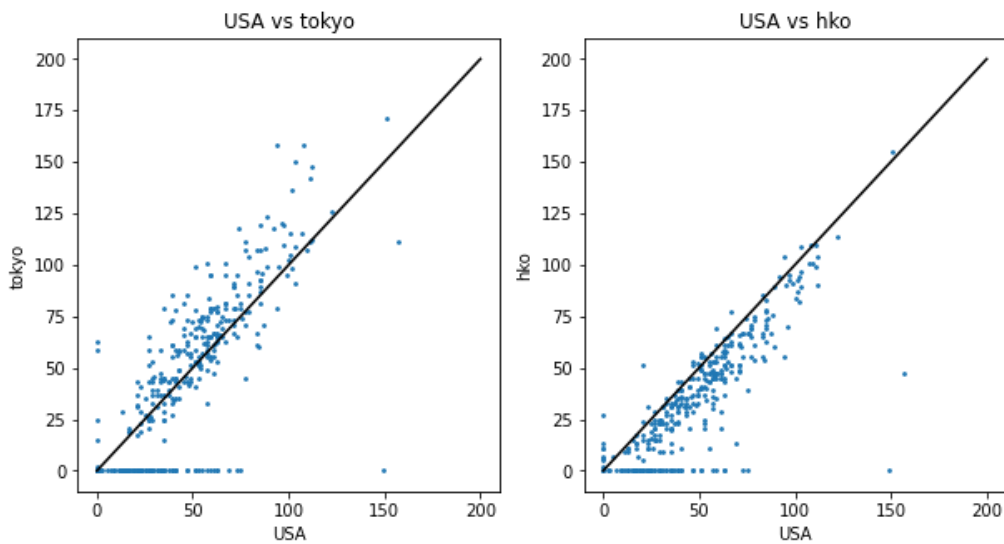


Figure 16: duration (in time steps) of the TC tracks of JMA center with respect USA (left) and of HKO center with respect USA (right)

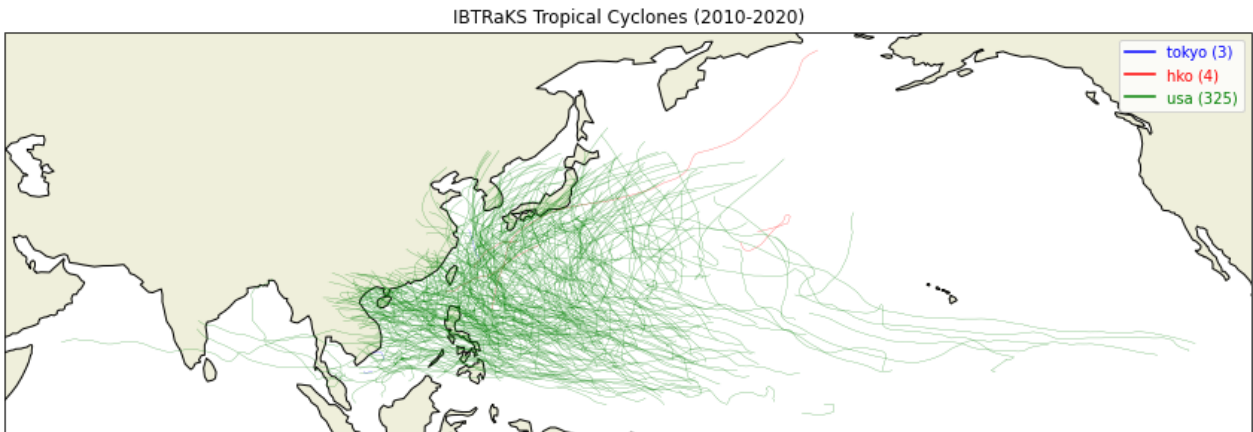


Figure 17: map of the TC tracks selected from the IBTrACS's USA \cup JMA \cup HKO sources for the West Pacific basin over 2010-2020.

4.1.1.6 Source selection for South Pacific basin

In the South Pacific, USA is only missing 6 tracks from Wellington and 13 from BoM, each of them missing many more from USA (68 and 71). USA tracks are longer than Wellington.

The final sources selected for South Pacific TC tracks is therefore defined as : USA \cup BoM \cup Wellington (for consistency with other basins - USA first - and to have radii wherever possible). The final TC tracks over 2010-2020 are shown in Figure 19.

Basin: SP

	usa	tokyo	hko	newdelhi	reunion	bom	nadi	wellington	ds824	td9636	td9635	neumann	mlc
usa	0	106	106	106	106	71	50	68	106	106	106	106	106
tokyo	0	0	0	0	0	0	0	0	0	0	0	0	0
hko	0	0	0	0	0	0	0	0	0	0	0	0	0
newdelhi	0	0	0	0	0	0	0	0	0	0	0	0	0
reunion	0	0	0	0	0	0	0	0	0	0	0	0	0
bom	13	48	48	48	48	0	38	38	48	48	48	48	48
nadi	0	56	56	56	56	46	0	19	56	56	56	56	56
wellington	6	44	44	44	44	34	7	0	44	44	44	44	44
ds824	0	0	0	0	0	0	0	0	0	0	0	0	0
td9636	0	0	0	0	0	0	0	0	0	0	0	0	0
td9635	0	0	0	0	0	0	0	0	0	0	0	0	0
neumann	0	0	0	0	0	0	0	0	0	0	0	0	0
mlc	0	0	0	0	0	0	0	0	0	0	0	0	0

Figure 18: Number of missed tracks from each WMO RSMC centre (column) with respect to other centers (lines), over 2010-2020 and for the South Pacific basin.

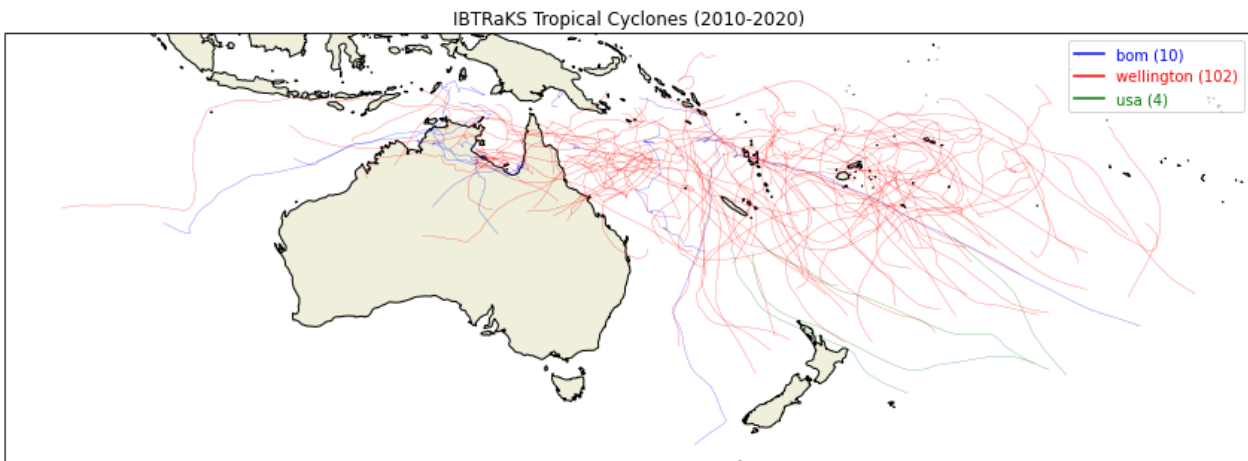


Figure 19: map of the TC tracks selected from the IBTrACS’s USA ∪ BoM ∪ Wellington sources for the South Pacific basin over 2010-2020.

4.1.1.7 TC tracks selection summary

To summarize, a combination of sources have been selected and used to generate one single set of tracks for the MAXSS storm Atlas. For each basin and by order of priority, the selection of sources from IBTrACS database is defined as follows:

- East Pacific: USA
- West Pacific: USA ∪ JMA ∪ HKO
- South Pacific: USA ∪ BoM ∪ Wellington
- North Atlantic: USA
- South Atlantic: USA (only 2 tracks, not shown here)
- North Indian: USA ∪ New Delhi
- South Indian: USA ∪ BoM ∪ Reunion

Note that USA source is always selected first for completeness with respect to other basins and to have wind radii wherever possible. All original tracks were then interpolated to every hour using an Hermit polynomial interpolator. The interpolation is also applied to R34, R50, R64, MWSP and SLP parameters. The intermediate locations (:15, :30,...) are kept when provided. We saved the tracks data into output track files in netcdf, csv and parquet format.

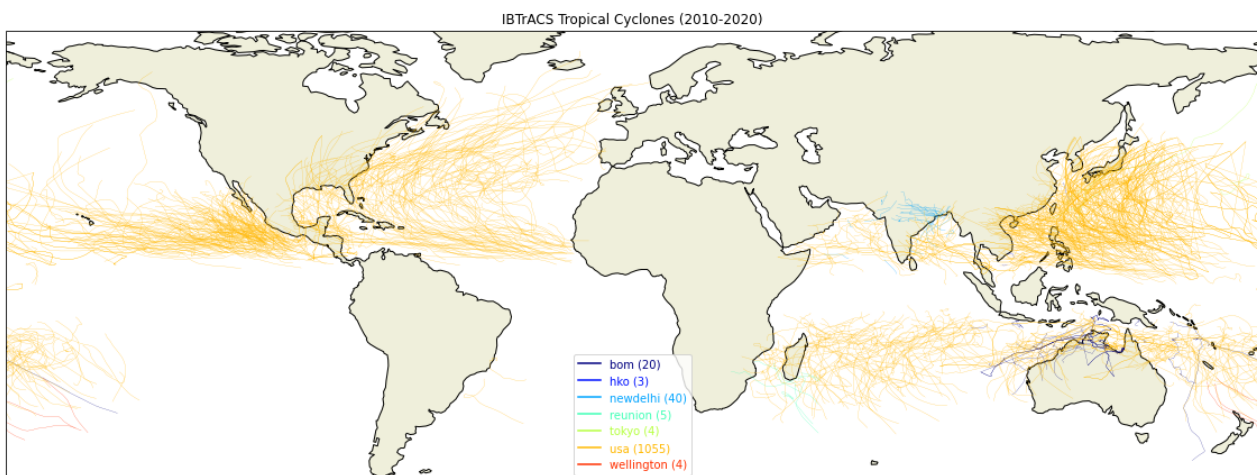


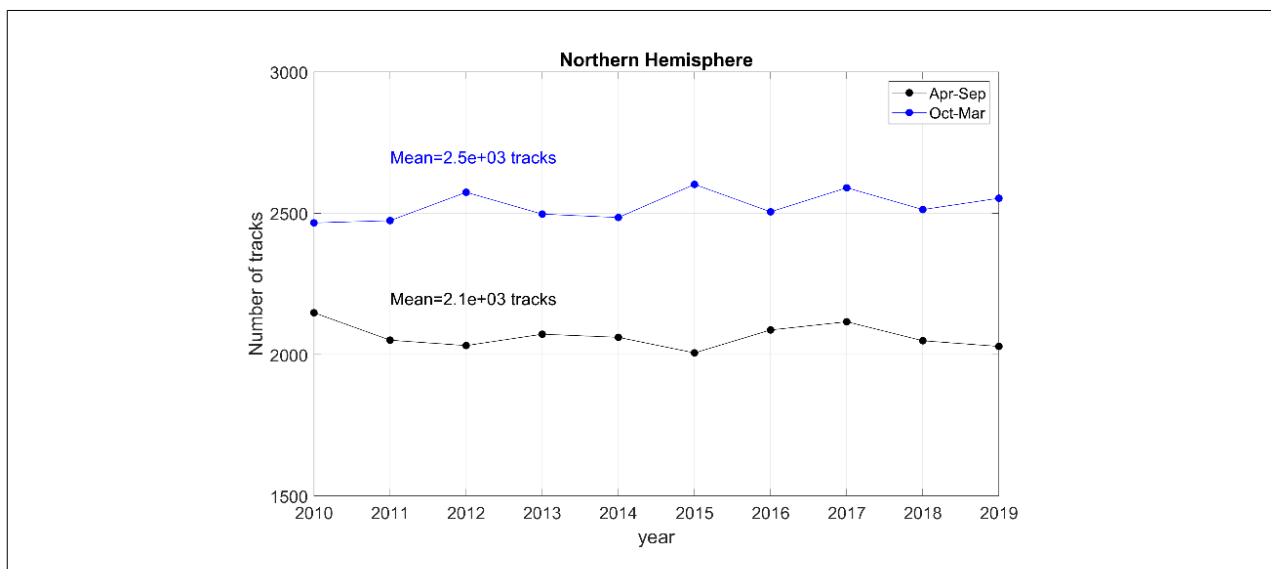
Figure 20: Ensemble of Tropical Cyclone tracks selected to build the MAXSS storm Atlas

4.1.2 Extra-Tropical Cyclones tracks

Sinclair (1994) highlighted the benefit of using vorticity instead of mean sea level pressure (MSLP) for the detection of cyclones in mid-latitudes, where the surface pressure gradient can be strong so that cyclones appear without a closed isobar. For this reason, the use of vorticity allows the early identification of cyclones that would only be detected by MSLP when intensification occurs or they move to higher latitudes. We also used the vorticity tracks as they are the most continuous. As illustrated in Figure 21 and Figure 22, the number of storm tracks in the original database is rather stable from year to year and is

very high (greater than 2000 per year, per season and per hemisphere) with a total number of 97000 storms over 2010-2019. This ERA5-based storm tracks database is dominated by TCs and pure « land storms » are included, as well as Polar lows. In order for the project to build a practical ETC storm Atlas, one need a significantly reduced number of events focused on the most intense ETCs. To this aim we applied the following filtering strategies:

- pure land storm tracks are removed,
- any storms that have the major part of their life cycle over land are excluded,
- To remove most TCs, any storms that have the major part of their life cycle within the tropics are excluded, where the tropics are defined here as the zonal region (30°S,30°N),
- To exclude most Polar Lows, any storms that have the major part of their life cycle within the polar regions are excluded, where the polar regions are defined as North of 66°N & South of 66°S.
- We only selected the most intense storms defined by a maximum 10 meter height wind speed during the storm lifetime $\max(U_{10}(t))$ greater than the 98th percentile pre-determined for each hemisphere & season.



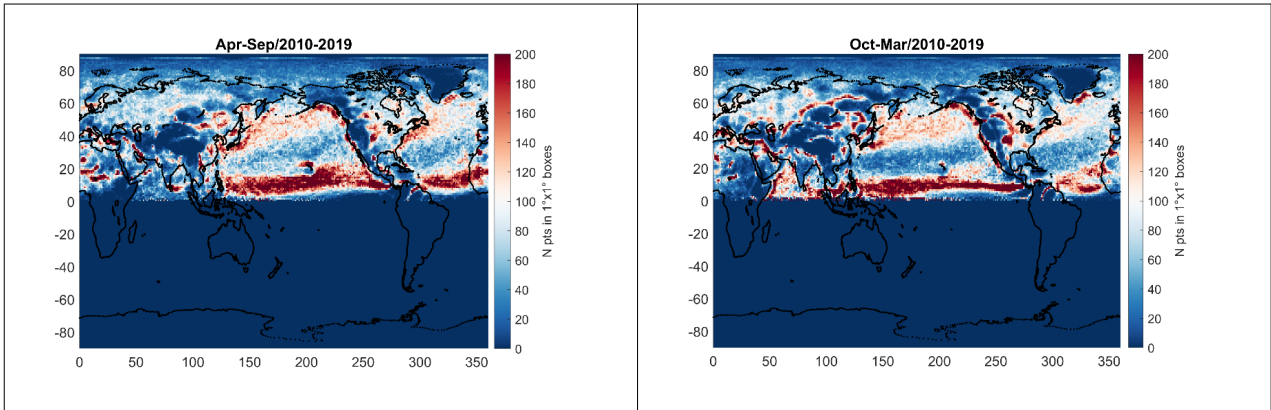


Figure 21: (Top) Number of storms per year in ERA5 reanalysis from 2010 to 2019 for the Northern Hemisphere and for both spring-summer (black) and autumn-winter (blue) seasons. (Bottom) Density of tracks per $1^{\circ} \times 1^{\circ}$ boxes for spring-summer (left) and autumn-winter (right) seasons.

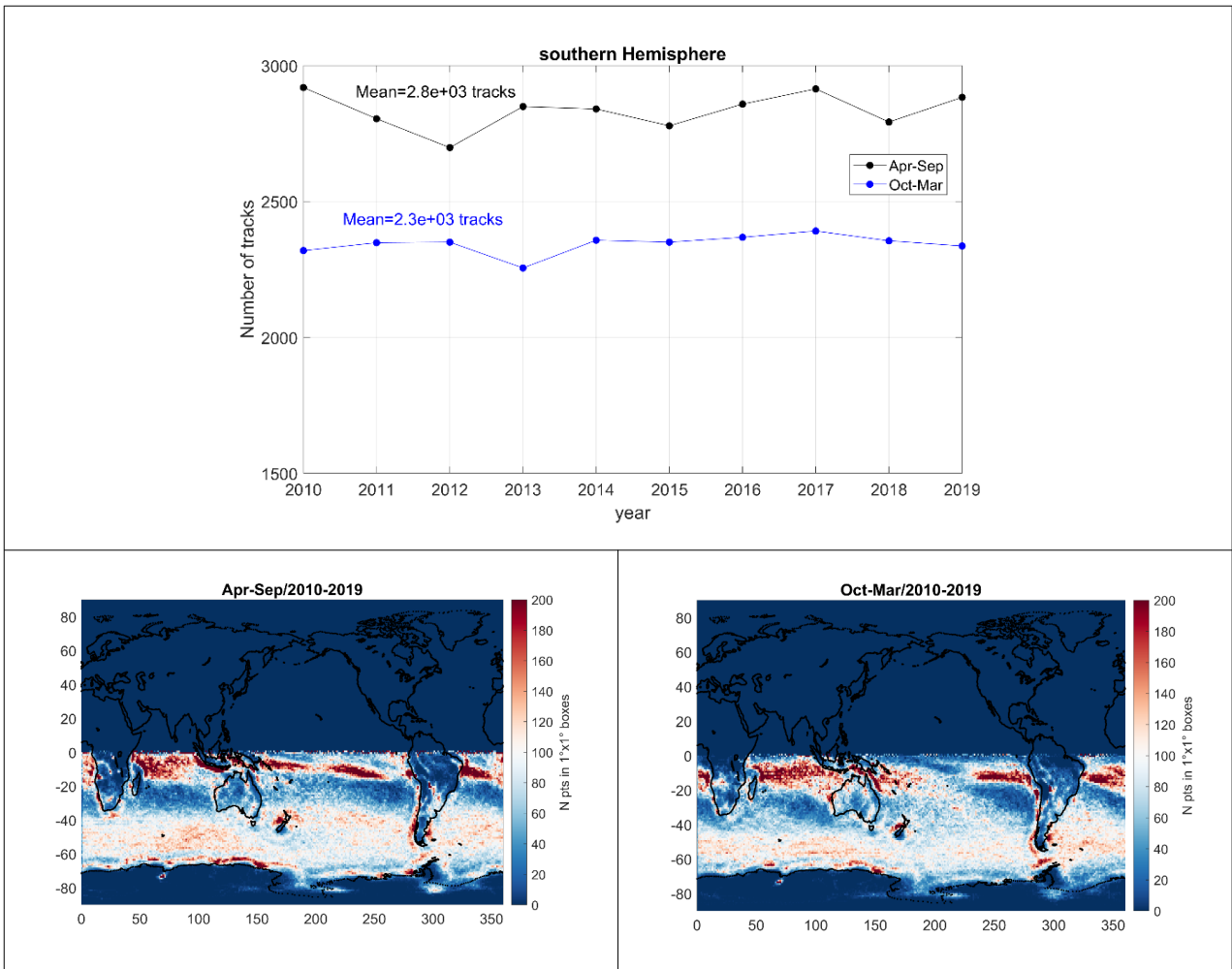


Figure 22: (Top) Number of storms per year in ERA5 reanalysis from 2010 to 2019 for the

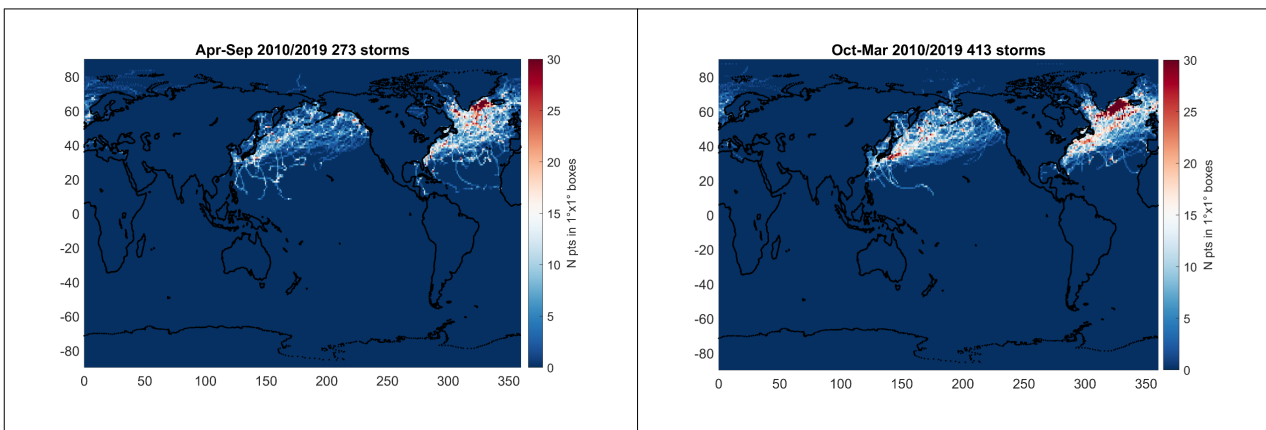
Southern Hemisphere and for both spring-summer (black) and autumn-winter (blue) seasons. (Bottom) Density of tracks per 1°x1° boxes for spring-summer (left) and autumn-winter (right) seasons.

The values of the 98th percentile of the maximum 10 meter height wind speed during storm lifetime were pre-determined for each hemisphere & season and are given in Table 1.

Region	North		South	
Season	Apr-Sep	Oct-Mar	Apr-Sep	Oct-Mar
98th percentile of the maximum intensity reached during lifetime (m/s)	23.5	27.9	29.7	27

Table 1: 98th percentile of the maximum 10 meter height wind speed during storm lifetime for each hemisphere & season

As illustrated in Figure 23, after applying such filtering strategy, the number of ETC reduces to ~150 storms /year (all regions and seasons).



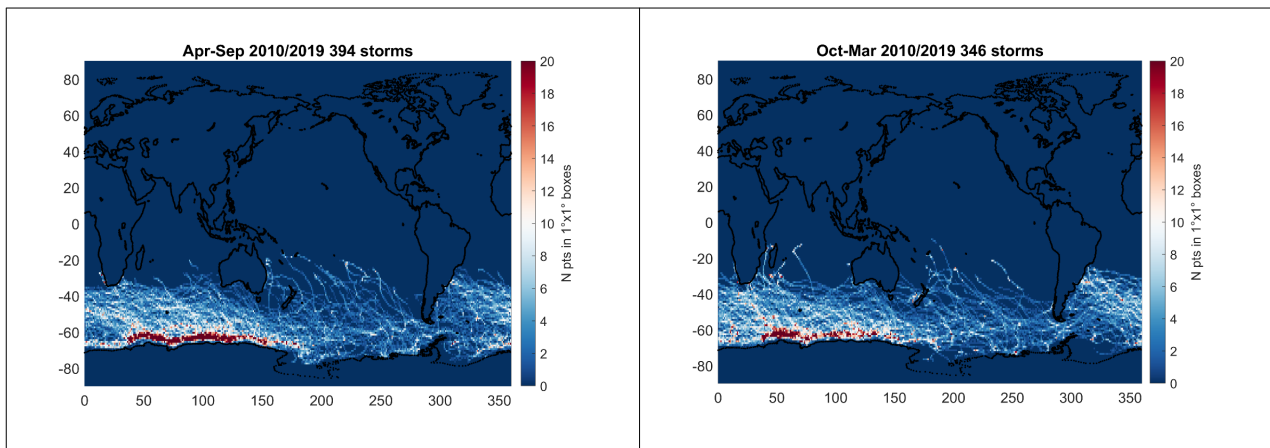


Figure 23: Number of selected ETC tracks per $1^\circ \times 1^\circ$ boxes per season (left panels are for Apr-Sep; right panels for Oct-Mar) and per hemisphere (top is North and bottom is south).

4.1.3 Polar Low tracks

For this version of the ATBD, we consider all tracks from the Rojo et al database in the Barents sea. In a next step, we shall also add some PLs for other regions extracted from the ERA5 storm track database used for ETCs (previous section).

5 STORM ATLAS GENERATION: STEP 2 COARSE COLLOCATION

Methodology: Step 2 Coarse Collocation

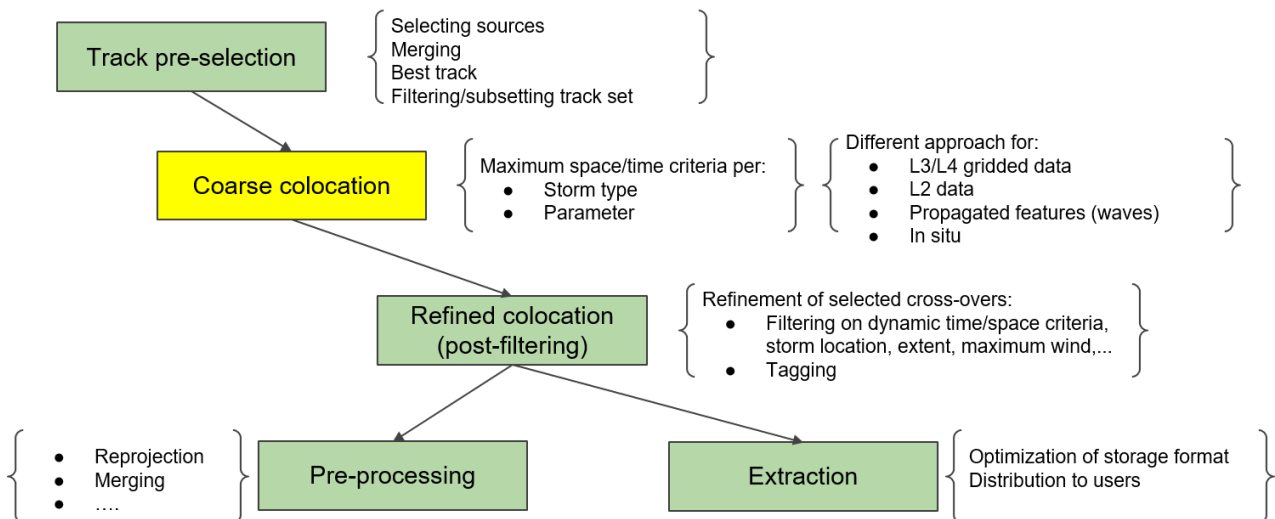


Figure 24: Atlas building algorithm Step 2: Coarse collocation

The space (dX) and time (dT) scales needed to gather the data around each storm may vary as a function of :

- The storm type: TC/ETC/PL, which all have all different characteristic space/time scales and dynamical evolution,
- The specific EO data parameters and associated space/time scales of the storm-induced physical or biogeochemical processes they do help to monitor,
- The sensing patterns of the EO data: grid (space/time composite L3/L4 satellite data, analyzed in situ, swath/image (L2 data, scatterometer, SAR image), along-track (altimetry), SAR wave mode, local in situ,...

The space radius dX (around the storm center track) and period dT over which we collect the storm Atlas input geophysical data around each storm trajectory were defined from the following coarse considerations as function of the types of storms and geophysical parameters.

			<p style="text-align: right;">MAXSS ATBD ESA Contract 4000132954/20/I-NB Delivery D21, Version 1.0.0 Date 06/10/2021 Page 42</p>
---	--	--	--

5.1 Tropical Cyclones scales

It is the TC size in terms of wind field that often determines potential tropical cyclone impacts (e.g., Powell and Reinhold 2007; Houston et al. 1999; Irish et al. 2008) and areal coverage and distribution of rainfall (e.g., Kidder et al. 2005; Matyas 2010). Size of Tropical Cyclone vary from 16 to 1,900 kilometers in diameter. Typical TC characteristic scales are the outer wind radius ranging from 50 to 1000 km, (Knaff et al., 2014) and the lifetime varying from several hours to more than a week (Hall & Kossin, 2019). Statistical properties of the distributions of the TC size parameters for Atlantic TCs between 1988 and 2002 have been conducted by Kumball and Mulekar (2004). As found, the gale-force wind radii (radi at 34 knts=17 m/s) is ranging from 45 km to ~700 kms. Most of the SST and SSS oceanic response to TC is concentrated within that domain (Reul et al., 2021). In addition, historical record of TC-centered IR imagery (1978–2011) and the basin-specific distributions of TC size reveal that, among other things, the eastern North Pacific TC basins have the smallest while western North Pacific have the largest TC size distributions estimate (Knaff et al., 2014). Large TCs are generally located at higher latitudes, poleward steering, and preferred in enhanced low-level vorticity environments. While there are significant variabilities in TC sizes (inner size defined by R_{max} and outer size defined by R_{34}), it shall be sufficient to chose a search space radius $dX = 1000$ km around the storm center track to collect EO data within most of the TC's wind-forced zone and in the general case. The dT quantity around TCs is dependent on the parameter analyzed and will be described further.

5.2 ETC characteristic scales

Composite analysis for air–sea turbulent fluxes, heat content, precipitable water, and precipitation of North Atlantic mid latitudinal winter cyclones have been performed by Rudeva and Gulev (2011) using NCEP–NCAR reanalysis data for the 60-yr period from 1948 to 2007. The composites were developed using an advanced methodology involving the coordinate transform of cyclones into a non-dimensional azimuthal coordinate system and the further collocation of fields. Composite analysis was performed for 576 oceanic cyclones generated in the Gulf Stream area in winter (January–March). In particular, they derived the the angular probability density function (PDF) of the actual cyclone radii along 36 directions for all 576 cyclones. As found, in the rear part of the cyclone the distribution of the cyclone radii is clearly less scattered compared to the forward part. For 50% of the modal cyclones, the radii in the back part vary from 400 to 700 km, while in the forward part this range increases to 400–800 km. Therefore, a search radius $dX \geq 1000$ km surrounding the identified cyclone position shall be enough to build up the ETC storm Atlas within a spatial domain including all the storm wind impact. The structure and evolution characteristics of 200 composited North Atlantic cyclones from 1989 to 2009 have been later studied by Dacre et al. (2012). An ETC atlas has been created to explore

			<p style="text-align: right;">MAXSS ATBD ESA Contract 4000132954/20/I-NB Delivery D21, Version 1.0.0 Date 06/10/2021 Page 43</p>
---	--	--	--

the mean structure and evolution of the 200 most intense North Atlantic cyclones identified in 20 winters of the ERA-Interim reanalysis data. Following Dacre et al. (2012), for the ETC, the MAXSS storm Atlas required EO fields (e.g., SST, SSS, wind, etc...) are extracted along the tracks of the selected cyclones within a radius $dX=2500$ km surrounding the identified cyclone position. In Dacre et al. (2012), the cyclone lifetime were also estimated ranging from several hours to 7 days. The Storm Atlas EO data are collected within an offset time dT relative to the time of maximum intensity of each cyclone, which varies as a function of the selected parameter (see table below) but is at minimum of ± 7 days.

5.3 Polar Lows characteristic scales

According to Rasmussen and Turner (2003), “A polar low is a small, but fairly intense maritime cyclone that forms poleward of the main baroclinic zone (the polar front or other major baroclinic zone). The horizontal scale of the polar low is approximately between 200 and 1000 kilometers and surface winds near or above gale force (15 m/s~30 kts).” The detailed characteristics of detected polar lows were analyzed in Smirnova et al. (2015) . They produced a climatology of polar lows using an approach based on satellite passive microwave data for polar low identification. A total of 637 polar lows were found in 14 extended winter seasons by combining total atmospheric water vapor content and sea surface wind speed fields retrieved from Special Sensor Microwave/Imager data. Most polar lows (42.5%) formed in the Norwegian Sea. As found about half of polar lows are small scale with 200–400 km diameter. The majority of polar lows do not exceed 500 km in horizontal scale. It should be noted that despite 1000 km diameter is an upper limit for initial selection of polar low like vortices, none of polar lows is expected to exceed 800 km. Most polar lows exist 9–18 h and only 10% last more than 1 day. The selected space radius dX (around the PL center track) and period dT over which we collect the Polar Low Atlas input are therefore 500 km radius and dT of at least ± 1 day.

5.4 Recovery time for SST and SSS response

As found in Dare and MacBride (2011) from a large SST dataset within TC wakes, the recovery of the ocean to cyclone passage is generally quite rapid with 44% of the studied data points recovering to climatological SST within 5 days, and 88% of the data points recovering within 30 days. Although differences exist between the mean results from the separate tropical cyclone basins, they are in broad agreement with the global mean results. Storm intensity and translation speed affect both the size of the SST response and the recovery time. The recovery e-folding time scale of the SST after TC passage have been also further obtained by Mei and Pasquero (2013) . As found, the area-averaged TC-induced SSTA largely decays within 1–2 weeks, with almost no dependence on the

			<p style="text-align: right;">MAXSS ATBD ESA Contract 4000132954/20/I-NB Delivery D21, Version 1.0.0 Date 06/10/2021 Page 44</p>
---	--	--	--

intensity of TCs and the magnitude of the anomaly. But, the recovery time of the SST has considerable case-to-case variability and is usually subject to environmental contaminations, including strong variations in wind strength and cloud cover. According to these studies, to determine SST anomalies left after TC passage, it is useful to collect SST data at least 2 weeks before the storm passage (to well characterize the pre-storm conditions) to slightly more than 1 months after it (to cover the full SST recovery time). For SST, we therefore used a DT ranging from -15 days to + 40 days .

Research shows that the upper ocean salinity response can persists about 10–12 days (Girishkumar et al. [2014](#)). Sun and Vecchi (2021) showed that on average, the passage of TCs over the ocean results in a saltier surface, with recovery time often more than 15 days but almost vanish after a month time. As for SST, we therefore chose to collect SSS data at least 2 weeks before the storm passage (to well characterize the pre-storm conditions) to slightly more than 1 months after it (to cover the full SSS recovery time), with a DT ranging from -15 days to + 40 days .

5.5 SSH and SLA long term response

The gridded and objectively analyzed SSH and SLA response to TC passage are derived from altimeters with limited spatio-temporal coverage of the storm events (which have characteristic scales < 1000 km and < 7 days). They usually merge altimeter data over more than 10 days period and might therefore mix pre- and post- storm signatures of the events. Short term SSH and SLA storm induced change can therefore be better studied based on swath observations, as described in §4.3.

Mei and Pasquero (2013) quantified cyclone-induced ocean warming by directly monitoring the thermal expansion of water in the wake of cyclones, using satellite-based sea surface height data that provide a unique way of tracking the changes in ocean heat content on seasonal and longer timescales. In particular, they determined the Temporal evolution of along-track-averaged composite SSHA (centimeters) associated with the passage of TCs of category-3 to -5 hurricane intensity in the Northern Hemisphere. As shown, the temporal evolution shows a rapid SSH increase during the first month, followed by a gradual increment that levels off after about 5 months. This behavior is consistent with recent observations showing that the warming by anomalous air–sea heat fluxes is initially confined to the top part of the mixed layer and is associated with a rapid recovery of the SST within a few weeks, whereas the bottom part of the TC-induced cold anomaly takes a much longer period to dissipate. To quantify the long-term change in ocean heat content induced by TCs we need to collect the SSHA averaged over a window that covers the quasi-steady stage in the period between 5 months and 7 months after the storm passage. This period is sufficiently long that the averaging window extends beyond the period of deepest winter mixed layer, thus ensuring that our estimate filters out short-term heating that does not survive beyond the winter season. At the same time, the

			<p style="text-align: right;">MAXSS ATBD ESA Contract 4000132954/20/I-NB Delivery D21, Version 1.0.0 Date 06/10/2021 Page 45</p>
---	--	--	--

averaging period is sufficiently near in time to the passage of the storm to minimize the amount of heat lost by large-scale horizontal advection. In the present Atlas, we therefore chose to collect the gridded SLA/SSH data from $dT=60$ days before to 210 days after the storm passage. Following Mei et al. (2013), we also collect the data within a spatial radius $dX=1500$ km around the storm tracks.

5.6 Upper ocean Biological response time scale

TCs induce phytoplankton blooms and primary production increase, which is mainly attributed to the increased nutrient supply in the euphotic zone induced by vertical mixing (or entrainment) and upwelling during a TC (Mooers 1975; Morimoto et al. 2009; Siswanto et al. 2009; Zheng et al. 2010; Chiang et al. 2011; Shibano et al. 2011; Hung et al. 2013; Huang and Oey 2015) and ocean restratification after the TC (Huang and Oey 2015; Lin and Oey 2016). The chlorophyll increases after a TC usually ranges from 5 to 91% (Babin et al. 2004; Zhao et al. 2017; Xu et al. 2017a), while a lingered slow-moving TC (Kai-Tak in year 2000) can even triggered 30-fold of surface chlorophyll-a concentration (Lin et al. 2003b). In Northern (Southern) Hemisphere, the chlorophyll increases usually biases to the right (left) side of the TC track (Lin et al. 2003b; Babin et al. 2004; Yin et al. 2007; Hanshaw et al. 2008; Shang et al. 2008; Zhao et al. 2008; Zheng et al. 2010; Shibano et al. 2011), although the rightward (leftward) bias is not obvious or may even occur towards the left (right) side of the TC track (Zheng et al. 2010; Shibano et al. 2011). The amplitude and scope of surface plankton blooms depend not only on the TC characteristics but also on the ocean background conditions (Lin et al. 2003b; Zhao et al. 2008; Chen and Tang 2012; Shang et al. 2015; Xu et al. 2017a). For example, weak and slow-moving TCs induce phytoplankton blooms with higher chlorophyll-a concentrations, while strong and fast-moving TCs induce blooms over a larger area (Zhao et al. 2008). A pre-existing cold core eddy plays an important role in the increase in chlorophyll-a concentration by TCs (Chen and Tang 2012; Shang et al. 2015; Xu et al. 2017a; Jin et al. 2020), and the concentration of pre-existing chlorophyll-a in cold core eddies is approximately 25–45% (8–25%) of that of the post-existing chlorophyll-a in cold core eddies for relatively high (low) TC transition speeds (Shang et al. 2015). The biological response in coastal regions is more complicated than that in the open ocean (Pan et al. 2017). TC-induced mixing, enhanced terrestrial runoff and resuspension are considered three major processes that contribute to the increased nutrient concentrations and subsequent primary production in the euphotic layer (Chen et al. 2003). The chlorophyll-a reaches its peak three days after nitrate peak after a TC (Pan et al. 2017), and TC-induced phytoplankton blooms usually last for two to three weeks (Babin et al. 2004; Chen and Tang 2012; Foltz et al. 2015; Wang 2020). Following, these biological response time scale found in these studies, we therefore chose to collect the ocean color data (Chlorophyll-A, CDOM and k_{490}) with a DT ranging from -15 days to + 40 days .

In addition to the previous coarse collocation dX and dT parameter definitions, there are

also consideration such as the specific data product space-time sampling or coverage that need to be taken into account in building the storm Atlas. For example, most In Situ salinity and temperature analysed fields are available monthly. In these cases, the dT parameter need to be extended accordingly to be able estimate both the pre- and –post-storm upper ocean conditions. If the EO data are gridded or if they are swath observations the space/time criteria also differ because the processes studied also differ (e.g., analysed SLA vs along-track SLA). We detail and summarize the refined collocation criteria in the table 2 below for each input data of the Storm Atlas algorithm.

	Source	Temporal Coverage	Spatial Resolution	Temporal Resolution	Reference	TC collocation criteria	ETC collocation criteria	PL collocation criteria
Gridded data								
Satellite SSS								
CATDS L3OS 2Q	CATDS / Boutin et al., 2018	2010-2019				1000 km 15 days bef. / 40 days after	2500 km 15 days bef. / 40 days after	
Remote Sensing Systems V4.0 SMAP Level 2C products	RSS / Meissner et al., 2018	2015-2019	70km 40km	et	www.remss.com/missions/smap/	1000 km 15 days bef. / 40 days after	2500 km 15 days bef. / 40 days after	
ESA CCI Sea Surface Salinity L4 v3.2	ESA CCI	2010-2019		daily -7 days running mean window average	ESACCI-SSS-L4-SSS-MERGED-OI-7DAY-RUNNINGMEA N-DAILY-25km': 'Boutin, J.; Vergely, J.-L.; Reul, N.; Catany, R.; Koehler, J.; Martin, A.; Rouffi, F.; Arias, M.; Chakroun, M.; Corato, G.; Estella-Perez, V.; Guimbard, S.; Hasson, A.; Josey, S.; Khvorostyanov, D.; Kolodziejczyk, N.; Mignot, J.; Olivier, L.; Reverdin, G.; Stammer, D.; Supply, A.; Thouvenin-	1000 km 15 days bef. / 40 days after	2500 km 15 days bef. / 40 days after	500 km 15 days bef. / 15 days after



					tab=overview'			
RSS MW_IR_OI L4 v5	RSS		9km	daily	Remote Sensing Systems. 2017. MWIR optimum interpolated SST data set. Ver. 5.0. PO.DAAC, CA, USA. Dataset accessed [YYYY-MM-DD] at https://doi.org/10.5067/GHM/WI-4FR05	1000 km 15 days bef. / 40 days after	2500 km 15 days bef. / 40 days after	
In Situ Temperature & Salinity analyses								
ISAS	Ifremer		0.5°x0.5°	monthly		1000km 1 month bef. / 1 month after.	2500 km 1 month bef. / 1 month after	
CORA	Ifremer							
SSH + SLA								
CEEMS / AVISO REP L4	CEEMS		0.25 deg	daily		1500 km 60 days bef. / 210 days aft.		
Ocean Colour								
ESA CCI Ocean Colour L3S chlorophyll_a	ESA CCI	1997-2020	4km	daily	Sathyendranath, S, Brewin, RJW, Brockmann, C, Brotas, V, Calton, B, Chuprin, A, Cipollini, P, Couto, AB, Dingle, J, Doerffer, R, Donlon, C, Dowell, M, Farman, A, Grant, M, Groom, S, Horseman, A, Jackson, T,	1000 km 15 days bef. / 40 days after		
ESA CCI Ocean Colour L3S CDOM								
ESA CCI Ocean Colour L3S K490								



--	--	--	--	--	--	--	--	--

Atmospheric Water Vapour & Cloud Liquid								
RSS Precipitable Water	RSS	1987-2020	0.25 deg	daily	http://www.remss.com/measurements/atmospheric-water-vapor/			
Rain Rate								

CMORPH (v1)			0.25 deg	3-hourly				
NASA Global Precipitation Measurement	Huffman et al., 2015		0.1 deg					
Tropical Rainfall Measuring Mission (TRMM) Multi-satellite Precipitation Analysis (TMPA) TRMM3B42 (V.7)			0.25 deg	3-hourly		1000 km 15 days bef. / 40 days after	1	
IMERG	Huffman et al., 2015	2000-2020	0.1 deg	30-minutes		1000 km 15 days bef. / 40 days after	2	
ERA5 Precipitation		1979-present	30 km	hourly		1000 km 15 days bef. / 40 days after		
Evaporation								
ESA Ocean Heat Flux Best	Bentamy et al., 2019	1992-2018				1000 km 15 days bef. / 40 days after	2	
ESA Ocean Heat Flux Reference	WHOI OAFflux, SeaFlux,...					1000 km 15 days bef. / 40 days after	1	
ERA5 Evaporation		1979-present	30 km	hourly		1000 km 15 days bef. / 40 days after		
Wind								
MAXSS L4 data		2010-2020	0.25°x0.25°	hourly		1000 km 15 days bef. / 40 days after		
ERA5 Wind		1979-present	30 km	hourly		1000 km 15 days bef. / 40 days after		

Along-track Swath Observations								
SSH								
IONS_008_062 CMEMS ALONG-TRACK L3 SEA SURFACE HEIGHTS, SEALEVEL_GLO_PHY_L3_REP_OBSERVATIONS_08_062	CMEMS		1 Hz			1000 km +/- 6 days		
SEALEVEL_GLO_PHY_L3_REP_OBSERVATIONS_08_062 [SASSA denoised version for Jason-3, S3A and Saral]	Ifremer		1 Hz			1000 km +/- 6 days		
Sea State								
ESA CCI Sea State L2P version 3 Altimetry + S1/SAR SWH v3	ESA CCI	2002-2020	1 Hz			1000 km +/-2 hrs		
Wind								
recalibrated scatterometer data for MAXSS project by ICM-CSIC: ASCAT-A ASCAT-B ASCAT-C HY-2A HY-2B Oceansat-2 Scatsat-1 Rapidscat	ICM		12.5 km to 25 km			1000 km +/-2 hrs		
recalibrated radiometer data	ICM		25 km			1000 km		

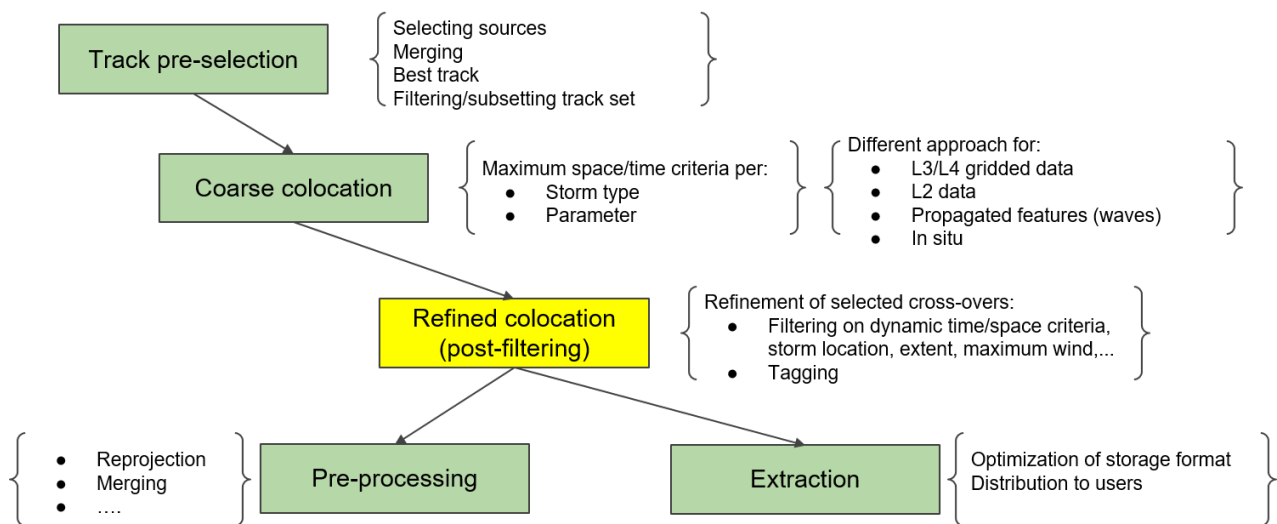
			<p style="text-align: right;"> MAXSS ATBD ESA Contract 4000132954/20/I-NB Delivery D21, Version 1.0.0 Date 06/10/2021 Page 52 </p>
---	--	--	--

for MAXSS project by ICM-CSIC: SMOS WindSat SMAP AMSR-2						+/-2 hrs		
--	--	--	--	--	--	----------	--	--

Table 2: List of datasets included in the Storm Atlas, and their respective colocation criteria for each storm category. Note: only the data in green background color are included into the Atlas for the preliminary version.

6 STORM ATLAS GENERATION: STEP 3 REFINED COLLOCATION

Methodology: Step 3 Refined Collocation



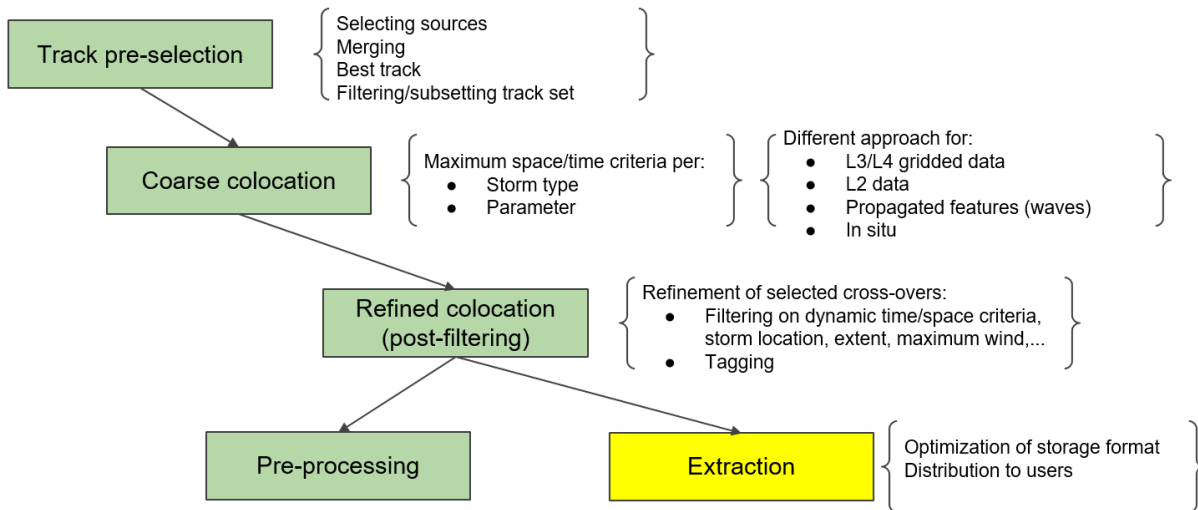
This step intends to characterize each found crossover between an observation source and the storm track, providing for instance:

- the relevance of the crossover with respect to the storm development at the observation time (R34 radius, maximum wind, etc...)
- properties on the quality of the crossover (intersection ration between the instrument and the storm, inclusion of the storm center or not, etc..)
- any property that could be inferred from the observation to classify the matchup

This step is not performed in the version 1 of the Storm Atlas.

7 STORM ATLAS GENERATION: STEP 4 DATA EXTRACTION AND PRE-PROCESSING

Methodology: step 4 Extraction

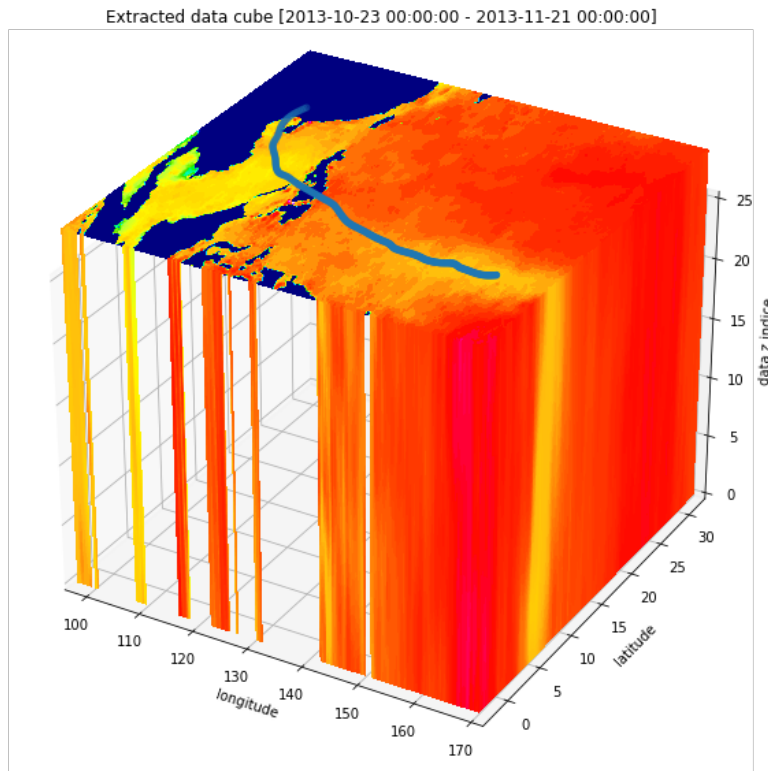


Given the collocation dT and dX criteria for each storm track and EO dataset the data are then extracted (and possibly pre-processed) to be saved in files following a defined storm archive organization, format and nomenclature. As described in what follows, the extraction methods differ if the products are gridded or swath observations.

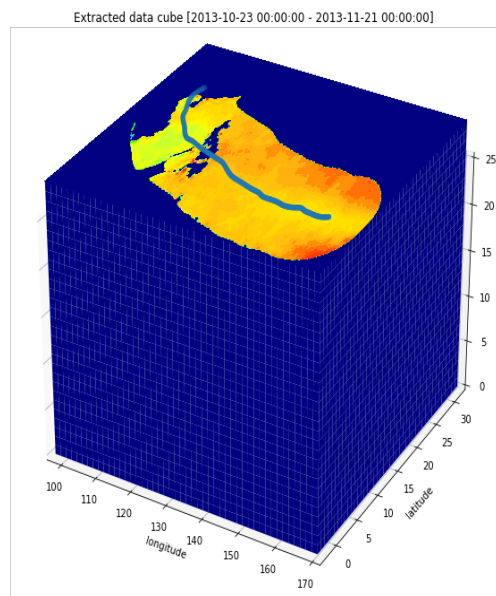
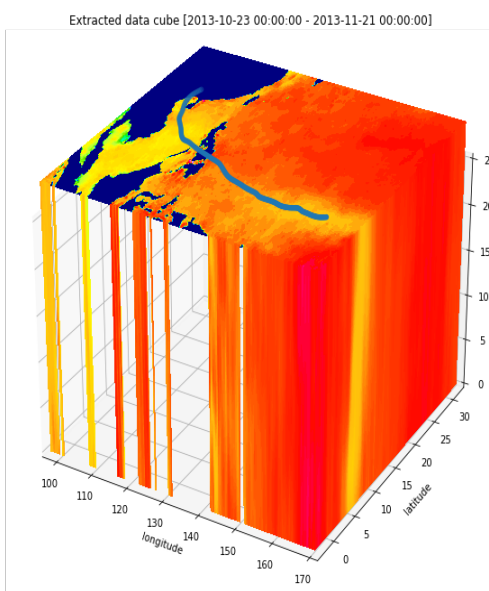
7.1 Gridded data

7.1.1 Extraction method

Each output file consists in a multidimensional data cube extracted from the source gridded data along the time axis over the region and time frame (including the collocation time window) covered by a given storm track. There is one output NetCDF4 file per storm and source gridded dataset, as illustrated in the example below:



In order to optimize the file size and to take advantage of NetCDF4 format internal compression, data out of storm path and wake (delimited by the spatial collocation radius) are extruded and replaced with fill values as illustrated below:.



			<p style="text-align: right;">MAXSS ATBD ESA Contract 4000132954/20/I-NB Delivery D21, Version 1.0.0 Date 06/10/2021 Page 56</p>
---	--	--	--

Gridded datasets which usually merge and average observations from multiple observation platforms or satellite passes are used in the Storm Atlas to provide the conditions and context preceding and following a storm passage. Therefore long temporal (dT) collocation criteria (from several days up to several months) are used; these criteria differ depending on the measured quantity.

7.1.2 Gridded product currently included into the MAXSS Storm Atlas

For the current version of the MTR storm Atlas, the gridded data from table 2 highlighted in green have been processed and included. Note that for this version, data were only extracted for TCs (using IBTRaCS storm track catalogue).

7.1.3 Output Content and Nomenclature

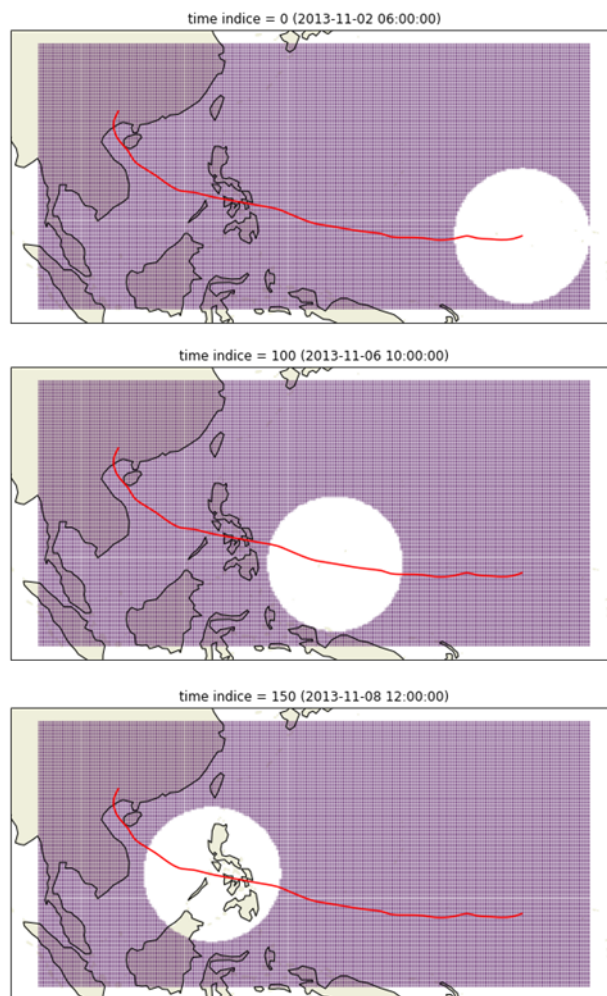
7.1.3.1 Content

The output files are saved in NeCDF4 and contained the following variables:

- Coordinate variables of the data cube
 - *lat, lon, time* contains the spatial and temporal coordinate values along the X, Y and T axis of the data cube
- Data variables
 - All variables copied from the source observation dataset within the data cube area, prefixed with *__eo__* string (*eo* standing for Earth Observation)
 - All coordinate and data variables from the storm track matched with the observation data, prefixed with *__track__*.
- Selection variables
 - *__data_start_time_indice* and *__data_end_time_indice* provide the first and last layer in the data cube framing the temporal window at the give track point.
 - *__data_nearest_time_indice* provides the temporally nearest layer in data cube to the track point.
 - *__data_spatial_mask* provides a selection mask over the data cube at a given track point (every hour): 1=inside the collocation radius, 0=outside. Use this over the data cube to spatially mask data out of the “column” centered on the

track point (image below).

- Traceability variables
 - ***__data_files*** : name of source observation file for each time step of the data cube



7.1.3.2 Nomenclature

There is one output NetCDF4 file per storm and observation product, named as follow:

MAXSS_<basin code>_<year>_<ATCF name>_<dataset_id>.nc

where:

- *basin code* is the code (EP: East-Pacific, NA: North-Atlantic, NI: North-Indian, SA:

South-Atlantic, SI: South-Indian, SP: South-Pacific, WP: West-Pacific) of the basin where the storm starts from

- *year* is the year of the storm track's start day
- *ATCF name* is the identifier from the Automated Tropical Cyclone Forecasting (ATCF) System of the storm, when existing (or an empty string if the storm was not named)
- *dataset_id* is the identifier of the source observation dataset, as listed in table **xx** below

Product title	MAXSS Product identifier
ESA CCI Sea Surface Salinity L4 v3.2	0
RSS MW_IR_OI L4 v5	0
ESA CCI Sea Surface Temperature L4	0
ESA CCI Ocean Colour / L3S chlor_a	0
ESA CCI Ocean Colour / L3S IOP	0
ESA CCI Ocean Colour / L3S KD	0
Tropical Rainfall Measuring Mission (TRMM) Multi-satellite Precipitation Analysis (TMPA) TRMM 3B42 (V.7)	0
ERA5 Precipitation	0
ERA5 Evaporation	0
MAXSS Blended L4	0
In Situ Temperature & Salinity analyses ISAS	0
CMEMS / AVISO REP L4	0

			<p style="text-align: right;">MAXSS ATBD ESA Contract 4000132954/20/I-NB Delivery D21, Version 1.0.0 Date 06/10/2021 Page 59</p>
---	--	--	--

For instance:

MAXSS_WP_WP312013_ESACCI-SEASURFACESALINITY-L4-SSS-MERGED_OI_7DAY_RUNNINGMEAN_DAILY_25km.nc

is the data files containing the observations from *ESACCI-SEASURFACESALINITY-L4-SSS-MERGED_OI_7DAY_RUNNINGMEAN_DAILY_25km* dataset for the storm with ATCF identifier *WP312013* in West Pacific (*WP*) basin.

7.2 Along-Track and Swath Data

7.2.1 Extraction method

Storm observations are collected from satellite along-track and swath (level 2) data to provide coincident measurements with the storm passage. Contrary to gridded merged products, the time colocation criteria (dT) used in this context are much narrower as shorter time scale processes are studied. They also depend on the measured quantity as some parameters may change at slower or faster time scales.

For along-track Sea Level altimetry observation over Tropical Cyclones, a larger colocation time criteria was used (+/-6 days) than for the other types of observation (wind and waves), in order to capture altimeter passes well before and after the storm passage (as per Combot et al, 2018).

The observations are extracted over each storm track using *felyx* open-source software (<https://felyx.ifremer.fr>), a tool designed to extract observation data over static or dynamic targets (measuring devices such as a buoy, a ship, etc... or a geophysical phenomenon).

Segments of satellite swath data are extracted each time the satellite crosses the storm track within a given time window (usually two hours), over the radius corresponding to the maximum extent of a storm, as illustrated on the figure 25:

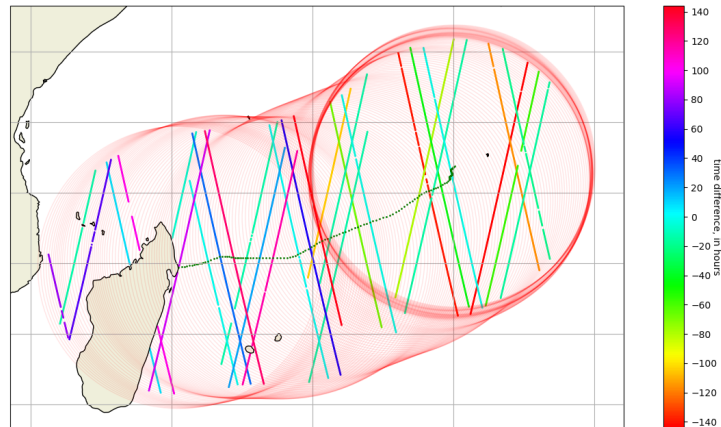


Figure 25: Exemple of Sentinel-3A SRAL along-track data extraction for TC ABELA. $dT = +/-6$ days, $R = 1000$ km

The extracted segments are centered on the closest track point in time and they have a constant size matching the maximum radius of a storm. The size (in number of measurements along each dimension of the extracted data) is dependent on the instrument spatial resolution. All the segments are stacked together into a single file per storm and data source. Similarly to the extractions from gridded products, measurements out of the storm path (whose width is given by the maximum spatial extent of a storm) are masked, as illustrated below.

GORDON 2018 - Sentinel-3 A

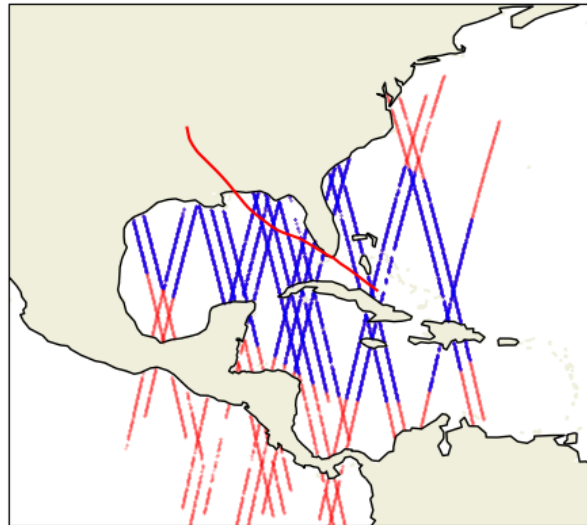
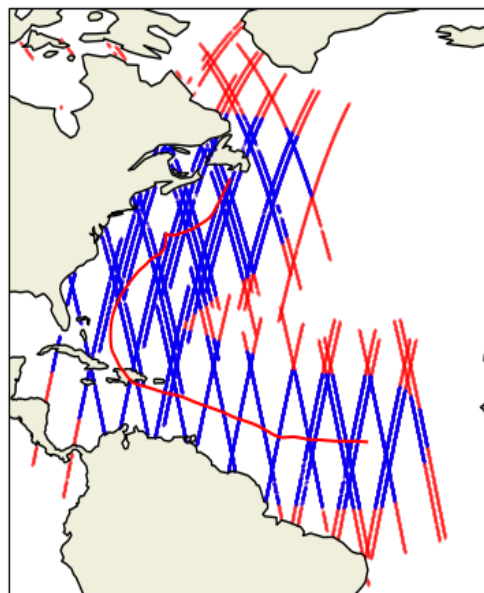


Figure 26: Use `data_spatial_mask` selection mask to only keep data points within track 1000 km radius

For sea level altimetry measurements, longer segments are extracted (500 1Hz values, ~ 3000 km) in order to cover completely the cyclone's wake when it is moving along a south / north axis approximately. Since a larger time criteria (+/- 6 days) is used in this case, it is meant to cover the sea level change over the whole storm wake within the storm maximum radius.

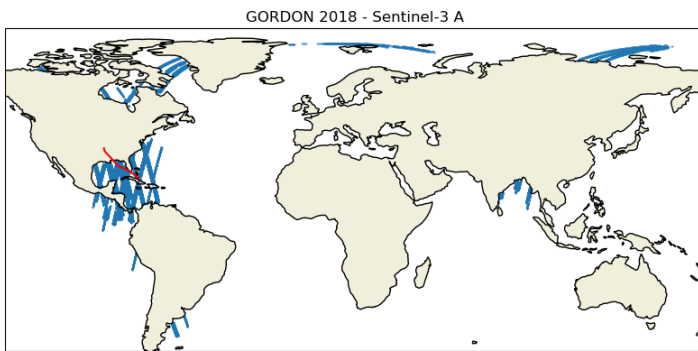
BERYL 2018 - Sentinel-3 A



			<p style="text-align: right;">MAXSS ATBD ESA Contract 4000132954/20/I-NB Delivery D21, Version 1.0.0 Date 06/10/2021 Page 62</p>
---	--	--	--

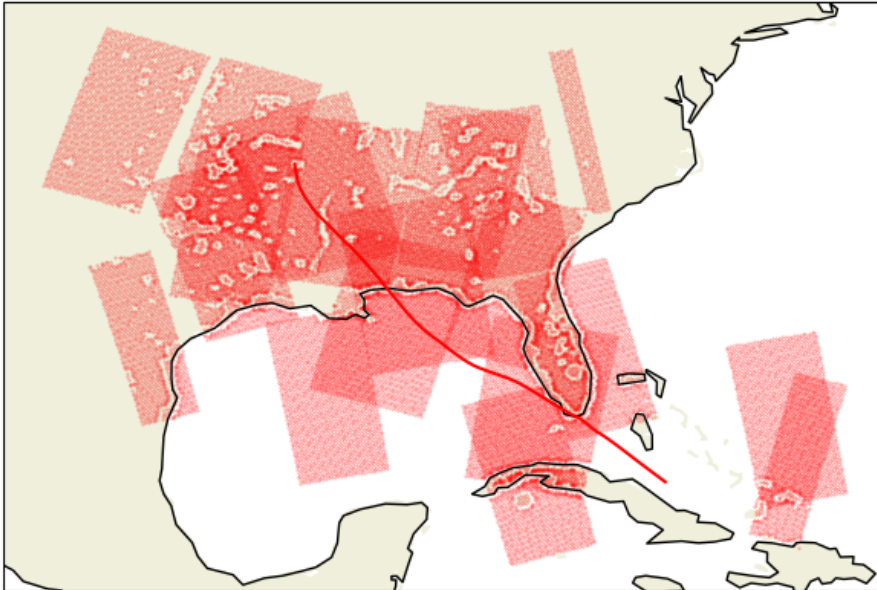
Some caveats

Some products (such as the CMEMS L3 Along-Track Sea Level altimetry product) are heavily edited and concatenate non continuous along-track segments. This creates some discontinuities within a data file. Extracting a fixed number of contiguous measurements centered on the track intersection (500 measurements in this case) result in the extracted segment containing measurement way out of the storm area, while being contiguous in the file. This is illustrated on the example below : the extracted Storm Atlas file for this specific storm (Gordon, 2018) and altimeter (Sentinel-3 A) contains measurements (in blue) very far from the storm track itself in the Gulf of Mexico. These unfitting measurements can be easily ignored using the *data_spatial_mask* variable provided in the file.



Some products include data over land (though most of the time they are invalid). We don't discriminate between land and sea surface in the colocation and extraction process. This result is some observations being useless (and often actually filled with fill values). This is illustrated in the example below, showing all crossovers between ASCAT-A scatterometer and Gordon, 2018. besides, ASCAT is a double swath instrument with both swaths merged into a single 2 dimensional array. Extracting a subset (N rows x N cells) may results in some parts of the subset being out of the actual storm maximum radius.

GORDON 2018 - ASCAT onboard Metop-A



7.2.2 Swath Data currently included into the Storm Atlas

For the current version of the MTR storm Atlas, the swath and along-track data from table 2 highlighted in green have been processed and included. Note that for this version, data were only extracted for TCs (using IBTRaCS storm track catalogue).

7.2.3 Output Content and Nomenclature

There is one NetCDF4 file per storm and observation product, named as follow:

MAXSS_<basin code>_<year>_<ATCF name>_<dataset_id>.nc

where:

- *basin code* is the code (EP: East-Pacific, NA: North-Atlantic, NI: North-Indian, SA: South-Atlantic, SI: South-Indian, SP: South-Pacific, WP: West-Pacific) of the basin where the storm starts from
- *year* is the year of the storm track's start day
- *ATCF name* is the identifier from the Automated Tropical Cyclone Forecasting (ATCF) System of the storm, when existing (or an empty string if the storm was not named)

- *dataset_id* is the identifier of the source observation dataset, as given in the table below.

Product title	MAXSS Product identifier
CCI Sea State L2P Altimeter + S1/SAR SWH v3	
CMEMS ALONG-TRACK L3 SEA SURFACE HEIGHTS , SEALEVEL_GLO_PHY_L3_REP_OBSERVATIO NS_008_062	SEALEVEL_GLO_PHY_L3_REP_OBSERVATIO NS_008_062_Cryosat-2 SEALEVEL_GLO_PHY_L3_REP_OBSERVATIO NS_008_062_HY2A SEALEVEL_GLO_PHY_L3_REP_OBSERVATIO NS_008_062_HY2B SEALEVEL_GLO_PHY_L3_REP_OBSERVATIO NS_008_062_Jason-1 SEALEVEL_GLO_PHY_L3_REP_OBSERVATIO NS_008_062_Jason-2 SEALEVEL_GLO_PHY_L3_REP_OBSERVATIO NS_008_062_Jason-3 SEALEVEL_GLO_PHY_L3_REP_OBSERVATIO NS_008_062_S3A SEALEVEL_GLO_PHY_L3_REP_OBSERVATIO NS_008_062_S3B SEALEVEL_GLO_PHY_L3_REP_OBSERVATIO NS_008_062_SARAL

For instance:

MAXSS_WP_WP312013_ESACCI-SEASURFACESALINITY-L4-SSS-MERGED_OI_7DAY_RUNNINGMEAN_DAILY_25km.nc

is the data files containing the observations from *ESACCI-SEASURFACESALINITY-L4-SSS-MERGED_OI_7DAY_RUNNINGMEAN_DAILY_25km* dataset for the storm with ATCF identifier *WP312013* in West Pacific (*WP*) basin.

7.3 Argo floats

A collocation of all cyclones tracks is done globally with all individual argo float profiles measurements (pressure, temperature, salinity). The Argo data are taken from the french CORIOLIS GDAC (<ftp://ftp.ifremer.fr/ifremer/argo>). Only measurements with quality

			<p style="text-align: right;">MAXSS ATBD ESA Contract 4000132954/20/I-NB Delivery D21, Version 1.0.0 Date 06/10/2021 Page 65</p>
---	--	--	--

flags equal to 1 or 2 (good and probably good) are used, and both delayed mode and real time data profiles are treated.

For the collocation, we process all cyclone tracks one by one in a loop. Some input parameters are set and may be changed if needed. We assume a spherical earth of radius = 6378206.4 meters (Clarke1866). The first large space-time window of collocation is of 30 days before/after the first/last date of the cyclone track, and concerning spatial limits, they are at least 300km off the cyclone tracks north/south/east/west extreme positions (and if e.g. collocation radius is of 1000km then this value goes to 1000km+5%=1050km). Once this first large space-time window has been computed, then we extract all the Argo profiles data that are present in it. Those Argo data are the basic instantaneous observations that will all be saved in the NetCDF output file (1 output file per cyclone track).

From those argo profiles positions, we then perform a fine collocation with the cyclone track through a 2-step linear interpolation along the track. Here we used 2 different values for the input parameter being the search radius of collocation: 1000km, and a varying radius equal to the r34 value given by IBTrACS database (or a minimum value of 55km i.e. about 30 nmiles, if r34 not defined or too small), which will end up in having 2 sets of output files. To reach an accuracy similar to the one of Argo data in positioning (about 1000m or less, a few 10's of minutes), we set the interpolation parameters at 2 min and 200m, which means we interpolate the cyclone track to such resolutions in space and time (minimum of the 2 depending on the cyclone local velocity). Then our collocation computation has a precision error of about 1 min and 100m, which should be less (and not the limiting error) compared to the position errors of cyclone tracks or Argo floats. For all Argo profiles that falls within the fine collocation area, we flag them and compute a set of spatio-temporal variables of their position compare to the cyclone track with the same fine resolution (distance to the cyclone track, time of entry/exit of the cyclone into the profile collocation area etc...). Multiple collocation may sometimes occur (e.g. if a cyclone comes back on its path) and are also handled. To finish, several so-called Advanced Ocean Variables are computed for all the Argo profiles of the large space-time window. Those are: temperature, salinity, density at 10 m depth, 3 types of mixed layer depths (isothermal, isopycnal, and an optimal mixed layer depth being the min of the 2 first ones), barrier layer thickness, D20, D26, heat content in 0-300m, sea steric height in 0-1000m, depth of the N2 maximum in 0-200m, depth of the pycnocline maximum below the isopycnal-mixed layer depth. The output NetCDF files should encompass a short description of each variable, with units and min/max values.

7.4 Data Organization and Access

The Storm Atlas data files can be accessed both through HTTPS and FTP respectively at the following URLs:

- <https://data-maxss.ifremer.fr/>

			<p style="text-align: right;">MAXSS ATBD ESA Contract 4000132954/20/I-NB Delivery D21, Version 1.0.0 Date 06/10/2021 Page 66</p>
---	--	--	--

- <ftp://ftp.ifremer.fr/ifremer/cersat/projects/maxss/>

The data file organization is as follow:

storm_atlas

```

<track source (e.g. ibtracs)>
  <basin (e.g. north-atlantic)>
    <year>
      <storm folder>

```

where:

- *track source* is the name of the track catalogue used to provide the best tracks with which the observation data were matched
- *basin* is the basin (East-Pacific, North-Atlantic, North-Indian, South-Atlantic, South-Indian, South-Pacific, West-Pacific) of the basin where the storm starts from
- *year* is the year of the storm track's start day
- *storm folder* is the directory that contains all the collocated observation data files for a given storm.

In the case of tropical storms, and in order to ease the search for a particular storm, the *storm folder* uses the following naming convention, combining different namings for a given storm: *<track code>_<ATCF name>_<storm name>*

where:

- *track code* is the identifier of the storm in the convention of the used storm catalogue
- *ATCF name* is the storm identifier in the Automated Tropical Cyclone Forecasting (ATCF) System, when existing (empty string otherwise)
- *storm name* is the storm name as provided by the World Meteorological Organization (WMO), when existing (empty string otherwise)

For instance: **2018227N37315_AL052018_ERNESTO** (*2018227N37315* is the IBTRaCS identifier, *AL052018* the ATCF identifier and *ERNESTO* the WMO storm name).

Note that ATCF and/or WMO names may be missing for some storms, in which case they

			MAXSS ATBD ESA Contract 4000132954/20/I-NB Delivery D21, Version 1.0.0 Date 06/10/2021 Page 67
---	--	--	--

are replaced by empty strings, resulting in incomplete folder names such as:
2010200N26127__.

8 ANNEX 1 EXAMPLE OF FORMAT FOR GRIDDED DATA

```
netcdf          MAXSS_NA_2019_AL112019_ESACCI-SEASURFACESALINITY-L4-SSS-  
MERGED_OI_7DAY_RUNNINGMEAN_DAILY_25km {
```

```
dimensions:
```

```
    time = 58 ;  
    lat = 91 ;  
    lon = 84 ;  
    track_time = 38 ;  
    string88 = 88 ;  
    string8 = 8 ;  
    string1 = 1 ;  
    string2 = 2 ;  
    string3 = 3 ;  
    string6 = 6 ;  
    string4 = 4 ;  
    string13 = 13 ;
```

```
variables:
```

```
    short __eo_total_nobs(time, lat, lon) ;  
        __eo_total_nobs:long_name = "Number of SSS in the time interval" ;  
        __eo_total_nobs:valid_min = 0s ;  
        __eo_total_nobs:valid_max = 10000s ;  
    short __eo_noutliers(time, lat, lon) ;  
        __eo_noutliers:long_name = "Count of the Number of Outliers within this  
bin cell" ;  
        __eo_noutliers:valid_min = 0s ;  
        __eo_noutliers:valid_max = 10000s ;  
    float __eo_sss_random_error(time, lat, lon) ;  
        __eo_sss_random_error:_FillValue = 1.e+20f ;  
        __eo_sss_random_error:long_name = "Sea Surface Salinity Random Error" ;  
        __eo_sss_random_error:valid_min = 0.f ;  
        __eo_sss_random_error:valid_max = 100.f ;  
        __eo_sss_random_error:ancilliary = "pct_var" ;  
    double track_time(track_time) ;  
        track_time:_FillValue = 1.e+20 ;  
        track_time:units = "seconds since 1981-01-01" ;
```

```
    track_time:calendar = "proleptic_gregorian" ;
float lon(lon) ;
    lon:_FillValue = NaNf ;
    lon:least_significant_digit = 3 ;
    lon:long_name = "longitude" ;
    lon:units = "degrees_east" ;
    lon:standard_name = "longitude" ;
    lon:valid_min = -180.f ;
    lon:valid_max = 180.f ;
    lon:axis = "X" ;
    lon:valid_range = -180.f, 180.f ;
    lon:comment = "geographical coordinates, WGS84 projection" ;
float lat(lat) ;
    lat:_FillValue = NaNf ;
    lat:least_significant_digit = 3 ;
    lat:long_name = "latitude" ;
    lat:units = "degrees_north" ;
    lat:standard_name = "latitude" ;
    lat:valid_min = -90.f ;
    lat:valid_max = 90.f ;
    lat:axis = "Y" ;
    lat:valid_range = -90.f, 90.f ;
    lat:comment = "geographical coordinates, WGS84 projection" ;
    lat:coordinates = "lon lat" ;
byte data_spatial_mask(track_time, lat, lon) ;
    data_spatial_mask:flag_values = 0, 1 ;
    data_spatial_mask:flag_meanings = "out_of_storm_radius
within_storm_radius" ;
int data_nearest_time_indice(track_time) ;
byte __eo_isc_qc(time, lat, lon) ;
    __eo_isc_qc:long_name = "Ice Sea Contamination Quality Check, 0=Good;
1=Bad" ;
    __eo_isc_qc:valid_min = 0b ;
    __eo_isc_qc:valid_max = 1b ;
int data_end_time_indice(track_time) ;
byte __eo_sss_qc(time, lat, lon) ;
    __eo_sss_qc:long_name = "Sea Surface Salinity Quality, 0=Good; 1=Bad" ;
```

```

__eo_sss_qc:valid_min = 0b ;
__eo_sss_qc:valid_max = 1b ;
double time(time) ;
time:_FillValue = 1.e+20 ;
time:long_name = "time" ;
time:standard_name = "time" ;
time:axis = "T" ;
time:units = "seconds since 1981-01-01" ;
time:calendar = "proleptic_gregorian" ;
int data_start_time_indice(track_time) ;
float __eo_pct_var(time, lat, lon) ;
__eo_pct_var:_FillValue = 1.e+20f ;
__eo_pct_var:long_name = "Percentage of SSS_variability that is expected
to be not explained by the products" ;
__eo_pct_var:units = "%" ;
__eo_pct_var:valid_min = 0.f ;
__eo_pct_var:valid_max = 100.f ;
byte __eo_lsc_qc(time, lat, lon) ;
__eo_lsc_qc:long_name = "Land Sea Contamination Quality Check, 0=Good;
1=Bad" ;
__eo_lsc_qc:valid_min = 0b ;
__eo_lsc_qc:valid_max = 1b ;
float __eo_sss(time, lat, lon) ;
__eo_sss:_FillValue = 1.e+20f ;
__eo_sss:long_name = "Unbiased merged Sea Surface Salinity" ;
__eo_sss:standard_name = "sea_surface_salinity" ;
__eo_sss:valid_min = 0.f ;
__eo_sss:valid_max = 50.f ;
__eo_sss:ancilliary = "noutliers total_nobs sss_qc" ;
char data_files(time, string88) ;
data_files:_Encoding = "utf-8" ;
char __track_atcf_id(track_time, string8) ;
__track_atcf_id:long_name = "ATCF ID for the storm" ;
__track_atcf_id:standard_name =
"automated_tropical_cyclone_forecasting_system_storm_identifler" ;
__track_atcf_id:coverage_content_type = "thematicClassification" ;
__track_atcf_id:_Encoding = "utf-8" ;

```

```
float __track_lat(track_time) ;
    __track_lat:_FillValue = 1.e+20f ;
    __track_lat:long_name = "latitude" ;
    __track_lat:standard_name = "latitude" ;
    __track_lat:units = "degrees_north" ;
    __track_lat:description = "This is merged position based on the
position(s) from the various source datasets." ;
    __track_lat>Note = "Variable:lat can be missing since the tracks are
stored in a fixed 2-D grid where tracks have varying lengths" ;
    __track_lat:coverage_content_type = "coordinate" ;
float __track_lon(track_time) ;
    __track_lon:_FillValue = 1.e+20f ;
    __track_lon:long_name = "longitude" ;
    __track_lon:standard_name = "longitude" ;
    __track_lon:units = "degrees_east" ;
    __track_lon:description = "This is merged position based on the
position(s) from the various source datasets." ;
    __track_lon>Note = "Variable:lon can be missing since the tracks are
stored in a fixed 2-D grid where tracks have varying lengths" ;
    __track_lon:coverage_content_type = "coordinate" ;
char __track_record(track_time, string1) ;
    __track_record:long_name = "Storm record type" ;
    __track_record:description = "C - Closest approach to a coast, not
followed by a landfall, G - Genesis, I - An intensity peak in terms of both
pressure and wind, L - Landfall (center of system crossing a coastline), P -
Minimum in central pressure, R - Provides additional detail on the intensity of
the cyclone when rapid changes are underway, S - Change of status of the
system, T - Provides additional detail on the track (position) of the cyclone,
W - Maximum sustained wind speed" ;
    __track_record:coverage_content_type = "thematicClassification" ;
    __track_record:_Encoding = "utf-8" ;
char __track_status(track_time, string2) ;
    __track_status:long_name = "Storm status" ;
    __track_status:description = " DB - disturbance, TD - tropical
depression, TS - tropical storm, TY - typhoon, ST - super typhoon, TC -
tropical cyclone, HU, HR - hurricane, SD - subtropical depression, SS -
subtropical storm, EX - extratropical systems, PT - post tropical, IN -
inland, DS - dissipating, LO - low, WV - tropical wave, ET - extrapolated,
MD - monsoon depression, XX - unknown." ;
    __track_status:coverage_content_type = "thematicClassification" ;
    __track_status:_Encoding = "utf-8" ;
float __track_wind(track_time) ;
```

```

__track_wind:_FillValue = 1.e+20f ;
__track_wind:long_name = "Maximum sustained wind speed" ;
__track_wind:standard_name =
"tropical_cyclone_maximum_sustained_wind_speed" ;
__track_wind:units = "kts" ;
__track_wind:valid_min = 1.f ;
__track_wind:valid_max = 250.f ;
__track_wind:coverage_content_type = "physicalMeasurement" ;
float __track_pres(track_time) ;
__track_pres:_FillValue = 1.e+20f ;
__track_pres:long_name = "Minimum central pressure" ;
__track_pres:units = "mb" ;
__track_pres:valid_min = 700.f ;
__track_pres:valid_max = 1050.f ;
__track_pres:coverage_content_type = "physicalMeasurement" ;
byte __track_sshs(track_time) ;
__track_sshs:long_name = "Saffir-Simpson Hurricane Wind Scale
Category" ;
__track_sshs:units = "1" ;
__track_sshs:valid_min = -5b ;
__track_sshs:valid_max = 5b ;
__track_sshs:flag_values = -5, -4, -3, -2, -1, 0, 1, 2, 3, 4, 5 ;
__track_sshs:flag_names = "unknown_type_XX post_tropical_ET_EX_PT
misc_disturbances_WV_LO_DB_DS_IN_MD subtropical_SS_SD
tropical_depression_w_lt_34 tropical_storm_wind_35-63 hurricane_cat_1_wind_64-
82 hurricane_cat_2_wind_83-95 hurricane_cat_3_wind_96-112
hurricane_cat_4_wind_113-136 hurricane_cat_5_wind_137+" ;
__track_sshs:coverage_content_type = "thematicClassification" ;
float __track_r34_ne(track_time) ;
__track_r34_ne:_FillValue = 1.e+20f ;
__track_r34_ne:long_name = "Radius of 34 knot winds" ;
__track_r34_ne:units = "nmile" ;
__track_r34_ne:valid_min = 1.f ;
__track_r34_ne:valid_max = 1000.f ;
__track_r34_ne:coverage_content_type = "physicalMeasurement" ;
float __track_r50_ne(track_time) ;
__track_r50_ne:_FillValue = 1.e+20f ;
__track_r50_ne:long_name = "Radius of 50 knot winds" ;

```

```
__track_r50_ne:units = "nmile" ;
__track_r50_ne:valid_min = 1.f ;
__track_r50_ne:valid_max = 1000.f ;
__track_r50_ne:coverage_content_type = "physicalMeasurement" ;
float __track_r64_ne(track_time) ;
__track_r64_ne:_FillValue = 1.e+20f ;
__track_r64_ne:long_name = "Radius of 64 knot winds" ;
__track_r64_ne:units = "nmile" ;
__track_r64_ne:valid_min = 1.f ;
__track_r64_ne:valid_max = 1000.f ;
__track_r64_ne:coverage_content_type = "physicalMeasurement" ;
float __track_poci(track_time) ;
__track_poci:_FillValue = 1.e+20f ;
__track_poci:long_name = "Pressure of outermost closed isobar (not best
tracked)" ;
__track_poci:units = "mb" ;
__track_poci:valid_min = 700.f ;
__track_poci:valid_max = 1050.f ;
__track_poci:coverage_content_type = "physicalMeasurement" ;
float __track_roci(track_time) ;
__track_roci:_FillValue = 1.e+20f ;
__track_roci:long_name = "Pressure of outermost closed isobar (not best
tracked)" ;
__track_roci:units = "nmile" ;
__track_roci:valid_min = 1.f ;
__track_roci:valid_max = 1000.f ;
__track_roci:coverage_content_type = "physicalMeasurement" ;
float __track_rmw(track_time) ;
__track_rmw:_FillValue = 1.e+20f ;
__track_rmw:long_name = "Radius of maximum winds (not best tracked)" ;
__track_rmw:standard_name =
"radius_of_tropical_cyclone_maximum_sustained_wind_speed" ;
__track_rmw:units = "nmile" ;
__track_rmw:valid_min = 1.f ;
__track_rmw:valid_max = 1000.f ;
__track_rmw:coverage_content_type = "physicalMeasurement" ;
float __track_eye(track_time) ;
```

```
__track_eye:_FillValue = 1.e+20f ;
__track_eye:long_name = "Eye diameter (not best tracked)" ;
__track_eye:standard_name = "radius_of_tropical_cyclone_eye" ;
__track_eye:units = "nmile" ;
__track_eye:valid_min = 1.f ;
__track_eye:valid_max = 250.f ;
__track_eye:coverage_content_type = "physicalMeasurement" ;
float __track_gust(track_time) ;
__track_gust:_FillValue = 1.e+20f ;
__track_gust:long_name = "Maximum reported wind gust from a US agency" ;
__track_gust:standard_name = "wind_speed_of_gust" ;
__track_gust:units = "kts" ;
__track_gust:valid_min = 1.f ;
__track_gust:valid_max = 350.f ;
__track_gust:coverage_content_type = "physicalMeasurement" ;
float __track_seahgt(track_time) ;
__track_seahgt:_FillValue = 1.e+20f ;
__track_seahgt:long_name = "Wave height for given radii" ;
__track_seahgt:units = "ft" ;
__track_seahgt:valid_min = 1.f ;
__track_seahgt:valid_max = 998.f ;
__track_seahgt:coverage_content_type = "physicalMeasurement" ;
float __track_searad_ne(track_time) ;
__track_searad_ne:_FillValue = 1.e+20f ;
__track_searad_ne:long_name = "Radial extent of given sea height" ;
__track_searad_ne:units = "nmile" ;
__track_searad_ne:valid_min = 1.f ;
__track_searad_ne:valid_max = 998.f ;
__track_searad_ne:coverage_content_type = "physicalMeasurement" ;
char __track_center(track_time, string3) ;
__track_center:_Encoding = "utf-8" ;
float __track_r34_se(track_time) ;
__track_r34_se:_FillValue = 1.e+20f ;
__track_r34_se:long_name = "Radius of 34 knot winds" ;
__track_r34_se:units = "nmile" ;
__track_r34_se:valid_min = 1.f ;
```

```
__track_r34_se:valid_max = 1000.f ;
__track_r34_se:coverage_content_type = "physicalMeasurement" ;
float __track_r50_se(track_time) ;
__track_r50_se:_FillValue = 1.e+20f ;
__track_r50_se:long_name = "Radius of 50 knot winds" ;
__track_r50_se:units = "nmile" ;
__track_r50_se:valid_min = 1.f ;
__track_r50_se:valid_max = 1000.f ;
__track_r50_se:coverage_content_type = "physicalMeasurement" ;
float __track_r64_se(track_time) ;
__track_r64_se:_FillValue = 1.e+20f ;
__track_r64_se:long_name = "Radius of 64 knot winds" ;
__track_r64_se:units = "nmile" ;
__track_r64_se:valid_min = 1.f ;
__track_r64_se:valid_max = 1000.f ;
__track_r64_se:coverage_content_type = "physicalMeasurement" ;
float __track_searad_se(track_time) ;
__track_searad_se:_FillValue = 1.e+20f ;
__track_searad_se:long_name = "Radial extent of given sea height" ;
__track_searad_se:units = "nmile" ;
__track_searad_se:valid_min = 1.f ;
__track_searad_se:valid_max = 998.f ;
__track_searad_se:coverage_content_type = "physicalMeasurement" ;
float __track_r34_sw(track_time) ;
__track_r34_sw:_FillValue = 1.e+20f ;
__track_r34_sw:long_name = "Radius of 34 knot winds" ;
__track_r34_sw:units = "nmile" ;
__track_r34_sw:valid_min = 1.f ;
__track_r34_sw:valid_max = 1000.f ;
__track_r34_sw:coverage_content_type = "physicalMeasurement" ;
float __track_r50_sw(track_time) ;
__track_r50_sw:_FillValue = 1.e+20f ;
__track_r50_sw:long_name = "Radius of 50 knot winds" ;
__track_r50_sw:units = "nmile" ;
__track_r50_sw:valid_min = 1.f ;
__track_r50_sw:valid_max = 1000.f ;
```

```
__track_r50_sw:coverage_content_type = "physicalMeasurement" ;
float __track_r64_sw(track_time) ;
__track_r64_sw:_FillValue = 1.e+20f ;
__track_r64_sw:long_name = "Radius of 64 knot winds" ;
__track_r64_sw:units = "nmile" ;
__track_r64_sw:valid_min = 1.f ;
__track_r64_sw:valid_max = 1000.f ;
__track_r64_sw:coverage_content_type = "physicalMeasurement" ;
float __track_searad_sw(track_time) ;
__track_searad_sw:_FillValue = 1.e+20f ;
__track_searad_sw:long_name = "Radial extent of given sea height" ;
__track_searad_sw:units = "nmile" ;
__track_searad_sw:valid_min = 1.f ;
__track_searad_sw:valid_max = 998.f ;
__track_searad_sw:coverage_content_type = "physicalMeasurement" ;
float __track_r34_nw(track_time) ;
__track_r34_nw:_FillValue = 1.e+20f ;
__track_r34_nw:long_name = "Radius of 34 knot winds" ;
__track_r34_nw:units = "nmile" ;
__track_r34_nw:valid_min = 1.f ;
__track_r34_nw:valid_max = 1000.f ;
__track_r34_nw:coverage_content_type = "physicalMeasurement" ;
float __track_r50_nw(track_time) ;
__track_r50_nw:_FillValue = 1.e+20f ;
__track_r50_nw:long_name = "Radius of 50 knot winds" ;
__track_r50_nw:units = "nmile" ;
__track_r50_nw:valid_min = 1.f ;
__track_r50_nw:valid_max = 1000.f ;
__track_r50_nw:coverage_content_type = "physicalMeasurement" ;
float __track_r64_nw(track_time) ;
__track_r64_nw:_FillValue = 1.e+20f ;
__track_r64_nw:long_name = "Radius of 64 knot winds" ;
__track_r64_nw:units = "nmile" ;
__track_r64_nw:valid_min = 1.f ;
__track_r64_nw:valid_max = 1000.f ;
__track_r64_nw:coverage_content_type = "physicalMeasurement" ;
```

```
float __track_searad_nw(track_time) ;
    __track_searad_nw:_FillValue = 1.e+20f ;
    __track_searad_nw:long_name = "Radial extent of given sea height" ;
    __track_searad_nw:units = "nmile" ;
    __track_searad_nw:valid_min = 1.f ;
    __track_searad_nw:valid_max = 998.f ;
    __track_searad_nw:coverage_content_type = "physicalMeasurement" ;
char __track_basin(track_time, string2) ;
    __track_basin:long_name = "Current basin" ;
    __track_basin:Note = "EP=East_Pacific NA=North_Atlantic NI=North_Indian
SA=South_Atlantic SI=South_Indian SP=South_Pacific WP=Western_Pacific" ;
    __track_basin:coverage_content_type = "thematicClassification" ;
    __track_basin:_Encoding = "utf-8" ;
char __track_name(track_time, string6) ;
    __track_name:long_name = "Name of system" ;
    __track_name:description = "May be a combination of names from different
agencies" ;
    __track_name:coverage_content_type = "thematicClassification" ;
    __track_name:_Encoding = "utf-8" ;
char __track_track_type(track_time, string4) ;
    __track_track_type:long_name = "Name of track type" ;
    __track_track_type:description = "Tracks are either MAIN or SPUR. Spur
tracks have points that either merge with or split from another track (or
both). Main tracks are regular tracks. Spur tracks should be treated with
caution." ;
    __track_track_type:coverage_content_type = "thematicClassification" ;
    __track_track_type:_Encoding = "utf-8" ;
char __track_main_track_sid(track_time, string13) ;
    __track_main_track_sid:long_name = "SID of the main track associated
with this storm." ;
    __track_main_track_sid:description = "If this track is a main, then this
is the same as serial_id. If a spur, it namesthe associated main track." ;
    __track_main_track_sid:coverage_content_type =
"thematicClassification" ;
    __track_main_track_sid:_Encoding = "utf-8" ;
float __track_dist2land(track_time) ;
    __track_dist2land:_FillValue = 1.e+20f ;
    __track_dist2land:long_name = "Distance to Land at current location" ;
    __track_dist2land:units = "km" ;
```

			MAXSS ATBD ESA Contract 4000132954/20/I-NB Delivery D21, Version 1.0.0 Date 06/10/2021 Page 78
---	--	--	--

```

__track_dist2land:description = "Distance to the nearest land point.
Also acts as a land mask since 0km = over land. Uses present location ONLY." ;
__track_dist2land:coverage_content_type = "modelResult" ;
float __track_landfall(track_time) ;
__track_landfall:_FillValue = 1.e+20f ;
__track_landfall:long_name = "Minimum distance to land between current
location and next." ;
__track_landfall:units = "km" ;
__track_landfall:description = "Describes landfall conditions between
the present observation and the next (usually 3 hours) by providing minimum
distance to land. So a value of 0 implies that the storm crosses a coastline
prior to the next observation." ;
__track_landfall:coverage_content_type = "modelResult" ;
float __track_storm_speed(track_time) ;
__track_storm_speed:_FillValue = 1.e+20f ;
__track_storm_speed:long_name = "Storm translation speed" ;
__track_storm_speed:units = "kts" ;
__track_storm_speed:valid_min = 0.f ;
__track_storm_speed:valid_max = 998.f ;
__track_storm_speed:coverage_content_type = "physicalMeasurement" ;
float __track_storm_dir(track_time) ;
__track_storm_dir:_FillValue = 1.e+20f ;
__track_storm_dir:long_name = "Storm translation direction" ;
__track_storm_dir:units = "degrees" ;
__track_storm_dir:valid_min = 0.f ;
__track_storm_dir:valid_max = 360.f ;
__track_storm_dir>Note = "Unit is degrees east of north" ;
__track_storm_dir:coverage_content_type = "physicalMeasurement" ;
float __track_ci(track_time) ;
__track_ci:_FillValue = 1.e+20f ;
__track_ci:long_name = "Dvorak Current Intensity (CI)" ;
__track_ci:standard_name =
"dvorak_tropical_cyclone_current_intensity_number" ;
__track_ci:units = "1" ;
__track_ci:valid_min = 0.f ;
__track_ci:valid_max = 8.f ;
__track_ci:coverage_content_type = "thematicClassification" ;
float __track_dp(track_time) ;

```

```
__track_dp:_FillValue = 1.e+20f ;
__track_dp:long_name = "Storm pressure drop" ;
__track_dp:units = "mb" ;
__track_dp:valid_min = 1.f ;
__track_dp:valid_max = 250.f ;
__track_dp:coverage_content_type = "physicalMeasurement" ;
float __track_tnum(track_time) ;
__track_tnum:_FillValue = 1.e+20f ;
__track_tnum:long_name = "Dvorak T number" ;
__track_tnum:units = "1" ;
__track_tnum:valid_min = 0.f ;
__track_tnum:valid_max = 8.f ;
__track_tnum:coverage_content_type = "thematicClassification" ;
float __track_gust_per(track_time) ;
__track_gust_per:_FillValue = 1.e+20f ;
__track_gust_per:long_name = "Time period of the wind gust from BoM" ;
__track_gust_per:units = "second" ;
__track_gust_per:valid_min = 1.f ;
__track_gust_per:valid_max = 9999.f ;
__track_gust_per:coverage_content_type = "physicalMeasurement" ;
float __track_r50_dir(track_time) ;
__track_r50_dir:_FillValue = 1.e+20f ;
__track_r50_dir:long_name = "Direction of maximum radius of 50 knots
winds" ;
__track_r50_dir:valid_min = 0.f ;
__track_r50_dir:valid_max = 9.f ;
__track_r50_dir:flag_values = 1, 2, 3, 4, 5, 6, 7, 8, 9 ;
__track_r50_dir:flag_names = "Northeast East Southeast South Southwest
West Northwest North Symmetric_Circle" ;
__track_r50_dir:coverage_content_type = "thematicClassification" ;
float __track_r50_long(track_time) ;
__track_r50_long:_FillValue = 1.e+20f ;
__track_r50_long:long_name = "Maximum radius of 50 knots winds" ;
__track_r50_long:units = "nmile" ;
__track_r50_long:valid_min = 1.f ;
__track_r50_long:valid_max = 1000.f ;
__track_r50_long:coverage_content_type = "physicalMeasurement" ;
```

```
float __track_r50_short(track_time) ;
    __track_r50_short:_FillValue = 1.e+20f ;
    __track_r50_short:long_name = "Minimum radius of 50 knots winds" ;
    __track_r50_short:units = "nmile" ;
    __track_r50_short:valid_min = 1.f ;
    __track_r50_short:valid_max = 1000.f ;
    __track_r50_short:coverage_content_type = "physicalMeasurement" ;
float __track_r30_dir(track_time) ;
    __track_r30_dir:_FillValue = 1.e+20f ;
    __track_r30_dir:long_name = "Direction of maximum radius of 30 knots
winds" ;
    __track_r30_dir:valid_min = 0.f ;
    __track_r30_dir:valid_max = 9.f ;
    __track_r30_dir:flag_values = 1, 2, 3, 4, 5, 6, 7, 8, 9 ;
    __track_r30_dir:flag_names = "Northeast East Southeast South Southwest
West Northwest North Symmetric_Circle" ;
    __track_r30_dir:coverage_content_type = "thematicClassification" ;
float __track_r30_long(track_time) ;
    __track_r30_long:_FillValue = 1.e+20f ;
    __track_r30_long:long_name = "Direction of maximum radius of 30 knots
winds" ;
    __track_r30_long:units = "nmile" ;
    __track_r30_long:valid_min = 1.f ;
    __track_r30_long:valid_max = 1000.f ;
    __track_r30_long:coverage_content_type = "physicalMeasurement" ;
float __track_r30_short(track_time) ;
    __track_r30_short:_FillValue = 1.e+20f ;
    __track_r30_short:long_name = "Minimum radius of 30 knots winds" ;
    __track_r30_short:units = "nmile" ;
    __track_r30_short:valid_min = 1.f ;
    __track_r30_short:valid_max = 1000.f ;
    __track_r30_short:coverage_content_type = "physicalMeasurement" ;

// global attributes:
    :__eo_creation_time = "27-Apr-2021 02:09:31" ;
    :__eo_title = "ESA CCI Sea Surface Salinity ECV produced at a spatial
resolution of 50 km and time resolution of one week and spatially resampled on
25 km EASE grid and 1 day of time sampling" ;
```

```
:__eo_institution = "ACRI-ST, LOCEAN" ;
__eo_source = "SMOS CCI v3 L20S reprocessing (ERA5,ref OTT SSS:ISAS,
RFI filtering) from DPGS L1 v620, L20S v662 modified as in
DOI:10.1109/tgrs.2020.3030488, SMAP L2 RSS v4.0 - DOI:10.5067/SMP40-2SOCS,
Aquarius L3 v5.0 - DOI:10.5067/AQR50-3SQCS" ;
__eo_history = " " ;
__eo_references = "http://cci.esa.int/salinity - DOI:XXXXX" ;
__eo_product_version = "3.2" ;
__eo_format_version = "CCI Data Standards v2.2" ;
__eo_Conventions = "CF-1.8" ;
__eo_summary = "ESA CCI Sea Surface Salinity" ;
__eo_keywords = "Ocean, Ocean Salinity, Sea Surface Salinity,
Satellite" ;
__eo_key_variables = "sss,sss_random_error" ;
__eo_naming_authority = "European Space Agency - ESA Climate Office" ;
__eo_keywords_vocabulary = "NASA Global Change Master Directory (GCMD)
Science Keywords" ;
__eo_cdm_data_type = "Grid" ;
__eo_comment = "Data are based on a 7-day running mean objectively
interpolated" ;
__eo_creator_name = "ACRI-ST, LOCEAN" ;
__eo_creator_email = "jean-luc.vergely@acri-st.fr" ;
__eo_creator_url = "http://cci.esa.int/salinity" ;
__eo_project = "Climate Change Initiative - European Space Agency" ;
__eo_geospatial_lat_min = -83.5171356201172 ;
__eo_geospatial_lat_max = 83.5171356201172 ;
__eo_geospatial_lon_min = -179.870315551758 ;
__eo_geospatial_lon_max = 179.870315551758 ;
__eo_license = "ESA CCI Data Policy: free and open access" ;
__eo_standard_name_vocabulary = "NetCDF Climate and Forecast (CF)
Metadata Convention version 1.8" ;
__eo_platform = "PROTEUS,SAC-D,SMAP" ;
__eo_sensor = "SMOS/MIRAS,Aquarius,SMAP" ;
__eo_spatial_resolution = "50km" ;
__eo_geospatial_lat_units = "degrees_north" ;
__eo_geospatial_lon_units = "degrees_east" ;
__eo_geospatial_vertical_min = 0. ;
__eo_geospatial_vertical_max = 0. ;
__eo_date_created = "20210427T020931Z" ;
```

```
:__eo_date_modified = "" ;
:__eo_time_coverage_start = "2019-08-29T00:00:00Z" ;
:__eo_time_coverage_end = "2019-09-05T23:59:59Z" ;
:__eo_time_coverage_duration = "P7D" ;
:__eo_time_coverage_resolution = "P1D" ;
      :__eo_id = "ESACCI-SEASURFACESALINITY-L4-SSS-
MERGED_OI_7DAY_RUNNINGMEAN_DAILY_25km-20190902-fv3.2.nc" ;
:__eo_tracking_id = "0bfd72ed-112a-4210-9342-6c6e0b891c2b" ;
:__eo_spatial_grid = "25km EASE 2 cylindrical grid" ;
:time_coverage_start = "2019-09-02T00:00:00Z" ;
:time_coverage_end = "2019-10-29T00:00:00Z" ;
:storm_atcf_name = "AL112019" ;
:storm_name = "IMELDA" ;
:storm_basin = "NA" ;
      :eo_dataset_id = "ESACCI-SEASURFACESALINITY-L4-SSS-
MERGED_OI_7DAY_RUNNINGMEAN_DAILY_25km" ;
      :id = "MAXSS-StormAtlas-ESACCI-SEASURFACESALINITY-L4-SSS-
MERGED_OI_7DAY_RUNNINGMEAN_DAILY_25km-v1.0" ;
      :summary = "data extracted from ESACCI-SEASURFACESALINITY-L4-SSS-
MERGED_OI_7DAY_RUNNINGMEAN_DAILY_25km dataset for MAXSS Storm Atlas version
1" ;
:geospatial_lat_min = 19.49018f ;
:geospatial_lat_max = 39.84907f ;
:geospatial_lon_min = -105.951f ;
:geospatial_lon_max = -84.42363f ;
:geospatial_bounds = "POLYGON ((-84.42362976074219 19.49017906188965, -
84.42362976074219 39.84907150268555, -105.9510116577148 39.84907150268555, -
105.9510116577148 19.49017906188965, -84.42362976074219 19.49017906188965))" ;
:uuid = "7ec375b4-e39d-4c6f-a697-52e3ed5ceb7f" ;
:history = "2021-09-07T10:39:31: Initial creation" ;
:date_created = "2021-09-07T10:39:31" ;
:date_modified = "2021-09-07T10:39:31" ;
:date_issued = "2021-09-07T10:39:31" ;
:naming_authority = "fr.ifremer.cersat" ;
:cdm_data_type = "grid" ;
:acknowledgement = "Please acknowledge the use of these data with the
following statement: these data were produced by the Centre de Recherche et
d'Exploitation Satellitaire (CERSAT), at IFREMER, Plouzane (France) for ESA
funded project MAXSS (Marine Atmosphere extreme Satellite Synergy)" ;
:Conventions = "CF 1.7, ACDD 1.3, ISO 8601" ;
```

			MAXSS ATBD ESA Contract 4000132954/20/I-NB Delivery D21, Version 1.0.0 Date 06/10/2021 Page 83
---	--	--	--

```

:Metadata_Conventions = "Climate and Forecast (CF) 1.7, Attribute
Convention for Data Discovery (ACDD) 1.3" ;
:standard_name_vocabulary = "NetCDF Climate and Forecast (CF) Metadata
Convention" ;
:keywords_vocabulary = "NASA Global Change Master Directory (GCMD)
Science Keywords" ;
:format_version = "MAXSS v1.0" ;
:platform_vocabulary = "CEOS" ;
:instrument_vocabulary = "CEOS" ;
:institution = "European Space Agency, Institut Francais de Recherche et
d'Exploitation de la Mer (Ifremer)" ;
:institution_abbreviation = "ESA, Ifremer" ;
:project = "ESA / Marine Atmosphere extreme Satellite Synergy (MAXSS)" ;
:license = "data use free and open." ;
:publisher_name = "CERSAT" ;
:publisher_url = "http://cersat.ifremer.fr" ;
:publisher_email = "cersat@ifremer.fr" ;
:publisher_institution = "Ifremer" ;
:publisher_type = "institution" ;
:creator_name = "Jean-François Piollé" ;
:creator_email = "jfpiolle@ifremer.fr" ;
:creator_type = "person" ;
:creator_institution = "Ifremer" ;
:contributor_institution = "ESA" ;
:contributor_type = "institution" ;
:contributor_role = "funding" ;
:technical_support_contact = "cersat@ifremer.fr" ;
:scientific_support_contact = "Jean-François Piollé
(jfpiolle@ifremer.fr)" ;
:references = "https://www.maxss.org" ;
:processing_software = "maxss" ;
:product_version = "1.0.0" ;
:source = "maxss" ;
:source_version = "1.0.0" ;
:geospatial_lat_units = "degrees" ;
:geospatial_lon_units = "degrees" ;
:geospatial_bounds_crs = "WGS84" ;
}

```



9 ANNEX 2: EXAMPLE OF FORMAT FOR ALONG-TRACK DATA

```
netcdf MAXSS_SA_2010_SL502010_ESACCI-SEASTATE-L2P-SWH-Jason-1 {
```

```
dimensions:
```

```
  obs = 7 ;  
  time = 333 ;  
  string55 = 55 ;  
  string33 = 33 ;  
  track_time = 115 ;  
  string8 = 8 ;  
  string2 = 2 ;  
  string9 = 9 ;  
  string4 = 4 ;  
  string13 = 13 ;
```

```
variables:
```

```
  double __eo_swh_rms(obs, time) ;  
    __eo_swh_rms:_FillValue = 1.e+20 ;  
    __eo_swh_rms:least_significant_digit = 3LL ;  
    __eo_swh_rms:authority = "CF 1.7" ;  
    __eo_swh_rms:long_name = "RMS of the Ku band significant wave height  
(from high frequency measurements)" ;  
    __eo_swh_rms:units = "m" ;  
    __eo_swh_rms:coverage_content_type = "auxiliaryInformation" ;  
    __eo_swh_rms:band = "Ku" ;  
    __eo_swh_rms:coordinates = "lon lat" ;  
  ushort __eo_swh_rejection_flags(obs, time) ;  
    __eo_swh_rejection_flags:_FillValue = 65535US ;  
    __eo_swh_rejection_flags:least_significant_digit = 0LL ;  
    __eo_swh_rejection_flags:authority = "CF 1.7" ;  
    __eo_swh_rejection_flags:long_name = "consolidated instrument and ice  
flags" ;  
    __eo_swh_rejection_flags:flag_meanings = "not_water sea_ice swh_validity  
sigma0_validity waveform_validity ssh_validity swh_rms_outlier swh_outlier" ;  
    __eo_swh_rejection_flags:flag_masks = 1LL, 2LL, 4LL, 8LL, 16LL, 32LL,  
64LL, 128LL ;  
    __eo_swh_rejection_flags:coverage_content_type = "qualityInformation" ;
```

```
__eo_swh_rejection_flags:band = "Ku" ;
__eo_swh_rejection_flags:rms_threshold_lut = "cci_swh_rms_LUT_jason-
1.dat" ;
__eo_swh_rejection_flags:coordinates = "lon lat" ;
float __eo_mean_wave_direction_model(obs, time) ;
__eo_mean_wave_direction_model:_FillValue = 1.e+20f ;
__eo_mean_wave_direction_model:least_significant_digit = 3LL ;
__eo_mean_wave_direction_model:long_name = "Mean wave direction" ;
__eo_mean_wave_direction_model:units = "degree" ;
__eo_mean_wave_direction_model:source = "Copernicus ERA5 Reanalysis by
ECMWF" ;
__eo_mean_wave_direction_model:coordinates = "lat lon" ;
float __eo_mean_wave_period_model(obs, time) ;
__eo_mean_wave_period_model:_FillValue = 1.e+20f ;
__eo_mean_wave_period_model:least_significant_digit = 3LL ;
__eo_mean_wave_period_model:long_name = "Mean wave period" ;
__eo_mean_wave_period_model:units = "s" ;
__eo_mean_wave_period_model:source = "Copernicus ERA5 Reanalysis by
ECMWF" ;
__eo_mean_wave_period_model:coordinates = "lat lon" ;
float __eo_wind_speed_model_u(obs, time) ;
__eo_wind_speed_model_u:_FillValue = 1.e+20f ;
__eo_wind_speed_model_u:least_significant_digit = 3LL ;
__eo_wind_speed_model_u:units = "m s-1" ;
__eo_wind_speed_model_u:long_name = "10 metre U wind component" ;
__eo_wind_speed_model_u:source = "Copernicus ERA5 Reanalysis by ECMWF" ;
__eo_wind_speed_model_u:coordinates = "lon lat" ;
float __eo_primary_swell_direction_model(obs, time) ;
__eo_primary_swell_direction_model:_FillValue = 1.e+20f ;
__eo_primary_swell_direction_model:least_significant_digit = 3LL ;
__eo_primary_swell_direction_model:long_name = "Mean wave direction of
first swell partition" ;
__eo_primary_swell_direction_model:units = "degree" ;
__eo_primary_swell_direction_model:source = "Copernicus ERA5 Reanalysis
by ECMWF" ;
__eo_primary_swell_direction_model:coordinates = "lat lon" ;
double __eo_sea_ice_fraction(obs, time) ;
__eo_sea_ice_fraction:_FillValue = 1.e+20 ;
```

```
__eo_sea_ice_fraction:least_significant_digit = 2LL ;
__eo_sea_ice_fraction:authority = "CF 1.7" ;
__eo_sea_ice_fraction:long_name = "sea ice fraction" ;
__eo_sea_ice_fraction:units = "1" ;
__eo_sea_ice_fraction:coverage_content_type = "auxiliaryInformation" ;
__eo_sea_ice_fraction:standard_name = "sea_ice_area_fraction" ;
__eo_sea_ice_fraction:coordinates = "lon lat" ;
float __eo_surface_air_temperature(obs, time) ;
__eo_surface_air_temperature:_FillValue = 1.e+20f ;
__eo_surface_air_temperature:least_significant_digit = 3LL ;
__eo_surface_air_temperature:units = "K" ;
__eo_surface_air_temperature:long_name = "2 metre temperature" ;
__eo_surface_air_temperature:source = "Copernicus ERA5 Reanalysis by
ECMWF" ;
__eo_surface_air_temperature:coordinates = "lon lat" ;
ubyte __eo_sigma0_num_valid(obs, time) ;
__eo_sigma0_num_valid:_FillValue = 255UB ;
__eo_sigma0_num_valid:least_significant_digit = 0LL ;
__eo_sigma0_num_valid:authority = "CF 1.7" ;
__eo_sigma0_num_valid:long_name = "number of high frequency valid points
used to compute Ku band backscatter coefficient" ;
__eo_sigma0_num_valid:units = "1" ;
__eo_sigma0_num_valid:coverage_content_type = "auxiliaryInformation" ;
__eo_sigma0_num_valid:band = "Ku" ;
__eo_sigma0_num_valid:coordinates = "lon lat" ;
double __eo_distance_to_coast(obs, time) ;
__eo_distance_to_coast:_FillValue = 1.e+20 ;
__eo_distance_to_coast:coverage_content_type = "auxiliaryInformation" ;
__eo_distance_to_coast:source = "Distance to Nearest Coastline: 0.01-
Degree Grid, by NASA Goddard Space Flight Center (GSFC) Ocean Color Group" ;
__eo_distance_to_coast:institution = "NASA/GFSC" ;
__eo_distance_to_coast:long_name = "distance to nearest coast" ;
__eo_distance_to_coast:units = "m" ;
__eo_distance_to_coast:coordinates = "lat lon" ;
float __eo_peak_wave_period_model(obs, time) ;
__eo_peak_wave_period_model:_FillValue = 1.e+20f ;
__eo_peak_wave_period_model:least_significant_digit = 3LL ;
```

```
__eo_peak_wave_period_model:long_name = "Peak wave period" ;
__eo_peak_wave_period_model:units = "s" ;
__eo_peak_wave_period_model:source = "Copernicus ERA5 Reanalysis by
ECMWF" ;
__eo_peak_wave_period_model:coordinates = "lat lon" ;
float __eo_surface_air_pressure(obs, time) ;
__eo_surface_air_pressure:_FillValue = 1.e+20f ;
__eo_surface_air_pressure:least_significant_digit = 3LL ;
__eo_surface_air_pressure:units = "Pa" ;
__eo_surface_air_pressure:long_name = "Mean sea level pressure" ;
__eo_surface_air_pressure:standard_name =
"air_pressure_at_mean_sea_level" ;
__eo_surface_air_pressure:source = "Copernicus ERA5 Reanalysis by ECMWF"
;
__eo_surface_air_pressure:coordinates = "lon lat" ;
float __eo_swh_denoised(obs, time) ;
__eo_swh_denoised:_FillValue = 1.e+20f ;
__eo_swh_denoised:least_significant_digit = 3LL ;
__eo_swh_denoised:long_name = "Ku band adjusted significant wave height"
;
__eo_swh_denoised:units = "m" ;
__eo_swh_denoised:standard_name =
"sea_surface_wave_significant_height" ;
__eo_swh_denoised:authority = "CF 1.7" ;
__eo_swh_denoised:comment = "EMD denoising by Quilfen et al. applied to
swh_adjusted variable" ;
__eo_swh_denoised:ancillary_variables = "swh_quality
swh_rejection_flags" ;
__eo_swh_denoised:coverage_content_type = "physicalMeasurement" ;
__eo_swh_denoised:band = "Ku" ;
__eo_swh_denoised:adjustment_lut = "tab_calibration_lut_jason-1.dat" ;
__eo_swh_denoised:adjustment_reference = "CCI Sea State v2 Product
Specification Document, 2021" ;
__eo_swh_denoised:coordinates = "lon lat" ;
float __eo_bathymetry(obs, time) ;
__eo_bathymetry:_FillValue = 1.e+20f ;
__eo_bathymetry:coverage_content_type = "auxiliaryInformation" ;
__eo_bathymetry:source = "The GEBCO_2014 Grid, version 20150318,
www.gebco.net, doi:10.1002/2015EA000107" ;
```

```
__eo_bathymetry:institution = "IOC/IHO" ;
__eo_bathymetry:authority = "CF-1.7" ;
__eo_bathymetry:long_name = "ocean depth" ;
__eo_bathymetry:units = "m" ;
__eo_bathymetry:standard_name = "sea_floor_depth_below_mean_sea_level" ;
__eo_bathymetry:coordinates = "lon lat" ;
float __eo_swh_noise(obs, time) ;
__eo_swh_noise:_FillValue = 1.e+20f ;
__eo_swh_noise:least_significant_digit = 3LL ;
__eo_swh_noise:long_name = "high-frequency noise attached to
swh_adjusted" ;
__eo_swh_noise:units = "m" ;
__eo_swh_noise:authority = "CF 1.7" ;
__eo_swh_noise:comment = "EMD denoising by Quilfen et al. applied to
swh_adjusted variable" ;
__eo_swh_noise:ancillary_variables = "swh_quality swh_rejection_flags" ;
__eo_swh_noise:coverage_content_type = "physicalMeasurement" ;
__eo_swh_noise:band = "Ku" ;
__eo_swh_noise:adjustment_lut = "tab_calibration_lut_jason-1.dat" ;
__eo_swh_noise:adjustment_reference = "CCI Sea State v2 Product
Specification Document, 2021" ;
__eo_swh_noise:coordinates = "lon lat" ;
double __eo_wind_speed_alt(obs, time) ;
__eo_wind_speed_alt:_FillValue = 1.e+20 ;
__eo_wind_speed_alt:least_significant_digit = 3LL ;
__eo_wind_speed_alt:standard_name = "wind_speed" ;
__eo_wind_speed_alt:authority = "CF 1.7" ;
__eo_wind_speed_alt:long_name = "wind speed from Ku band altimeter, as
in GDR" ;
__eo_wind_speed_alt:units = "m s-1" ;
__eo_wind_speed_alt:ancillary_variables = "wind_speed_alt_quality" ;
__eo_wind_speed_alt:coverage_content_type = "physicalMeasurement" ;
__eo_wind_speed_alt:band = "Ku" ;
__eo_wind_speed_alt:coordinates = "lon lat" ;
float __eo_primary_swell_swh_model(obs, time) ;
__eo_primary_swell_swh_model:_FillValue = 1.e+20f ;
__eo_primary_swell_swh_model:least_significant_digit = 3LL ;
__eo_primary_swell_swh_model:long_name = "Significant wave height of
```

			MAXSS ATBD ESA Contract 4000132954/20/I-NB Delivery D21, Version 1.0.0 Date 06/10/2021 Page 90
---	--	--	--

```

first swell partition" ;
    __eo_primary_swell_swh_model:units = "m" ;
    __eo_primary_swell_swh_model:source = "Copernicus ERA5 Reanalysis by
ECMWF" ;
    __eo_primary_swell_swh_model:coordinates = "lat lon" ;
ubyte __eo_swh_num_valid(obs, time) ;
    __eo_swh_num_valid:_FillValue = 255UB ;
    __eo_swh_num_valid:least_significant_digit = 0LL ;
    __eo_swh_num_valid:authority = "CF 1.7" ;
    __eo_swh_num_valid:long_name = "number of high frequency valid points
used to compute Ku band significant wave height" ;
    __eo_swh_num_valid:units = "1" ;
    __eo_swh_num_valid:coverage_content_type = "auxiliaryInformation" ;
    __eo_swh_num_valid:band = "Ku" ;
    __eo_swh_num_valid:coordinates = "lon lat" ;
double __eo_total_column_liquid_water_content_rad(obs, time) ;
    __eo_total_column_liquid_water_content_rad:_FillValue = 1.e+20 ;
    __eo_total_column_liquid_water_content_rad:least_significant_digit = 3LL
;
    __eo_total_column_liquid_water_content_rad:standard_name =
"atmosphere_cloud_liquid_water_content" ;
    __eo_total_column_liquid_water_content_rad:authority = "CF 1.7" ;
    __eo_total_column_liquid_water_content_rad:long_name = "radiometer
liquid water content" ;
    __eo_total_column_liquid_water_content_rad:units = "kg m-2" ;
    __eo_total_column_liquid_water_content_rad:coverage_content_type =
"physicalMeasurement" ;
    __eo_total_column_liquid_water_content_rad:coordinates = "lon lat" ;
double __eo_swh(obs, time) ;
    __eo_swh:_FillValue = 1.e+20 ;
    __eo_swh:least_significant_digit = 3LL ;
    __eo_swh:standard_name = "sea_surface_wave_significant_height" ;
    __eo_swh:authority = "CF 1.7" ;
    __eo_swh:long_name = "Ku band significant wave height" ;
    __eo_swh:units = "m" ;
    __eo_swh:comment = "All instrumental corrections included. As available
from retracker and unedited." ;
    __eo_swh:ancillary_variables = "swh_quality swh_rejection_flags" ;
    __eo_swh:coverage_content_type = "physicalMeasurement" ;

```

```
__eo_swh:band = "Ku" ;
__eo_swh:coordinates = "lon lat" ;
double __eo_sigma0_rms(obs, time) ;
__eo_sigma0_rms:_FillValue = 1.e+20 ;
__eo_sigma0_rms:least_significant_digit = 3LL ;
__eo_sigma0_rms:authority = "CF 1.7" ;
__eo_sigma0_rms:long_name = "RMS of the high frequency Ku band
backscatter coefficient" ;
__eo_sigma0_rms:units = "dB" ;
__eo_sigma0_rms:coverage_content_type = "auxiliaryInformation" ;
__eo_sigma0_rms:band = "Ku" ;
__eo_sigma0_rms:coordinates = "lon lat" ;
float __eo_swh_model(obs, time) ;
__eo_swh_model:_FillValue = 1.e+20f ;
__eo_swh_model:least_significant_digit = 3LL ;
__eo_swh_model:long_name = "Significant height of combined wind waves
and swell" ;
__eo_swh_model:units = "m" ;
__eo_swh_model:source = "Copernicus ERA5 Reanalysis by ECMWF" ;
__eo_swh_model:coordinates = "lat lon" ;
double __eo_sigma0(obs, time) ;
__eo_sigma0:_FillValue = 1.e+20 ;
__eo_sigma0:least_significant_digit = 3LL ;
__eo_sigma0:standard_name =
"surface_backwards_scattering_coefficient_of_radar_wave" ;
__eo_sigma0:authority = "CF 1.7" ;
__eo_sigma0:long_name = "Ku band backscatter coefficient" ;
__eo_sigma0:units = "dB" ;
__eo_sigma0:comment = "All instrumental corrections included. As
available from retracker and unedited.." ;
__eo_sigma0:ancillary_variables = "sigma0_quality" ;
__eo_sigma0:coverage_content_type = "physicalMeasurement" ;
__eo_sigma0:band = "Ku" ;
__eo_sigma0:coordinates = "lon lat" ;
float __eo_swh_denoised_uncertainty(obs, time) ;
__eo_swh_denoised_uncertainty:_FillValue = 1.e+20f ;
__eo_swh_denoised_uncertainty:least_significant_digit = 3LL ;
__eo_swh_denoised_uncertainty:long_name = "uncertainty attached to
```

			MAXSS ATBD ESA Contract 4000132954/20/I-NB Delivery D21, Version 1.0.0 Date 06/10/2021 Page 92
---	--	--	--

```

swh_adjusted" ;
    __eo_swh_denoised_uncertainty:units = "m" ;
    __eo_swh_denoised_uncertainty:authority = "CF 1.7" ;
    __eo_swh_denoised_uncertainty:comment = "EMD denoising by Quilfen et al.
applied to sw_h_adjusted variable" ;
    __eo_swh_denoised_uncertainty:ancillary_variables = "sw_h_quality
sw_h_rejection_flags" ;
    __eo_swh_denoised_uncertainty:coverage_content_type =
"physicalMeasurement" ;
    __eo_swh_denoised_uncertainty:band = "Ku" ;
    __eo_swh_denoised_uncertainty:adjustment_lut =
"tab_calibration_lut_jason-1.dat" ;
    __eo_swh_denoised_uncertainty:adjustment_reference = "CCI Sea State v2
Product Specification Document, 2021" ;
    __eo_swh_denoised_uncertainty:coordinates = "lon lat" ;
float __eo_wind_speed_model_v(obs, time) ;
    __eo_wind_speed_model_v:_FillValue = 1.e+20f ;
    __eo_wind_speed_model_v:least_significant_digit = 3LL ;
    __eo_wind_speed_model_v:units = "m s-1" ;
    __eo_wind_speed_model_v:long_name = "10 metre V wind component" ;
    __eo_wind_speed_model_v:source = "Copernicus ERA5 Reanalysis by ECMWF" ;
    __eo_wind_speed_model_v:coordinates = "lon lat" ;
ubyte __eo_swh_quality(obs, time) ;
    __eo_swh_quality:least_significant_digit = 0LL ;
    __eo_swh_quality:authority = "CF 1.7" ;
    __eo_swh_quality:long_name = "quality of Ku band significant wave height
measurement" ;
    __eo_swh_quality:flag_values = 0LL, 1LL, 2LL, 3LL ;
    __eo_swh_quality:flag_meanings = "undefined bad acceptable good" ;
    __eo_swh_quality:coverage_content_type = "qualityInformation" ;
    __eo_swh_quality:band = "Ku" ;
    __eo_swh_quality:coordinates = "lon lat" ;
double __eo_swh_adjusted(obs, time) ;
    __eo_swh_adjusted:_FillValue = 1.e+20 ;
    __eo_swh_adjusted:least_significant_digit = 3LL ;
    __eo_swh_adjusted:standard_name =
"sea_surface_wave_significant_height" ;
    __eo_swh_adjusted:authority = "CF 1.7" ;
    __eo_swh_adjusted:long_name = "Ku band adjusted significant wave height"

```

			MAXSS ATBD ESA Contract 4000132954/20/I-NB Delivery D21, Version 1.0.0 Date 06/10/2021 Page 93
---	--	--	--

```

;
    __eo_swh_adjusted:units = "m" ;
    __eo_swh_adjusted:comment = "All instrumental corrections included.
Adjusted and unedited" ;
    __eo_swh_adjusted:ancillary_variables = "swh_quality
swh_rejection_flags" ;
    __eo_swh_adjusted:coverage_content_type = "physicalMeasurement" ;
    __eo_swh_adjusted:band = "Ku" ;
    __eo_swh_adjusted:adjustment_lut = "tab_calibration_lut_jason-1.dat" ;
    __eo_swh_adjusted:adjustment_reference = "CCI Sea State v2 Product
Specification Document, 2021" ;
    __eo_swh_adjusted:coordinates = "lon lat" ;
double __eo_swh_uncertainty(obs, time) ;
    __eo_swh_uncertainty:_FillValue = 1.e+20 ;
    __eo_swh_uncertainty:least_significant_digit = 3LL ;
    __eo_swh_uncertainty:authority = "CF 1.7" ;
    __eo_swh_uncertainty:long_name = "best estimate of significant wave
height standard error" ;
    __eo_swh_uncertainty:units = "m" ;
    __eo_swh_uncertainty:comment = "Standard error calculated from buoy
colocations" ;
    __eo_swh_uncertainty:coverage_content_type = "qualityInformation" ;
    __eo_swh_uncertainty:formula = "1.96 * 0.054 * SWH + 0.095" ;
    __eo_swh_uncertainty:reference = "CCI Sea State v2 Product Specification
Document, 2021" ;
    __eo_swh_uncertainty:coordinates = "lon lat" ;
float lat(obs, time) ;
    lat:_FillValue = 1.e+20f ;
    lat:least_significant_digit = 3LL ;
    lat:axis = "Y" ;
    lat:standard_name = "latitude" ;
    lat:units = "degree_north" ;
    lat:valid_range = -90.f, 90.f ;
float lon(obs, time) ;
    lon:_FillValue = 1.e+20f ;
    lon:least_significant_digit = 3LL ;
    lon:axis = "X" ;
    lon:standard_name = "longitude" ;

```

```
lon:units = "degree_east" ;
lon:valid_range = -180.f, 180.f ;
double eo_time(obs, time) ;
eo_time:_FillValue = NaN ;
eo_time:long_name = "measurement time" ;
eo_time:standard_name = "time" ;
eo_time:axis = "T" ;
eo_time:units = "seconds since 1981-01-01" ;
eo_time:calendar = "proleptic_gregorian" ;
byte data_spatial_mask(obs, time) ;
data_spatial_mask:long_name = "name of source file for E0 data" ;
data_spatial_mask:flag_values = 0LL, 1LL ;
data_spatial_mask:flag_meanings = "out_of_storm_radius
within_storm_radius" ;
data_spatial_mask:coordinates = "eo_time lat lon" ;
data_spatial_mask:dtype = "bool" ;
char data_files(obs, string55) ;
data_files:long_name = "name of source file for E0 data" ;
char data_files_slices(obs, string33) ;
data_files_slices:long_name = "slices in source file of the extracted E0
data" ;
int64 track_nearest_point_indice(obs) ;
track_nearest_point_indice:long_name = "indice in track of the closest
point to the E0 data subset" ;
track_nearest_point_indice:comment = "the nearest track point is defined
as the one with the minimum time difference to the E0 observations among the
track points within the search radius" ;
double track_nearest_point_distance(obs) ;
track_nearest_point_distance:_FillValue = 1.e+20 ;
track_nearest_point_distance:long_name = "distance between the center of
the E0 data subset and the nearest track point, in meters" ;
track_nearest_point_distance:comment = "the nearest track point is
defined as the one with the minimum time difference to the E0 observations
among the track points within the search radius" ;
track_nearest_point_distance:units = "m" ;
double track_nearest_point_time_difference(obs) ;
track_nearest_point_time_difference:_FillValue = 1.e+20 ;
track_nearest_point_time_difference:long_name = "time difference between
the center of the E0 data subset and the nearest track point, in seconds (E0
time minus track time)" ;
```

			MAXSS ATBD ESA Contract 4000132954/20/I-NB Delivery D21, Version 1.0.0 Date 06/10/2021 Page 95
---	--	--	--

```

track_nearest_point_time_difference:comment = "the nearest track point
is defined as the one with the minimum time difference to the E0 observations
among the track points within the search radius" ;
track_nearest_point_time_difference:units = "s" ;
int64 track_time(track_time) ;
track_time:units = "seconds since 1981-01-01" ;
track_time:calendar = "proleptic_gregorian" ;
char __track_atcf_id(track_time, string8) ;
__track_atcf_id:long_name = "ATCF ID for the storm" ;
__track_atcf_id:standard_name =
"automated_tropical_cyclone_forecasting_system_storm_identifler" ;
__track_atcf_id:coverage_content_type = "thematicClassification" ;
float __track_lat(track_time) ;
__track_lat:_FillValue = 1.e+20f ;
__track_lat:long_name = "latitude" ;
__track_lat:standard_name = "latitude" ;
__track_lat:units = "degrees_north" ;
__track_lat:description = "This is merged position based on the
position(s) from the various source datasets." ;
__track_lat>Note = "Variable:lat can be missing since the tracks are
stored in a fixed 2-D grid where tracks have varying lengths" ;
__track_lat:coverage_content_type = "coordinate" ;
float __track_lon(track_time) ;
__track_lon:_FillValue = 1.e+20f ;
__track_lon:long_name = "longitude" ;
__track_lon:standard_name = "longitude" ;
__track_lon:units = "degrees_east" ;
__track_lon:description = "This is merged position based on the
position(s) from the various source datasets." ;
__track_lon>Note = "Variable:lon can be missing since the tracks are
stored in a fixed 2-D grid where tracks have varying lengths" ;
__track_lon:coverage_content_type = "coordinate" ;
char __track_record(track_time, string8) ;
__track_record:long_name = "Storm record type" ;
string __track_record:description = "C - Closest approach to a coast,
not followed by a landfall, G - Genesis, I - An intensity peak in terms of both
pressure and wind, L - Landfall (center of system crossing a coastline), P -
Minimum in central pressure, R - Provides additional detail on the intensity of
the cyclone when rapid changes are underway, S - Change of status of the
system, T - Provides additional detail on the track (position) of the cyclone,
W - Maximum sustained wind speed" ;

```

			MAXSS ATBD ESA Contract 4000132954/20/I-NB Delivery D21, Version 1.0.0 Date 06/10/2021 Page 96
---	--	--	--

```

__track_record:coverage_content_type = "thematicClassification" ;
char __track_status(track_time, string2) ;
__track_status:long_name = "Storm status" ;
__track_status:description = " DB - disturbance, TD - tropical
depression, TS - tropical storm, TY - typhoon, ST - super typhoon, TC -
tropical cyclone, HU, HR - hurricane, SD - subtropical depression, SS -
subtropical storm, EX - extratropical systems, PT - post tropical, IN -
inland, DS - dissipating, LO - low, WV - tropical wave, ET - extrapolated,
MD - monsoon depression, XX - unknown." ;
__track_status:coverage_content_type = "thematicClassification" ;
float __track_wind(track_time) ;
__track_wind:_FillValue = 1.e+20f ;
__track_wind:long_name = "Maximum sustained wind speed" ;
__track_wind:standard_name =
"tropical_cyclone_maximum_sustained_wind_speed" ;
__track_wind:units = "kts" ;
__track_wind:valid_min = 1LL ;
__track_wind:valid_max = 250LL ;
__track_wind:coverage_content_type = "physicalMeasurement" ;
float __track_pres(track_time) ;
__track_pres:_FillValue = 1.e+20f ;
__track_pres:long_name = "Minimum central pressure" ;
__track_pres:units = "mb" ;
__track_pres:valid_min = 700LL ;
__track_pres:valid_max = 1050LL ;
__track_pres:coverage_content_type = "physicalMeasurement" ;
byte __track_sshs(track_time) ;
__track_sshs:long_name = "Saffir-Simpson Hurricane Wind Scale
Category" ;
__track_sshs:units = "1" ;
__track_sshs:valid_min = -5LL ;
__track_sshs:valid_max = 5LL ;
__track_sshs:flag_values = -5LL, -4LL, -3LL, -2LL, -1LL, 0LL, 1LL, 2LL,
3LL, 4LL, 5LL ;
__track_sshs:flag_names = "unknown_type_XX post_tropical_ET_EX_PT
misc_disturbances_WV_LO_DB_DS_IN_MD subtropical_SS_SD
tropical_depression_w_lt_34 tropical_storm_wind_35-63 hurricane_cat_1_wind_64-
82 hurricane_cat_2_wind_83-95 hurricane_cat_3_wind_96-112
hurricane_cat_4_wind_113-136 hurricane_cat_5_wind_137+" ;
__track_sshs:coverage_content_type = "thematicClassification" ;
float __track_r34_ne(track_time) ;

```

```
__track_r34_ne:_FillValue = 1.e+20f ;
__track_r34_ne:long_name = "Radius of 34 knot winds" ;
__track_r34_ne:units = "nmile" ;
__track_r34_ne:valid_min = 1LL ;
__track_r34_ne:valid_max = 1000LL ;
__track_r34_ne:coverage_content_type = "physicalMeasurement" ;
float __track_r50_ne(track_time) ;
__track_r50_ne:_FillValue = 1.e+20f ;
__track_r50_ne:long_name = "Radius of 50 knot winds" ;
__track_r50_ne:units = "nmile" ;
__track_r50_ne:valid_min = 1LL ;
__track_r50_ne:valid_max = 1000LL ;
__track_r50_ne:coverage_content_type = "physicalMeasurement" ;
float __track_r64_ne(track_time) ;
__track_r64_ne:_FillValue = 1.e+20f ;
__track_r64_ne:long_name = "Radius of 64 knot winds" ;
__track_r64_ne:units = "nmile" ;
__track_r64_ne:valid_min = 1LL ;
__track_r64_ne:valid_max = 1000LL ;
__track_r64_ne:coverage_content_type = "physicalMeasurement" ;
float __track_poci(track_time) ;
__track_poci:_FillValue = 1.e+20f ;
__track_poci:long_name = "Pressure of outermost closed isobar (not best
tracked)" ;
__track_poci:units = "mb" ;
__track_poci:valid_min = 700LL ;
__track_poci:valid_max = 1050LL ;
__track_poci:coverage_content_type = "physicalMeasurement" ;
float __track_roci(track_time) ;
__track_roci:_FillValue = 1.e+20f ;
__track_roci:long_name = "Pressure of outermost closed isobar (not best
tracked)" ;
__track_roci:units = "nmile" ;
__track_roci:valid_min = 1LL ;
__track_roci:valid_max = 1000LL ;
__track_roci:coverage_content_type = "physicalMeasurement" ;
float __track_rmw(track_time) ;
```

```
__track_rmw:_FillValue = 1.e+20f ;
__track_rmw:long_name = "Radius of maximum winds (not best tracked)" ;
__track_rmw:standard_name =
"radius_of_tropical_cyclone_maximum_sustained_wind_speed" ;
__track_rmw:units = "nmile" ;
__track_rmw:valid_min = 1LL ;
__track_rmw:valid_max = 1000LL ;
__track_rmw:coverage_content_type = "physicalMeasurement" ;
float __track_eye(track_time) ;
__track_eye:_FillValue = 1.e+20f ;
__track_eye:long_name = "Eye diameter (not best tracked)" ;
__track_eye:standard_name = "radius_of_tropical_cyclone_eye" ;
__track_eye:units = "nmile" ;
__track_eye:valid_min = 1LL ;
__track_eye:valid_max = 250LL ;
__track_eye:coverage_content_type = "physicalMeasurement" ;
float __track_gust(track_time) ;
__track_gust:_FillValue = 1.e+20f ;
__track_gust:long_name = "Maximum reported wind gust from a US agency" ;
__track_gust:standard_name = "wind_speed_of_gust" ;
__track_gust:units = "kts" ;
__track_gust:valid_min = 1LL ;
__track_gust:valid_max = 350LL ;
__track_gust:coverage_content_type = "physicalMeasurement" ;
float __track_seahgt(track_time) ;
__track_seahgt:_FillValue = 1.e+20f ;
__track_seahgt:long_name = "Wave height for given radii" ;
__track_seahgt:units = "ft" ;
__track_seahgt:valid_min = 1LL ;
__track_seahgt:valid_max = 998LL ;
__track_seahgt:coverage_content_type = "physicalMeasurement" ;
float __track_searad_ne(track_time) ;
__track_searad_ne:_FillValue = 1.e+20f ;
__track_searad_ne:long_name = "Radial extent of given sea height" ;
__track_searad_ne:units = "nmile" ;
__track_searad_ne:valid_min = 1LL ;
__track_searad_ne:valid_max = 998LL ;
```

```
__track_searad_ne:coverage_content_type = "physicalMeasurement" ;
string __track_center(track_time) ;
float __track_r34_se(track_time) ;
__track_r34_se:_FillValue = 1.e+20f ;
__track_r34_se:long_name = "Radius of 34 knot winds" ;
__track_r34_se:units = "nmile" ;
__track_r34_se:valid_min = 1LL ;
__track_r34_se:valid_max = 1000LL ;
__track_r34_se:coverage_content_type = "physicalMeasurement" ;
float __track_r50_se(track_time) ;
__track_r50_se:_FillValue = 1.e+20f ;
__track_r50_se:long_name = "Radius of 50 knot winds" ;
__track_r50_se:units = "nmile" ;
__track_r50_se:valid_min = 1LL ;
__track_r50_se:valid_max = 1000LL ;
__track_r50_se:coverage_content_type = "physicalMeasurement" ;
float __track_r64_se(track_time) ;
__track_r64_se:_FillValue = 1.e+20f ;
__track_r64_se:long_name = "Radius of 64 knot winds" ;
__track_r64_se:units = "nmile" ;
__track_r64_se:valid_min = 1LL ;
__track_r64_se:valid_max = 1000LL ;
__track_r64_se:coverage_content_type = "physicalMeasurement" ;
float __track_searad_se(track_time) ;
__track_searad_se:_FillValue = 1.e+20f ;
__track_searad_se:long_name = "Radial extent of given sea height" ;
__track_searad_se:units = "nmile" ;
__track_searad_se:valid_min = 1LL ;
__track_searad_se:valid_max = 998LL ;
__track_searad_se:coverage_content_type = "physicalMeasurement" ;
float __track_r34_sw(track_time) ;
__track_r34_sw:_FillValue = 1.e+20f ;
__track_r34_sw:long_name = "Radius of 34 knot winds" ;
__track_r34_sw:units = "nmile" ;
__track_r34_sw:valid_min = 1LL ;
__track_r34_sw:valid_max = 1000LL ;
```

```
__track_r34_sw:coverage_content_type = "physicalMeasurement" ;
float __track_r50_sw(track_time) ;
__track_r50_sw:_FillValue = 1.e+20f ;
__track_r50_sw:long_name = "Radius of 50 knot winds" ;
__track_r50_sw:units = "nmile" ;
__track_r50_sw:valid_min = 1LL ;
__track_r50_sw:valid_max = 1000LL ;
__track_r50_sw:coverage_content_type = "physicalMeasurement" ;
float __track_r64_sw(track_time) ;
__track_r64_sw:_FillValue = 1.e+20f ;
__track_r64_sw:long_name = "Radius of 64 knot winds" ;
__track_r64_sw:units = "nmile" ;
__track_r64_sw:valid_min = 1LL ;
__track_r64_sw:valid_max = 1000LL ;
__track_r64_sw:coverage_content_type = "physicalMeasurement" ;
float __track_searad_sw(track_time) ;
__track_searad_sw:_FillValue = 1.e+20f ;
__track_searad_sw:long_name = "Radial extent of given sea height" ;
__track_searad_sw:units = "nmile" ;
__track_searad_sw:valid_min = 1LL ;
__track_searad_sw:valid_max = 998LL ;
__track_searad_sw:coverage_content_type = "physicalMeasurement" ;
float __track_r34_nw(track_time) ;
__track_r34_nw:_FillValue = 1.e+20f ;
__track_r34_nw:long_name = "Radius of 34 knot winds" ;
__track_r34_nw:units = "nmile" ;
__track_r34_nw:valid_min = 1LL ;
__track_r34_nw:valid_max = 1000LL ;
__track_r34_nw:coverage_content_type = "physicalMeasurement" ;
float __track_r50_nw(track_time) ;
__track_r50_nw:_FillValue = 1.e+20f ;
__track_r50_nw:long_name = "Radius of 50 knot winds" ;
__track_r50_nw:units = "nmile" ;
__track_r50_nw:valid_min = 1LL ;
__track_r50_nw:valid_max = 1000LL ;
__track_r50_nw:coverage_content_type = "physicalMeasurement" ;
```

```
float __track_r64_nw(track_time) ;
    __track_r64_nw:_FillValue = 1.e+20f ;
    __track_r64_nw:long_name = "Radius of 64 knot winds" ;
    __track_r64_nw:units = "nmile" ;
    __track_r64_nw:valid_min = 1LL ;
    __track_r64_nw:valid_max = 1000LL ;
    __track_r64_nw:coverage_content_type = "physicalMeasurement" ;
float __track_searad_nw(track_time) ;
    __track_searad_nw:_FillValue = 1.e+20f ;
    __track_searad_nw:long_name = "Radial extent of given sea height" ;
    __track_searad_nw:units = "nmile" ;
    __track_searad_nw:valid_min = 1LL ;
    __track_searad_nw:valid_max = 998LL ;
    __track_searad_nw:coverage_content_type = "physicalMeasurement" ;
char __track_basin(track_time, string2) ;
    __track_basin:long_name = "Current basin" ;
    __track_basin:Note = "EP=East_Pacific NA=North_Atlantic NI=North_Indian
SA=South_Atlantic SI=South_Indian SP=South_Pacific WP=Western_Pacific" ;
    __track_basin:coverage_content_type = "thematicClassification" ;
char __track_name(track_time, string9) ;
    __track_name:long_name = "Name of system" ;
    __track_name:description = "May be a combination of names from different
agencies" ;
    __track_name:coverage_content_type = "thematicClassification" ;
char __track_track_type(track_time, string4) ;
    __track_track_type:long_name = "Name of track type" ;
    __track_track_type:description = "Tracks are either MAIN or SPUR. Spur
tracks have points that either merge with or split from another track (or
both). Main tracks are regular tracks. Spur tracks should be treated with
caution." ;
    __track_track_type:coverage_content_type = "thematicClassification" ;
char __track_main_track_sid(track_time, string13) ;
    __track_main_track_sid:long_name = "SID of the main track associated
with this storm." ;
    __track_main_track_sid:description = "If this track is a main, then this
is the same as serial_id. If a spur, it namesthe associated main track." ;
    __track_main_track_sid:coverage_content_type =
"thematicClassification" ;
float __track_dist2land(track_time) ;
```

```
__track_dist2land:_FillValue = 1.e+20f ;
__track_dist2land:long_name = "Distance to Land at current location" ;
__track_dist2land:units = "km" ;
__track_dist2land:description = "Distance to the nearest land point.
Also acts as a land mask since 0km = over land. Uses present location ONLY." ;
__track_dist2land:coverage_content_type = "modelResult" ;
float __track_landfall(track_time) ;
__track_landfall:_FillValue = 1.e+20f ;
__track_landfall:long_name = "Minimum distance to land between current
location and next." ;
__track_landfall:units = "km" ;
__track_landfall:description = "Describes landfall conditions between
the present observation and the next (usually 3 hours) by providing minimum
distance to land. So a value of 0 implies that the storm crosses a coastline
prior to the next observation." ;
__track_landfall:coverage_content_type = "modelResult" ;
float __track_storm_speed(track_time) ;
__track_storm_speed:_FillValue = 1.e+20f ;
__track_storm_speed:long_name = "Storm translation speed" ;
__track_storm_speed:units = "kts" ;
__track_storm_speed:valid_min = 0LL ;
__track_storm_speed:valid_max = 998LL ;
__track_storm_speed:coverage_content_type = "physicalMeasurement" ;
float __track_storm_dir(track_time) ;
__track_storm_dir:_FillValue = 1.e+20f ;
__track_storm_dir:long_name = "Storm translation direction" ;
__track_storm_dir:units = "degrees" ;
__track_storm_dir:valid_min = 0LL ;
__track_storm_dir:valid_max = 360LL ;
__track_storm_dir>Note = "Unit is degrees east of north" ;
__track_storm_dir:coverage_content_type = "physicalMeasurement" ;
float __track_ci(track_time) ;
__track_ci:_FillValue = 1.e+20f ;
__track_ci:long_name = "Dvorak Current Intensity (CI)" ;
__track_ci:standard_name =
"dvorak_tropical_cyclone_current_intensity_number" ;
__track_ci:units = "1" ;
__track_ci:valid_min = 0. ;
```

```
__track_ci:valid_max = 8. ;
__track_ci:coverage_content_type = "thematicClassification" ;
float __track_dp(track_time) ;
__track_dp:_FillValue = 1.e+20f ;
__track_dp:long_name = "Storm pressure drop" ;
__track_dp:units = "mb" ;
__track_dp:valid_min = 1LL ;
__track_dp:valid_max = 250LL ;
__track_dp:coverage_content_type = "physicalMeasurement" ;
float __track_tnum(track_time) ;
__track_tnum:_FillValue = 1.e+20f ;
__track_tnum:long_name = "Dvorak T number" ;
__track_tnum:units = "1" ;
__track_tnum:valid_min = 0. ;
__track_tnum:valid_max = 8. ;
__track_tnum:coverage_content_type = "thematicClassification" ;
float __track_gust_per(track_time) ;
__track_gust_per:_FillValue = 1.e+20f ;
__track_gust_per:long_name = "Time period of the wind gust from BoM" ;
__track_gust_per:units = "second" ;
__track_gust_per:valid_min = 1LL ;
__track_gust_per:valid_max = 9999LL ;
__track_gust_per:coverage_content_type = "physicalMeasurement" ;
float __track_r50_dir(track_time) ;
__track_r50_dir:_FillValue = 1.e+20f ;
__track_r50_dir:long_name = "Direction of maximum radius of 50 knots
winds" ;
__track_r50_dir:valid_min = 0LL ;
__track_r50_dir:valid_max = 9LL ;
__track_r50_dir:flag_values = 1LL, 2LL, 3LL, 4LL, 5LL, 6LL, 7LL, 8LL,
9LL ;
__track_r50_dir:flag_names = "Northeast East Southeast South Southwest
West Northwest North Symmetric_Circle" ;
__track_r50_dir:coverage_content_type = "thematicClassification" ;
float __track_r50_long(track_time) ;
__track_r50_long:_FillValue = 1.e+20f ;
__track_r50_long:long_name = "Maximum radius of 50 knots winds" ;
```

```
__track_r50_long:units = "nmile" ;
__track_r50_long:valid_min = 1LL ;
__track_r50_long:valid_max = 1000LL ;
__track_r50_long:coverage_content_type = "physicalMeasurement" ;
float __track_r50_short(track_time) ;
__track_r50_short:_FillValue = 1.e+20f ;
__track_r50_short:long_name = "Minimum radius of 50 knots winds" ;
__track_r50_short:units = "nmile" ;
__track_r50_short:valid_min = 1LL ;
__track_r50_short:valid_max = 1000LL ;
__track_r50_short:coverage_content_type = "physicalMeasurement" ;
float __track_r30_dir(track_time) ;
__track_r30_dir:_FillValue = 1.e+20f ;
__track_r30_dir:long_name = "Direction of maximum radius of 30 knots
winds" ;
__track_r30_dir:valid_min = 0LL ;
__track_r30_dir:valid_max = 9LL ;
__track_r30_dir:flag_values = 1LL, 2LL, 3LL, 4LL, 5LL, 6LL, 7LL, 8LL,
9LL ;
__track_r30_dir:flag_names = "Northeast East Southeast South Southwest
West Northwest North Symmetric_Circle" ;
__track_r30_dir:coverage_content_type = "thematicClassification" ;
float __track_r30_long(track_time) ;
__track_r30_long:_FillValue = 1.e+20f ;
__track_r30_long:long_name = "Direction of maximum radius of 30 knots
winds" ;
__track_r30_long:units = "nmile" ;
__track_r30_long:valid_min = 1LL ;
__track_r30_long:valid_max = 1000LL ;
__track_r30_long:coverage_content_type = "physicalMeasurement" ;
float __track_r30_short(track_time) ;
__track_r30_short:_FillValue = 1.e+20f ;
__track_r30_short:long_name = "Minimum radius of 30 knots winds" ;
__track_r30_short:units = "nmile" ;
__track_r30_short:valid_min = 1LL ;
__track_r30_short:valid_max = 1000LL ;
__track_r30_short:coverage_content_type = "physicalMeasurement" ;
```

			MAXSS ATBD ESA Contract 4000132954/20/I-NB Delivery D21, Version 1.0.0 Date 06/10/2021 Page 105
---	--	--	---

```
// global attributes:
```

```

: __eo_Conventions = "CF-1.7, ACDD-1.3, ISO 8601" ;
: __eo_title = "ESA CCI Sea State L2P derived from Jason-1 GDR" ;
: __eo_id = "ESACCI-SEASTATE-L2P-SWH-Jason-1" ;
: __eo_institution = "Institut Francais de Recherche et d'Exploitation
de la Mer/Centre de Recherche et d'Exploitation satellitaire" ;
: __eo_institution_abbreviation = "ifremer/cersat" ;
: __eo_source = "CCI Sea State Jason-1 GDR to L2P Processor" ;
: __eo_references = "CCI Sea State Product Specification Document (PSD),
v1.1" ;
: __eo_summary = "This dataset contains along-track significant wave
height measurements from Jason-1 altimeter, cross-calibrated with other
altimetry missions and reference in situ measurements." ;
string : __eo_keywords = "Oceans > Ocean Waves > Significant Wave
Height", "Oceans > Ocean Waves > Sea State" ;
: __eo_keywords_vocabulary = "NASA Global Change Master Directory (GCMD)
Science Keywords" ;
: __eo_naming_authority = "fr.ifremer.cersat" ;
: __eo_cdm_data_type = "trajectory" ;
: __eo_featureType = "trajectory" ;
: __eo_comment = "These data were produced at ESACCI as part of the ESA
SST CCI project." ;
: __eo_creator_name = "Cersat" ;
: __eo_creator_url = "http://cersat.ifremer.fr" ;
: __eo_creator_email = "cersat@ifremer.fr" ;
: __eo_creator_institution = "Ifremer / Cersat" ;
: __eo_project = "Climate Change Initiative - European Space Agency" ;
: __eo_geospatial_lat_units = "degrees" ;
: __eo_geospatial_lon_units = "degrees" ;
: __eo_standard_name_vocabulary = "NetCDF Climate and Forecast (CF)
Metadata Convention" ;
: __eo_license = "ESA CCI Data Policy: free and open access" ;
: __eo_platform = "Jason-1" ;
: __eo_platform_type = "low earth orbit satellite" ;
: __eo_platform_vocabulary = "CCI" ;
: __eo_instrument = "Poseidon-2" ;
: __eo_instrument_type = "altimeter" ;
: __eo_instrument_vocabulary = "CCI" ;
: __eo_spatial_resolution = "5.8 km" ;

```

```
:__eo_cycle_number = 301 ;
:__eo_equator_crossing_longitude = "" ;
:__eo_netcdf_version_id = "4.7.4 of Oct 31 2021 03:02:48 $" ;
:__eo_acknowledgement = "Please acknowledge the use of these data with
the following statement: these data were obtained from the ESA CCI Sea State
project" ;
:__eo_format_version = "Data Standards v2.1" ;
:__eo_processing_level = "L2P" ;
:__eo_publisher_name = "ifremer/cersat" ;
:__eo_publisher_url = "http://cersat.ifremer.fr" ;
:__eo_publisher_email = "cersat@ifremer.fr" ;
:__eo_publisher_institution = "Ifremer / Cersat" ;
:__eo_scientific_support_contact = "Guillaume.Dodet@ifremer.fr" ;
:__eo_technical_support_contact = "cersat@ifremer.fr" ;
:__eo_key_variables = "swh_adjusted_denoised" ;
:__eo_band = "Ku" ;
:__eo_processing_software = "Cersat/Cerbere 1.0" ;
:__eo_Metadata_Conventions = "Climate and Forecast (CF) 1.7, Attribute
Convention for Data Discovery (ACDD) 1.3" ;
:__eo_geospatial_vertical_units = "meters above mean sea level" ;
:__eo_geospatial_vertical_positive = "up" ;
:__eo_product_version = "3.0" ;
:__eo_source_version = "3.0" ;
:storm_atcf_name = "SL502010" ;
:storm_id = "2010067S25317" ;
:storm_name = "" ;
:storm_basin = "SA" ;
:storm_source = "ibtracs" ;
:eo_dataset_id = "ESACCI-SEASTATE-L2P-SWH-Jason-1" ;
:id = "MAXSS-StormAtlas-ESACCI-SEASTATE-L2P-SWH-Jason-1-v1.0" ;
:summary = "data extracted from ESACCI-SEASTATE-L2P-SWH-Jason-1 dataset
for MAXSS Storm Atlas version 1" ;
:geospatial_lat_min = -42.8466796875 ;
:geospatial_lat_max = -2.94140625 ;
:geospatial_lon_min = -62.59375 ;
:geospatial_lon_max = -32.8818359375 ;
:geospatial_bounds = "POLYGON ((-32.8818359375 -42.8466796875, -
32.8818359375 -2.94140625, -62.59375 -2.94140625, -62.59375 -42.8466796875, -
```

			MAXSS ATBD ESA Contract 4000132954/20/I-NB Delivery D21, Version 1.0.0 Date 06/10/2021 Page 107
---	--	--	---

```
32.8818359375 -42.8466796875))" ;  
    :time_coverage_start = "2010-03-08T20:32:04" ;  
    :time_coverage_end = "2010-03-12T05:51:51" ;  
    :uuid = "73843e0f-d48c-496f-8f74-5cd455b2a634" ;  
    :history = "2022-03-01T15:24:01: Initial creation" ;  
    :date_created = "2022-03-01T15:24:01" ;  
    :date_modified = "2022-03-01T15:24:01" ;  
    :date_issued = "2022-03-01T15:24:01" ;  
}
```

10 ANNEX 3: EXAMPLE OF FORMAT FOR ARGO FLOAT DATA

```
netcdf MAXSS_NA_AL052016_GDAC_ARGO_AOV {
```

```
dimensions:
```

```
    strlen2 = 4 ;
    strlen3 = 13 ;
    strlen4 = 8 ;
    strlen5 = 2 ;
    n_pts_cyc = 104 ;
    dim1 = 4 ;
    dim2 = 2 ;
    dim3 = 2 ;
    n_argo_prf_tot = 592 ;
    strlen6 = 14 ;
    n_lev_argo_max = 1024 ;
    n_coloc_tot = 322 ;
    strlen1 = 158 ;
    nlines = 428 ;
    n_argo_prf_coloc = 321 ;
```

```
variables:
```

```
    int cyclone_index_in_datafile ;
        cyclone_index_in_datafile:long_name = "Index (in [0,1,...,ntotcyc-1]) of the cyclone in the Cyclone_Track_Data_Source file (cf global attributes)" ;
        cyclone_index_in_datafile:units = "n/a" ;
        cyclone_index_in_datafile:value = 617 ;
    char storm_name(strlen2) ;
        storm_name:long_name = "name of the system ; May be a combination of names from different agencies" ;
        storm_name:value = "EARL" ;
    char storm_sid(strlen3) ;
        storm_sid:long_name = "storm ibtracs serial ID" ;
        storm_sid:value = "2016215N16283" ;
    char atcf_id(strlen4) ;
        atcf_id:long_name = "ATCF ID for the storm"
= \"automated_tropical_cyclone_forecasting_system_storm_identifier\" ;
```

			MAXSS ATBD ESA Contract 4000132954/20/I-NB Delivery D21, Version 1.0.0 Date 06/10/2021 Page 109
---	--	--	---

```

        atcf_id:value = "AL052016" ;
char basin(strlen5) ;
        basin:long_name      =      "Current      basin      :      EP=East_Pacific
NA=North_Atlantic      NI=North_Indian      SA=South_Atlantic      SI=South_Indian
SP=South_Pacific WP=Western_Pacific" ;
        basin:value = "NA" ;
float lon_cyc(n_pts_cyc) ;
        lon_cyc:units = "degree_East" ;
        lon_cyc:long_name = "longitudes of the points along the cyclone
path (track of the cyclone center)" ;
        lon_cyc:valid_min = -97.5f ;
        lon_cyc:valid_max = -77.5f ;
float lat_cyc(n_pts_cyc) ;
        lat_cyc:units = "degree_North" ;
        lat_cyc:long_name = "latitudes of the points along the cyclone path
(track of the cyclone center)" ;
        lat_cyc:valid_min = 16.f ;
        lat_cyc:valid_max = 19.00867f ;
double time_cyc(n_pts_cyc) ;
        time_cyc:units = "days since 1950-01-01 00:00:00" ;
        time_cyc:long_name = "date/time UTC of the points along the cyclone
path (track of the cyclone center)" ;
        time_cyc:valid_min = 24320.25 ;
        time_cyc:valid_max = 24324.5 ;
float r34_max(n_pts_cyc) ;
        r34_max:units = "km" ;
        r34_max:long_name = "maximum radius of 34 knots winds (among the
four r34 values in the four quadrant ne/nw/se/sw)" ;
        r34_max:valid_min = 74.08f ;
        r34_max:valid_max = 222.24f ;
short sshs(n_pts_cyc) ;
        sshs:units = "n/a" ;
        sshs:long_name = "Saffir-Simpson Hurricane Wind Scale Category
(from usa_sshs in Cyclone_Track_Data_Source file)" ;
        sshs:valid_min = -5s ;
        sshs:valid_max = 1s ;
float geog_window_of_cyclone_domain(dim1) ;
        geog_window_of_cyclone_domain:units = "degE for lon, degN for
lat" ;

```

```

        geog_window_of_cyclone_domain:long_name           =           "="
[lon1,lon2(>lon1),lat1,lat2(>lat1)], geographic limits of the large spatial
window defined from the cyclone path (+ margins) to extract basic argo data
used for the colocalisation final process" ;

        geog_window_of_cyclone_domain:value = "[-108.000,-67.000 degE ;
6.000,29.000 degN ] " ;

        double time_window_of_cyclone_domain(dim2) ;

        time_window_of_cyclone_domain:units = "days since 1950-01-01
00:00:00" ;

        time_window_of_cyclone_domain:long_name = "large time window
[t_start,t_end] defined from the cyclone path dates (+ margins, cf
coloc_namelist var for details) to find basic argo data for the colocalisation
final process" ;

        time_window_of_cyclone_domain:valid_min = 24290.25 ;
        time_window_of_cyclone_domain:valid_max = 24354.5 ;
        time_window_of_cyclone_domain:dates_min_max           =
"20160703.250_20160905.500" ;

        float coloc_radius ;

        coloc_radius:units = "km" ;

        coloc_radius:long_name = "radius from the points of the cyclone
track used to define the spatial colocalisation disk" ;

        coloc_radius:valid_min = 1000.f ;
        coloc_radius:valid_max = 1000.f ;

        float coloc_delta_t(dim3) ;

        coloc_delta_t:units = "days" ;

        coloc_delta_t:long_name = "= time interval [t1,t2] (with t2>t1)
used to define the temporal colocalisation with cyclone track points. An argo
profile is colocalised in time iff we find some cyclone points such as
Tcyc_point-Targo is in [t1,t2] (if =bmiss only, then we do a space-only coloc,
then coloc occurs iff the given argo profile in our cyclone-space/time_window
is in coloc_radius distance of some cyclone track points)" ;

        coloc_delta_t:missing_value = 99999.f ;
        coloc_delta_t:valid_min = 99999.f ;
        coloc_delta_t:valid_max = 99999.f ;

        int n_argo_prf_tot ;

        n_argo_prf_tot:long_name = "number of argo casts (or profiles)
found in the basic space/time window of cyclone (based only on lon/lat/time
min/max of cyclone + margins)" ;

        n_argo_prf_tot:value = 592 ;

        int flag_cyclone_coloc ;

        flag_cyclone_coloc:long_name = "General output flag returned by the
argo/cyclone coloc process" ;

        flag_cyclone_coloc:legend = "Possible values = -100: no argo prf

```

			MAXSS ATBD ESA Contract 4000132954/20/I-NB Delivery D21, Version 1.0.0 Date 06/10/2021 Page 111
---	--	--	---

found in cyclone path lon/lat/time window (n_argo_prf_tot=0); -110: argo prf found in cyclone path window BUT no argo prf in exact coloc with cyclone path ; 1: at least 1 argo prf found in exact coloc with cyclone path (based on coloc params Rcoloc, DTcoloc etc...)" ;

```

    flag_cyclone_coloc:value = 1 ;
int nwmo_argo_prf(n_argo_prf_tot) ;
    nwmo_argo_prf:units = "ID number" ;
    nwmo_argo_prf:long_name = "WMO unique ID number of the argo float
that has measured a given profile/cast" ;
int ncycle_argo_prf(n_argo_prf_tot) ;
    ncycle_argo_prf:units = "ID number" ;
    ncycle_argo_prf:long_name = "ID number/counter of a profile done by
an argo float (must be in [1,2,3...,n_profiles_tot_of_argo_float])" ;
char basin_name_argo_prf(n_argo_prf_tot, strlen6) ;
    basin_name_argo_prf:units = "n/a" ;
    basin_name_argo_prf:long_name = "name of the basin (Pacific,
Atlantic or Indian) where the argo profile/cast has been done (used to re-read
argo data if needed)" ;
double lon_argo_prf(n_argo_prf_tot) ;
    lon_argo_prf:units = "degree_East" ;
    lon_argo_prf:long_name = "longitudes of the argo profile" ;
    lon_argo_prf:valid_min = -107.9518 ;
    lon_argo_prf:valid_max = -67.041 ;
double lat_argo_prf(n_argo_prf_tot) ;
    lat_argo_prf:units = "degree_North" ;
    lat_argo_prf:long_name = "latitudes of the argo profile" ;
    lat_argo_prf:valid_min = 6.06341 ;
    lat_argo_prf:valid_max = 28.94813 ;
double time_argo_prf(n_argo_prf_tot) ;
    time_argo_prf:units = "days since 1950-01-01 00:00:00" ;
    time_argo_prf:long_name = "date/time UTC of the argo profile" ;
    time_argo_prf:valid_min = 24290.1453935187 ;
    time_argo_prf:valid_max = 24354.9280555556 ;
float pdep_argo_prf(n_argo_prf_tot, n_lev_argo_max) ;
    pdep_argo_prf:units = "m" ;
    pdep_argo_prf:long_name = "Depth of the argo profile measurement
(depth computed from pressure after Saunders & Fofonoff DSR 1976)" ;
    pdep_argo_prf:missing_value = 99999.f ;
    pdep_argo_prf:valid_min = 0.9538131f ;

```

```
    pdep_argo_prf:valid_max = 2026.869f ;
float press_argo_prf(n_argo_prf_tot, n_lev_argo_max) ;
    press_argo_prf:units = "db" ;
    press_argo_prf:long_name = "Pressure of the argo profile
measurement" ;
    press_argo_prf:missing_value = 99999.f ;
    press_argo_prf:valid_min = 0.96f ;
    press_argo_prf:valid_max = 2050.f ;
float temp_argo_prf(n_argo_prf_tot, n_lev_argo_max) ;
    temp_argo_prf:units = "degC" ;
    temp_argo_prf:long_name = "In situ temperature of the argo profile
measurement" ;
    temp_argo_prf:missing_value = 99999.f ;
    temp_argo_prf:valid_min = 2.067f ;
    temp_argo_prf:valid_max = 31.2f ;
float psal_argo_prf(n_argo_prf_tot, n_lev_argo_max) ;
    psal_argo_prf:units = "PSU" ;
    psal_argo_prf:long_name = "Salinity of the argo profile
measurement" ;
    psal_argo_prf:missing_value = 99999.f ;
    psal_argo_prf:valid_min = 28.151f ;
    psal_argo_prf:valid_max = 37.222f ;
float sigma0_argo_prf(n_argo_prf_tot, n_lev_argo_max) ;
    sigma0_argo_prf:units = "kg/m3" ;
    sigma0_argo_prf:long_name = "Potential density of sea water (with
reference depth = 0m, i.e. sigma0 = rho0 - 1000) of the argo profile
measurement" ;
    sigma0_argo_prf:missing_value = 99999.f ;
    sigma0_argo_prf:valid_min = 16.52519f ;
    sigma0_argo_prf:valid_max = 27.89243f ;
float temp_10_argo_prf(n_argo_prf_tot) ;
    temp_10_argo_prf:units = "degC" ;
    temp_10_argo_prf:long_name = "Temperature at 10m depth on the argo
profile (linear interp. between above/below levels)" ;
    temp_10_argo_prf:missing_value = 99999.f ;
    temp_10_argo_prf:valid_min = 22.51542f ;
    temp_10_argo_prf:valid_max = 30.87538f ;
float psal_10_argo_prf(n_argo_prf_tot) ;
```

```
    psal_10_argo_prf:units = "PSU" ;
    psal_10_argo_prf:long_name = "Salinity at 10m depth on the argo
profile (linear interp. between above/below levels)" ;
    psal_10_argo_prf:missing_value = 99999.f ;
    psal_10_argo_prf:valid_min = 31.9742f ;
    psal_10_argo_prf:valid_max = 36.816f ;
float sigma0_10_argo_prf(n_argo_prf_tot) ;
    sigma0_10_argo_prf:units = "kg/m3" ;
    sigma0_10_argo_prf:long_name = "Surface potential density at 10m
depth on the argo profile (linear interp. between above/below levels)" ;
    sigma0_10_argo_prf:missing_value = 99999.f ;
    sigma0_10_argo_prf:valid_min = 19.27144f ;
    sigma0_10_argo_prf:valid_max = 23.4831f ;
float mld_dt02_argo_prf(n_argo_prf_tot) ;
    mld_dt02_argo_prf:units = "m" ;
    mld_dt02_argo_prf:long_name = "Mixed Layer Depth on the argo
profile (= proxy of the isothermal layer depth, with a temperature threshold
criterion = +/- 0.2 degC, difference from 10m depth value)" ;
    mld_dt02_argo_prf:missing_value = 99999.f ;
    mld_dt02_argo_prf:valid_min = -60.44828f ;
    mld_dt02_argo_prf:valid_max = 101.3597f ;
float mld_dreqdt02_argo_prf(n_argo_prf_tot) ;
    mld_dreqdt02_argo_prf:units = "m" ;
    mld_dreqdt02_argo_prf:long_name = "Mixed Layer Depth on the argo
profile (= proxy of the isopycnal layer depth, with a variable density
threshold equivalent to a 0.2 degC variation, difference from 10m depth value)"
;
    mld_dreqdt02_argo_prf:missing_value = 99999.f ;
    mld_dreqdt02_argo_prf:valid_min = -40.25415f ;
    mld_dreqdt02_argo_prf:valid_max = 103.0409f ;
float mld_mindtr02_argo_prf(n_argo_prf_tot) ;
    mld_mindtr02_argo_prf:units = "m" ;
    mld_mindtr02_argo_prf:long_name = "Mixed Layer Depth on the argo
profile (proxy of the T and S homogeneous surface layer of the ocean); with a
temperature & density criterion from 10m depth :
min[mld_dt02_argo_prf,mld_dreqdt02_argo_prf])" ;
    mld_mindtr02_argo_prf:missing_value = 99999.f ;
    mld_mindtr02_argo_prf:valid_min = -40.25415f ;
    mld_mindtr02_argo_prf:valid_max = 100.5199f ;
float blt02_argo_prf(n_argo_prf_tot) ;
```

```
    blt02_argo_prf:units = "m" ;
    blt02_argo_prf:long_name = "Barrier Layer Thickness on the argo
profile (negative values correspond to a compensated layer thickness); computed
by difference between the top of thermocline depth (depth where T decreases by
0.2 degC compared to value at 10m depth) minus mld_dreqdt02_argo_prf
variable" ;
    blt02_argo_prf:missing_value = 99999.f ;
    blt02_argo_prf:valid_min = -13.61635f ;
    blt02_argo_prf:valid_max = 46.45999f ;
float d20_argo_prf(n_argo_prf_tot) ;
    d20_argo_prf:units = "m" ;
    d20_argo_prf:long_name = "Depth of the 20 degC isotherm on the argo
profile" ;
    d20_argo_prf:missing_value = 99999.f ;
    d20_argo_prf:valid_min = 12.61973f ;
    d20_argo_prf:valid_max = 317.6269f ;
float d26_argo_prf(n_argo_prf_tot) ;
    d26_argo_prf:units = "m" ;
    d26_argo_prf:long_name = "Depth of the 26 degC isotherm on the argo
profile" ;
    d26_argo_prf:missing_value = 99999.f ;
    d26_argo_prf:valid_min = 5.753272f ;
    d26_argo_prf:valid_max = 195.2923f ;
float hc300_argo_prf(n_argo_prf_tot) ;
    hc300_argo_prf:units = "Joules (TBC...)" ;
    hc300_argo_prf:long_name = "Heat content between 0 and 300 m depth,
from the argo profile" ;
    hc300_argo_prf:missing_value = 99999.f ;
    hc300_argo_prf:valid_min = 16301.62f ;
    hc300_argo_prf:valid_max = 32198.28f ;
float ssh_0_1000_argo_prf(n_argo_prf_tot) ;
    ssh_0_1000_argo_prf:units = "m" ;
    ssh_0_1000_argo_prf:long_name = "sea steric height = integral of
[ ( rho(0degC,35psu,p) / rho(T,S,p) - 1 ) * dz ] from z = 0 to 1000 m (e.g.
Tomczak and Godfrey 1994, regional oceanog. book)" ;
    ssh_0_1000_argo_prf:missing_value = 99999.f ;
    ssh_0_1000_argo_prf:valid_min = 0.9032522f ;
    ssh_0_1000_argo_prf:valid_max = 2.492419f ;
float n2max_0_200_argo_prf(n_argo_prf_tot) ;
```

```

n2max_0_200_argo_prf:units = "sec-2" ;
n2max_0_200_argo_prf:long_name = "max of N2 (Brunt-Vaisala
Frequency squared=  $g^2*d\_rho/d\_p$  ) profile in 0-200m depth range" ;
n2max_0_200_argo_prf:missing_value = 99999.f ;
n2max_0_200_argo_prf:valid_min = 2.527944e-05f ;
n2max_0_200_argo_prf:valid_max = 0.01714766f ;
float depth_of_n2max_0_200_argo_prf(n_argo_prf_tot) ;
depth_of_n2max_0_200_argo_prf:units = "m" ;
depth_of_n2max_0_200_argo_prf:long_name = "depth of
n2max_0_200_argo_prf (N2 max in 0-200 m depth)" ;
depth_of_n2max_0_200_argo_prf:missing_value = 99999.f ;
depth_of_n2max_0_200_argo_prf:valid_min = 1.529814f ;
depth_of_n2max_0_200_argo_prf:valid_max = 199.7153f ;
float pycnocline_max_below_mld_argo_prf(n_argo_prf_tot) ;
pycnocline_max_below_mld_argo_prf:units = "kg/m3/m" ;
pycnocline_max_below_mld_argo_prf:long_name = "maximum value of
 $d(\sigma_\theta)/dz$  below the mld = mld_mindtr02_argo_prf (and until 1000m, or until
max profile depth if mld>800m) ; NB: should mostly occur at same depth as
n2max_0_200_argo_prf with a relation of  $n2=(-g/rho)*d\sigma_\theta/dz$ " ;
pycnocline_max_below_mld_argo_prf:missing_value = 99999.f ;
pycnocline_max_below_mld_argo_prf:valid_min = 0.02467912f ;
pycnocline_max_below_mld_argo_prf:valid_max = 0.6135837f ;
float depth_of_pycnocline_max_below_mld_argo_prf(n_argo_prf_tot) ;
depth_of_pycnocline_max_below_mld_argo_prf:units = "m" ;
depth_of_pycnocline_max_below_mld_argo_prf:long_name = "depth where
maximum value of  $d(\sigma_\theta)/dz$  below the mld occurs" ;
depth_of_pycnocline_max_below_mld_argo_prf:missing_value =
99999.f ;
depth_of_pycnocline_max_below_mld_argo_prf:valid_min = 10.87757f ;
depth_of_pycnocline_max_below_mld_argo_prf:valid_max = 217.5564f ;
int n_argo_prf_coloc ;
n_argo_prf_coloc:long_name = "number of argo casts (or profiles)
with at least 1 colocalisation with the cyclone track (based on coloc
space/time box and parameters)" ;
n_argo_prf_coloc:value = 321 ;
int flag_coloc_argo_prf(n_argo_prf_tot) ;
flag_coloc_argo_prf:long_name = "Coloc flag for each argo
profile/cast" ;
flag_coloc_argo_prf:legend = "Possible values = -100: argo-prf in
cyclone x/t window but no coloc at all; -110: argo-prf is spatially inside
max(coloc_radius) distance to the cyclone path BUT it is not in final

```

			MAXSS ATBD ESA Contract 4000132954/20/I-NB Delivery D21, Version 1.0.0 Date 06/10/2021 Page 116
---	--	--	---

space(/time) coloc area of the cyclone path; 1: argo-prf has been successfully colocalised with some points of the cyclone track" ;

```
flag_coloc_argo_prf:valid_min = -110 ;
```

```
flag_coloc_argo_prf:valid_max = 1 ;
```

```
short n_coloc_per_argo_prf(n_argo_prf_tot) ;
```

n_coloc_per_argo_prf:long_name = "Number of colocalisation per argo profile. A colocalisation for an argo-profile is defined here as a continuous part of the cyclone track that is included in the spatio(-temporal) area around the argo-profile and defined by coloc radius and delta_t. n_coloc_per_argo_prf can be greater than 1 e.g. if the cyclone comes back on its path and passes twice over a given argo profile position, then for this argo profile we can have n_coloc_per_argo_prf=2 (such values of 2 or more should be rather rare but those multiple coloc. may occur). NB: Total(n_coloc_per_argo_prf) = n_coloc_tot" ;

```
n_coloc_per_argo_prf:valid_min = 0s ;
```

```
n_coloc_per_argo_prf:valid_max = 2s ;
```

```
int n_coloc_tot ;
```

n_coloc_tot:long_name = "total number of colocalisation(s) found for this cyclone track (based on coloc parameters). NB: see variable \'n_coloc_per_argo_prf\' long_name attribute for the definition of what is called a colocalisation here." ;

```
n_coloc_tot:value = 322 ;
```

```
int index_of_argo_prf_for_each_coloc(n_coloc_tot) ;
```

index_of_argo_prf_for_each_coloc:long_name = "For each colocalisation found, this index gives the index number of the argo profile to which the coloc. is associated (in [1,2,...,n_argo_prf_tot]). If same argo index occurs several times, then those multiple coloc. for the same argo should be in chronological order" ;

```
index_of_argo_prf_for_each_coloc:valid_min = 3 ;
```

```
index_of_argo_prf_for_each_coloc:valid_max = 592 ;
```

```
int flag_argo_prf_under_cyclone(n_coloc_tot) ;
```

flag_argo_prf_under_cyclone:long_name = "Flag for each argo profile/cast colocalised, tells whether the argo profile measurements occur before/after/during the cyclone is in the coloc. area" ;

flag_argo_prf_under_cyclone:legend = "Possible values : -1: cyclone goes over the argo coloc zone BEFORE argo profile measurements; 0: cyclone coloc starts BEFORE and leaves AFTER argo measurement.; 1: cyclone goes over the argo coloc zone AFTER argo measurement." ;

```
flag_argo_prf_under_cyclone:valid_min = -1 ;
```

```
flag_argo_prf_under_cyclone:valid_max = 1 ;
```

```
int flag_cyclone_cross_coloc(n_coloc_tot) ;
```

flag_cyclone_cross_coloc:long_name = "Flag for each argo profile/cast colocalised, tells whether the cyclone crosses the x/y/t coloc zone or starts/ends in it..." ;

```
flag_cyclone_cross_coloc:legend = "Possible values = 1: cyclone
crosses the coloc. area; 2: cyclone starts in coloc. area and leaves it; 3:
cyclone enters in coloc. area and finishes in it; 4: whole cyclone track is in
coloc. area " ;

flag_cyclone_cross_coloc:valid_min = 1 ;
flag_cyclone_cross_coloc:valid_max = 3 ;

double lon_cyc_in(n_coloc_tot) ;
lon_cyc_in:units = "degree_East" ;
lon_cyc_in:long_name = "longitude of the cyclone center when it
comes into the coloc x/y/t zone" ;
lon_cyc_in:valid_min = -97.4915301829062 ;
lon_cyc_in:valid_max = -77.5 ;

double lat_cyc_in(n_coloc_tot) ;
lat_cyc_in:units = "degree_North" ;
lat_cyc_in:long_name = "latitude of the cyclone center when it
comes into the coloc x/y/t zone" ;
lat_cyc_in:valid_min = 16.0087723709759 ;
lat_cyc_in:valid_max = 19.0084071462335 ;

double time_cyc_in(n_coloc_tot) ;
time_cyc_in:units = "days since 1950-01-01 00:00:00" ;
time_cyc_in:long_name = "date/time UTC when the cyclone center
comes into the coloc x/y/t zone" ;
time_cyc_in:valid_min = 24320.25 ;
time_cyc_in:valid_max = 24324.4980263156 ;

double dist_cyc_in(n_coloc_tot) ;
dist_cyc_in:units = "km" ;
dist_cyc_in:long_name = "distance between the colocalised argo prf
and the cyclone center when it comes into the coloc x/y/t zone (or maybe when
it starts)" ;
dist_cyc_in:valid_min = 78.0188359818526 ;
dist_cyc_in:valid_max = 1000.0897822012 ;

double dt_cyc_in(n_coloc_tot) ;
dt_cyc_in:units = "days" ;
dt_cyc_in:long_name = "time difference between the colocalised argo
prf date and the time when the cyclone center comes into the coloc x/y/t zone
(t_cyc_in-t_argo)" ;
dt_cyc_in:valid_min = -34.6780555555597 ;
dt_cyc_in:valid_max = 33.1102970317006 ;

double rclc_cyc_in(n_coloc_tot) ;
rclc_cyc_in:units = "km" ;
```

```
    rclc_cyc_in:long_name = "Colocalisation radius when the cyclone
center comes into the coloc x/y/t zone" ;
    rclc_cyc_in:valid_min = 1000. ;
    rclc_cyc_in:valid_max = 1000. ;
    double lon_cyc_out(n_coloc_tot) ;
    lon_cyc_out:units = "degree_East" ;
    lon_cyc_out:long_name = "longitude of the cyclone center when it
goes out of the coloc x/y/t zone" ;
    lon_cyc_out:valid_min = -97.5 ;
    lon_cyc_out:valid_max = -77.5944318819747 ;
    double lat_cyc_out(n_coloc_tot) ;
    lat_cyc_out:units = "degree_North" ;
    lat_cyc_out:long_name = "latitude of the cyclone center when it
goes out of the coloc x/y/t zone" ;
    lat_cyc_out:valid_min = 16.0017550812851 ;
    lat_cyc_out:valid_max = 19.0039252663984 ;
    double time_cyc_out(n_coloc_tot) ;
    time_cyc_out:units = "days since 1950-01-01 00:00:00" ;
    time_cyc_out:long_name = "date/time UTC when the cyclone center
goes out of the coloc x/y/t zone" ;
    time_cyc_out:valid_min = 24320.2637527236 ;
    time_cyc_out:valid_max = 24324.5 ;
    double dist_cyc_out(n_coloc_tot) ;
    dist_cyc_out:units = "km" ;
    dist_cyc_out:long_name = "distance between the colocalised argo prf
and the cyclone center when it goes out of the coloc x/y/t zone (or maybe when
it finishes)" ;
    dist_cyc_out:valid_min = 510.590957084457 ;
    dist_cyc_out:valid_max = 1000.09415709222 ;
    double dt_cyc_out(n_coloc_tot) ;
    dt_cyc_out:units = "days" ;
    dt_cyc_out:long_name = "time difference between the colocalised
argo prf date and time when the cyclone center goes out of the coloc x/y/t zone
(t_cyc_out-t_argo)" ;
    dt_cyc_out:valid_min = -32.970543582458 ;
    dt_cyc_out:valid_max = 33.9960416667163 ;
    double rclc_cyc_out(n_coloc_tot) ;
    rclc_cyc_out:units = "km" ;
    rclc_cyc_out:long_name = "Colocalisation radius when the cyclone
```

```
center goes out of the coloc x/y/t zone" ;
    rclc_cyc_out:valid_min = 1000. ;
    rclc_cyc_out:valid_max = 1000. ;
double lon_cyc_distmin(n_coloc_tot) ;
    lon_cyc_distmin:units = "degree_East" ;
    lon_cyc_distmin:long_name = "longitude of the cyclone center when
it is at its minimum distance from its colocalised argo prf" ;
    lon_cyc_distmin:valid_min = -97.5 ;
    lon_cyc_distmin:valid_max = -77.5 ;
double lat_cyc_distmin(n_coloc_tot) ;
    lat_cyc_distmin:units = "degree_North" ;
    lat_cyc_distmin:long_name = "latitude of the cyclone center when it
is at its minimum distance from its colocalised argo prf" ;
    lat_cyc_distmin:valid_min = 16.0331001281738 ;
    lat_cyc_distmin:valid_max = 19.0086688995361 ;
double time_cyc_distmin(n_coloc_tot) ;
    time_cyc_distmin:units = "days since 1950-01-01 00:00:00" ;
    time_cyc_distmin:long_name = "date/time UTC when the cyclone center
is at its minimum distance from its colocalised argo prf" ;
    time_cyc_distmin:valid_min = 24320.25 ;
    time_cyc_distmin:valid_max = 24324.5 ;
double distmin_cyc(n_coloc_tot) ;
    distmin_cyc:units = "km" ;
    distmin_cyc:long_name = "minimum distance between the colocalised
argo prf and the cyclone center (in/during the continuous coloc x/y/t zone)" ;
    distmin_cyc:valid_min = 78.0188359818526 ;
    distmin_cyc:valid_max = 999.371662234403 ;
double dt_cyc_distmin(n_coloc_tot) ;
    dt_cyc_distmin:units = "days" ;
    dt_cyc_distmin:long_name = "time difference between the colocalised
argo prf date and time when the cyclone center is at minimum distance
(t_cyc_dmin-t_argo)" ;
    dt_cyc_distmin:valid_min = -33.9694675924256 ;
    dt_cyc_distmin:valid_max = 33.4303365387022 ;
double lon_cyc_dtmin(n_coloc_tot) ;
    lon_cyc_dtmin:units = "degree_East" ;
    lon_cyc_dtmin:long_name = "longitude of the cyclone center when it
is closest in time from its colocalised argo prf" ;
    lon_cyc_dtmin:valid_min = -97.5 ;
```

```
lon_cyc_dtmin:valid_max = -77.5 ;
double lat_cyc_dtmin(n_coloc_tot) ;
    lat_cyc_dtmin:units = "degree_North" ;
    lat_cyc_dtmin:long_name = "latitude of the cyclone center when it
is closest in time from its colocalised argo prf" ;
    lat_cyc_dtmin:valid_min = 16.0179007497319 ;
    lat_cyc_dtmin:valid_max = 19.0084071462335 ;
double time_cyc_dtmin(n_coloc_tot) ;
    time_cyc_dtmin:units = "days since 1950-01-01 00:00:00" ;
    time_cyc_dtmin:long_name = "date/time UTC when the cyclone center
is closest in time from its colocalised argo prf" ;
    time_cyc_dtmin:valid_min = 24320.25 ;
    time_cyc_dtmin:valid_max = 24324.5 ;
double dist_cyc_dtmin(n_coloc_tot) ;
    dist_cyc_dtmin:units = "km" ;
    dist_cyc_dtmin:long_name = "distance between the colocalised argo
prf and the cyclone center when the cyclone is closest in time from its
colocalised argo prf" ;
    dist_cyc_dtmin:valid_min = 78.0188359818526 ;
    dist_cyc_dtmin:valid_max = 1000.09126287149 ;
double dtmin_cyc(n_coloc_tot) ;
    dtmin_cyc:units = "days" ;
    dtmin_cyc:long_name = "time difference between the colocalised argo
prf date and time when the cyclone center is closest in time (t_cyc_dtmin-
t_argo)" ;
    dtmin_cyc:valid_min = 8.2673504948616e-06 ;
    dtmin_cyc:valid_max = 33.1102970317006 ;
double rclc_min(n_coloc_tot) ;
    rclc_min:units = "km" ;
    rclc_min:long_name = "Minimum value of the colocalisation radius
in/during the continuous x/y/t coloc zone" ;
    rclc_min:valid_min = 1000. ;
    rclc_min:valid_max = 1000. ;
double rclc_max(n_coloc_tot) ;
    rclc_max:units = "km" ;
    rclc_max:long_name = "Maximum value of the colocalisation radius
in/during the continuous x/y/t coloc zone" ;
    rclc_max:valid_min = 1000. ;
    rclc_max:valid_max = 1000. ;
```

```
double rclc_ave(n_coloc_tot) ;
    rclc_ave:units = "km" ;
    rclc_ave:long_name = "Average value of the colocalisation radius
over/during the continuous x/y/t coloc zone" ;
    rclc_ave:valid_min = 1000. ;
    rclc_ave:valid_max = 1000. ;
double coloc_duration(n_coloc_tot) ;
    coloc_duration:units = "days" ;
    coloc_duration:long_name = "Duration of the colocalisation, time
integral during which the cyclone is colocalised with its argo prf (=t_cyc_in-
t_cyc_out)" ;
    coloc_duration:valid_min = 0.00197368441149592 ;
    coloc_duration:valid_max = 3.70432692300528 ;
double coloc_length(n_coloc_tot) ;
    coloc_length:units = "km" ;
    coloc_length:long_name = "Length of the colocalisation, distance
integral over the cyclone track during its continuous colocalisation with the
argo prf" ;
    coloc_length:valid_min = 0.891827244256648 ;
    coloc_length:valid_max = 1973.02435946072 ;
double coloc_duration_before(n_coloc_tot) ;
    coloc_duration_before:units = "days" ;
    coloc_duration_before:long_name = "Duration of the colocalisation
BEFORE the argo measurements = time integral from time the cyclone enters
coloc. area until it leaves the area (or until the argo measurements time if
the latter is before t_cyc_out). It is =0. if cyclone enters coloc area after
argo measurements. By doing the total over possible multiple colocs, this may
result in a proxy of mixing duration before an argo measurements if Rcoloc is
appropriate (e.g. Rclc=r34)" ;
    coloc_duration_before:valid_min = 0. ;
    coloc_duration_before:valid_max = 3.70432692300528 ;
double coloc_length_before(n_coloc_tot) ;
    coloc_length_before:units = "km" ;
    coloc_length_before:long_name = "Total length of cyclone track
during the colocalisation and BEFORE the possible argo measurements time. It is
=0. if cyclone enters coloc area after argo measurements" ;
    coloc_length_before:valid_min = 0. ;
    coloc_length_before:valid_max = 1973.02435946072 ;
char coloc_namelist(nlines, strlen1) ;
    coloc_namelist:long_name = "the namelist used for colocalisation
(i.e. input coloc parameters). NB: it is an IDL script, stored here as a string
vector, lines starting with \'\' character are comments" ;
```

			MAXSS ATBD ESA Contract 4000132954/20/I-NB Delivery D21, Version 1.0.0 Date 06/10/2021 Page 122
---	--	--	---

```
// global attributes:
```

```
    :Dataset_Id = "Advanced Ocean Variables (mld, blt, N2max, D20...)
computed from GDAC individual Argo profiles, colocalised with cyclone tracks
(GDAC_ARGO_AOV)" ;
```

```
    :Production = "Clement de Boyer Montegut, IFREMER, LOPS laboratory
(UMR6523, Univ. of Brest/Cnrs/Ifremer/Ird), Brest, France (deboyer@ifremer.fr)
for the ESA MAXSS project" ;
```

```
    :Program_Name = "coloc_argo_cyclone.pro - stamp_date of the main
prog run : 2022_02_28_18h23m56s" ;
```

```
    :Colocalisation_Precision = "max errors on track coloc
positions/times computed: DX = 100.0 m ; DT = 0.4 min ; For info/comparison:
argo position/time accuracy is resp. about 1500m or less / order of 10 min
(TBC), for cyclone input positions/times accuracy still to be defined (km?,
10min?)" ;
```

```
    :Cyclone_Track_Data_Source = "ESA MAXSS project file :
ibtracs.nc" ;
```

```
    :Earth_Model = "Coloc (e.g. distances between points) computed on a
spherical Earth model, with radius = Clarke 1866 equatorial radius = 6378206.40
meters" ;
```

```
    :Timestamp = "Mon Feb 28 22:45:55 2022" ;
```

```
}
```